# CALOXINS: A NOVEL CLASS OF PLASMA MEMBRANE $Ca^{2+}$ PUMP INHIBITORS

# CALOXINS: A NOVEL CLASS OF PLASMA MEMBRANE $Ca^{2+}$PUMP INHIBITORS

by

JYOTI PANDE, B.Sc., M.Sc.

A Thesis
Submitted to the School of Graduate Studies
in Partial Fulfillment of the Requirements
for the Degree
Doctor of Philosophy
Biology

McMaster University

Doctor of Philosophy (2008) McMaster University

(Biology) Hamilton, Ontario

TITLE: Caloxins: a novel class of plasma membrane $Ca^{2+}$ pump inhibitors

AUTHOR: Jyoti Pande, B.Sc., M.Sc. (McMaster University)

SUPERVISOR: Professor A.K. Grover

# OF PAGES: xiii, 172

## ABSTRACT

Ionized calcium ($Ca^{2+}$) is a signaling messenger that controls numerous cellular processes essential for life. The fidelity of $Ca^{2+}$ signaling depends on the mechanisms that dynamically regulate its cytosolic concentration and maintain it at a low level in a resting cell. Plasma Membrane $Ca^{2+}$ ATPase (PMCA) is a high affinity $Ca^{2+}$ extrusion pathway involved in $Ca^{2+}$ homeostasis and signal transduction. PMCA are encoded by 4 genes (PMCA1-4), which are expressed in a tissue dependent manner. The diversity of PMCA isoforms is further increased by alternative splicing. Changes in PMCA activity occur in heart failure and hypertension. Specific inhibitors of other ion transporters such as thapsigargin and digoxin, have made their mark in cell biology, but the currently used inhibitors of PMCA (vanadate and eosin) are non-specific. Thus, selective inhibitors of PMCA are needed to discern its role in $Ca^{2+}$ signaling in physiology and pathophysiology. We introduced the concept of caloxins - peptides that specifically inhibit the activity of PMCA by binding to one of its five extracellular domains (exdoms) 1 to 5. The earlier caloxins including 2a1 and 3a1 were obtained by screening a phage display random 12-amino acid peptide (Ph.D-12) library for binding to synthetic peptides based on the exdom sequences. However, they all had low affinity.

The objective of this research was to develop caloxins with high affinity and PMCA4 isoform selectivity. A two-step screening method was developed to screen the Ph.D-12 library to first bind to the synthetic exdom of PMCA4,

followed by affinity chromatography using PMCA protein purified from human erythrocyte ghosts (mainly PMCA4). This method was used to obtain caloxins 1b1 and 1b2 to bind to the N and C-terminal halves of the exdom 1 of PMCA4, respectively. Both caloxins 1b1 and 1b2 had a 10-fold higher affinity than the prototype caloxin 2a1 and showed slight PMCA4 isoform preference. To engineer inhibitors with greater affinity and PMCA4 isoform selectivity, Ph.D caloxin 1b1-like peptide library was constructed. Most of the peptides expressed in this library differed from caloxin 1b1 in 0, 1, 2 or 3 amino acid residues at random. The library was screened to obtain several peptides one of which was caloxin 1c2. Caloxin 1c2 had 200-fold higher affinity than caloxin 2a1 and was isoform selective, with greater than 10-fold affinity for PMCA4 than for PMCA isoforms 1, 2 or 3. Thus, caloxin 1c2 is the first high affinity PMCA inhibitor that also is selective for an individual PMCA isoform.

The second aim of this research was to establish that caloxin 1c2 binds to PMCA protein in erythrocyte ghosts. Two photoreactive caloxin 1c2-derivatives containing the photoactivable residue benzoylphenylalanine (Bpa) and a C-terminal biotin tag were used. Bpa substituted tryptophan at position 3 (3Bpa1c2-biotin) and serine at position 16 (16Bpa1c2-biotin) in caloxin 1c2. Both the derivatives inhibited PMCA activity in the erythrocyte ghosts. The intensity of the biotin label in the photolabeled erythrocyte ghosts was much stronger with 3Bpa1c2-biotin, which was then used in the subsequent experiments. The photolabeled proteins in erythrocyte ghosts were detected as a 250-270 kDa

doublet in Western blots using streptavidin and the PMCA specific antibody. The degree of photolabeling depended on the UV-crosslinking time, and on the concentrations of 3Bpa1c2-biotin and the ghost protein. The selectivity of the photolabeling site was confirmed by decreased photolabel incorporation at 250-270 kDa doublet in the presence of excess caloxin 1c2 and the synthetic exdom 1X peptide of PMCA4. The photolabeled erythrocyte ghosts were solubilized and analyzed by immunoprecipitation with the PMCA specific antibody. The immunoprecipitate showed a 250-270 kDa doublet in Western blots using streptavidin. This confirmed that PMCA protein was photolabeled by the photoreactive derivatives of caloxin 1c2. Thus, caloxin 1c2 inhibits PMCA activity by binding to the exdom 1X of PMCA4.

My work in M.Sc. initiated the concept of caloxins in the literature. This research has taken it to the stage where we can obtain caloxins selective for individual PMCA isoforms. This contrasts with the relative paucity of inhibitors specific for individual isoforms of other ion pumps. The high affinity isoform selective caloxin 1c2 and previous caloxins are being used to study PMCA physiology in our lab and by other researchers. Since caloxins act when added extracellularly and it is possible to obtain PMCA isoform selective caloxins, it is anticipated that they will aid in understanding the role of PMCA in signal transduction and homeostasis in health and disease.

## PUBLICATIONS

List of Publications as a result of the present study:

Pande J, Szewczyk MM, Kuszczak I, Grover S, Escher, E, Grover, AK. Functional effects of caloxin 1c2, a novel engineered selective inhibitor of plasma membrane Ca2+ pump isoform 4, on coronary artery. J. Cell. Mol. Med. 2008; 12(3):1049-60.

Szewczyk M.M, Pande J, and Grover A.K. Caloxins: a novel class of selective plasma membrane Ca(2+) pump inhibitors obtained using biotechnology. Pflugers Arch. 2008; 456:255-266

Pande J, Mallhi KK, Sawh A, Szewczyk MM, Simpson F, Grover AK. Aortic smooth muscle and endothelial plasma membrane Ca2+ pump isoforms are inhibited differently by the extracellular inhibitor caloxin 1b1. Am.J.Physiol Cell Physiol 2006; 290:C1341-C1349

Pande J, Grover AK. Plasma membrane calcium pumps in smooth muscle: from fictional molecules to novel inhibitors. Can.J.Physiol Pharmacol. 2005; 83:743-754. (invited review)

Pande J, Mallhi KK, Grover AK. A novel plasma membrane Ca(2+)-pump inhibitor:
caloxin 1A1. Eur.J.Pharmacol. 2005; 508:1-6.

List of Publications related to present study:

Pande J, Mallhi KK, Grover AK. Role of third extracellular domain of plasma membrane Ca2+-Mg2+-ATPase based on the novel inhibitor caloxin 3A1. Cell Calcium 2005; 37:245-250.

Holmes ME, Chaudhary J*, Grover AK. Mechanism of action of the novel plasma membrane Ca(2+)-pump inhibitor caloxin. Cell Calcium 2003; 33:241-245.

Chaudhary J*, Walia M, Matharu J, Escher E, Grover AK. Caloxin: a novel plasma membrane Ca2+ pump inhibitor. Am.J.Physiol Cell Physiol 2001; 280:C1027-C1030 (M.Sc. thesis)
* Pande J is married name of Chaudhary J

## ACKNOWLEDGEMENTS

I dedicate this thesis to my father who values higher education and has always been a constant source of encouragement. This thesis would have never been completed had you not been there to support me. I hope in everything I do, I can make you half as proud of me as I am of you.

Above all, I would like to express my sincere gratitude to Dr. A.K. Grover, for giving me the opportunity to work in his lab. I am grateful for his esteemed guidance and support throughout the course of my study. I will forever be grateful for his patience in accommodating my schedule that helped me to complete my work. I would also like to thank my committee members, Dr. Werstiuk and Dr. Nurse for their helpful comments and encouragement. Thanks to Heart and Stroke foundation of Canada for the financial support during the studies.

I have had the opportunity to work with wonderful people in the lab and have made good friends along the way. Magda, it was nice to work with you on the same project and I thankyou for your friendship. Through my project, I got aquainted with many wonderful people.

I would like to thank Sue Samson who shares her technical skills with all the lab members and ensures the smooth running of the lab.

I would like to acknowledge my loving mom, parents in law, brothers Deepak and Sandeeep, and their families that make everything worthwhile. Special thanks to Promy for always having the time to listen to my good and bad. I am grateful to you all for being there and enriching my life. May God give me the strength to become a better person and make you all proud.

My studies would not have been completed had it not been for the love, patience and support of my husband, Manish. I hope to always be by your side trying to be as great a life partner as you are.

I thank God for the countless blessings!

TABLE OF CONTENTS

ABSTRACT ..... III
PUBLICATIONS ..... VI
ACKNOWLEDGEMENTS ..... VII
LIST OF ILLUSTRATIONS ..... XI
LIST OF ABBREVIATIONS ..... XIII
1.0 INTRODUCTION ..... 1
1.1 Overview of $Ca^{2+}$ Homeostasis ..... 1
1.2 Mechanisms of maintaining low resting $[Ca^{2+}]_i$ ..... 4
1.2.1 PMCA ..... 5
1.2.1.1 General properties ..... 5
1.2.1.2 Structural organization of PMCA ..... 8
1.2.1.3 PMCA isoforms ..... 11
1.2.1.4 Tissue distribution of PMCA isoforms ..... 13
1.2.1.5 Regulation of PMCA ..... 15
1.2.1.5.1 Regulation by calmodulin ..... 16
1.2.1.5.2 Regulation by protein kinases ..... 20
1.2.1.5.3 Regulation by acidic phospholipids ..... 22
1.2.1.6 Potential role of PMCA ..... 24
1.2.2 $Ca^{2+}$ pumps of the intracellular organelles ..... 28
1.2.3 Other ion transporters in the PM ..... 30
1.2.4 $Ca^{2+}$ binding proteins ..... 31
1.3 Mechanisms of $Ca^{2+}$ elevation in the cytosol ..... 33
1.3.1 $Ca^{2+}$ entry channels ..... 33
1.3.2 $Ca^{2+}$ release channels ..... 35
1.4 Need for PMCA selective inhibitors ..... 37
1.5 The concept of Caloxins ..... 41
1.5.1 Screening the phage display (Ph.D) random peptide libraries ..... 41
1.5.2 Properties of the known caloxins ..... 42
1.6 Objectives of the present study ..... 44
2.0 MATERIALS AND METHODS ..... 48
2.1 Materials ..... 48
2.2 Two-step screening of Ph.D-12 library with PMCA4 exdom 1X as target. 49
2.2.1 Screening Ph.D-12 library using the synthetic exdom 1X target ..... 50
2.2.1.1 Amplification and precipitation of the eluted phage ..... 52
2.2.1.2 Determining phage titers ..... 53
2.2.1.3 Picking phage clones and amplification ..... 54
2.2.1.4 Isolation of plasmid DNA ..... 54
2.2.2 Screening Ph.D-12 library using PMCA affinity chromatography ..... 55
2.3 Assay for selectivity of phage binding to the exdom target ..... 57

2.4 Two-step screening of Ph.D-12 library with PMCA4 exdom 1Y as target. 58
2.5 Screening a cysteine bridge constrained Ph.D-C7C library ..... 58
2.6 Construction of the Ph.D caloxin 1b1-like peptide library ..... 58
2.6.1 Synthesis of a duplex from single stranded oligonucleotides ..... 59
2.6.2 Digestion of the oligonucleotide duplex ..... 60
2.6.3 Preparation of the M13KE vector ..... 61
2.6.4 Ligation of digested oligonucleotide duplex and M13KE vector ..... 61
2.6.5 Transformation of XL2-Blue Ultracompetent cells ..... 62
2.7 Construction of the Ph.D caloxin 1b2-like peptide library ..... 62
2.8 Photolabeling reaction ..... 63
2.9 PMCA immunoprecipitation from human erythrocyte ghosts ..... 65
2.10 Western blotting ..... 66
2.11 Preparation of the leaky human erythrocyte ghosts ..... 67
2.12 Protein estimation ..... 68
2.13 Coupled enzyme ATPase assay ..... 68
2.14 ATPase assay based on hydrolysis of radioactive ATP ..... 69
2.15 Phosphatase assay ..... 71
2.16 Acylphosphate assays ..... 71
2.17 Contractility studies and Cytosolic $Ca^{2+}$ measurements ..... 72
2.18 Data Analysis ..... 72

3.0 RESULTS ..... 73

3.1 Aim 1: Developing high affinity caloxins using the exdom 1X as target.... 73
3.1.1 Screening of the Ph.D-12 library ..... 74
3.1.1.1 Two-step screening of Ph.D-12 library using PMCA4 exdom 1X ..... 75
3.1.1.2 Selectivity of the obtained phage clone for the exdom 1X ..... 76
3.1.1.3 Caloxin 1b1 modulates the $Ca^{2+}$-$Mg^{2+}$ATPase activity of PMCA ..... 78
3.1.1.4 Inhibition constant of caloxin 1b1 for PMCA in erythrocyte ghosts..... 79
3.1.1.5 PMCA isoform preference of caloxin 1b1 ..... 81
3.1.1.6 Inhibition by caloxin 1b1 and its randomized peptide ..... 86
3.1.1.7 PMCA selectivity of caloxin 1b1 over other ATPases ..... 87
3.1.1.8 Effect of caloxin 1b1 on PMCA acylphosphate levels ..... 89
3.1.1.9 Physiological effects of caloxin 1b1 ..... 92
3.1.2 Limited mutagenesis of caloxin 1b1 to obtain caloxin 1c2 ..... 92
3.1.2.1 Construction of Ph.D caloxin 1b1-like peptide library ..... 93
3.1.2.2 First screening of Ph.D caloxin 1b1-like peptide library ..... 94
3.1.2.3 Competition between phage clones selected in the first screening..... 99
3.1.2.4 Inhibition of PMCA by caloxins 1c1, 1c2 and 1c3 ..... 100
3.1.2.5 PMCA isoform preference of caloxin 1c2 ..... 103
3.1.2.6 Physiological studies with caloxin 1c2 ..... 103
3.1.2.7 Caloxin 1c2 inhibition of PMCA in different species ..... 104
3.2 Aim 2: Determine the caloxin 1c2-binding domain on PMCA protein..... 107
3.2.1 Caloxin 1c2 derived photolabels inhibit PMCA activity ..... 108
3.2.2 Photolabeling erythrocyte ghosts with caloxin 1c2-derived photolabels 111

3.2.2.1 3Bpa1c2-biotin concentration dependence of photolabeling..... 113
3.2.2.2 Ghost protein concentration dependence of photolabeling..... 113
3.2.2.3 UV-irradiation time dependence of photolabeling ..... 115
3.2.3 Selectivity of the photolabeling site in erythrocyte ghosts ..... 116
3.2.4 Immunoprecipitation to establish that PMCA was photolabeled ..... 117
3.3 Aim 3: Develop caloxins using exdom 1Y for screening Ph.D libraries... 120
3.3.1 Two-step screening of Ph.D-12 library using exdom 1Y of PMCA4..... 120
3.3.2 Screening a cysteine bridge constrained Ph.D-C7C library..... 123

4.0 DISCUSSION ..... 130

4.1 Two-step screening and mutagenesis to improve affinity of caloxins..... 130
4.2 Screening the Ph.D-C7C library ..... 134
4.3 Selectivity of caloxins..... 136
4.4 Mechanism of inhibition by caloxins..... 137
4.5 PMCA-binding domain of caloxin 1c2..... 140
4.6 Studies using caloxins..... 143
4.7 Conclusions and Future experiments ..... 145

5.0 REFERENCES ..... 148

6.0 APPENDIX 1: PHYSIOLOGICAL STUDIES USING CALOXINS..... 163

A1.1 Effects of caloxin 1b1 on [Ca2+]i and the arterial contractility ..... 163
A1.2. Effect of caloxin 1c2 on the arterial contractility ..... 169
A1.3. Effect of caloxin 1a1 on cells stimulated with $Ca^{2+}$ ionophore..... 172

## LIST OF ILLUSTRATIONS


Fig. 1.1 Major candidates in Ca2+ homeostasis. ..... 3
Fig. 1.2. Extracellular domains (exdoms) in human PMCA1b protein. ..... 9
Fig. 2.1. Construction of Ph.D caloxin 1b1-like peptide library ..... 64
Fig. 3.1. Selectivity of phage clone ..... 77
Fig. 3.2. Traces showing the coupled enzyme assay for ATPase. ..... 80
Fig. 3.3. Caloxin 1b1 inhibition of PMCA activity in leaky human erythrocyte ghosts measured by coupled enzyme assay. ..... 82
Fig. 3.4. Caloxin 1b1 inhibition of PMCA activity in leaky human erythrocyte ghosts measured by hydrolysis of [$\gamma$-$^{33}$P]-ATP ..... 83
Fig. 3.5. Caloxin 1b1 inhibition of $Ca^{2+}$-$Mg^{2+}$ATPase activity of PMCA1-4 measured by coupled enzyme assay. ..... 85
Fig. 3.6. Effect of caloxin 1b1 on various ATPases. ..... 90
Fig. 3.7. Effect of caloxin 1b1 on the 140-kDa acylphosphate intermediate of PMCA. ..... 91
Fig. 3.8. Mixture of oligonucleotides encoding caloxin 1b1-like peptides. ..... 96
Fig. 3.9. Inhibition of PMCA activity in leaky human erythrocyte ghosts by caloxin 1b1 and its mutants ..... 102
Fig. 3.10. Caloxin 1c2 inhibition of $Ca^{2+}$-$Mg^{2+}$ATPase activity of PMCA isoforms 1-4 measured in a coupled enzyme assay. ..... 105
Fig. 3.11. Caloxin 1c2 inhibition of $Ca^{2+}$-$Mg^{2+}$ATPase activity of PMCA in leaky erythrocyte ghosts from different species. ..... 106
Fig. 3.12. Effect of caloxin 1c2-derived photolabels on PMCA activity in leaky human erythrocyte ghosts measured by the $Ca^{2+}$ stimulated hydrolysis of [$\gamma$-$^{33}$P]-ATP. ..... 110
Fig. 3.13. Photolabeling of erythrocyte ghosts by caloxin 1c2-derived photolabels. ..... 112
Fig. 3.14. 3Bpa1c2-biotin concentration dependence of photolabeling. ..... 114
Fig. 3.15. Erythrocyte ghost protein concentration dependence of photolabeling. ..... 114
Fig. 3.16. The effect of increasing length of UV irradiation on photolabeling. . 115
Fig. 3.17. Caloxin 1c2 competes with 3Bpa1c2-biotin for photolabeling of the erythrocyte ghosts. ..... 118
Fig. 3.18. The synthetic exdom 1X peptide of PMCA4 competes with the erythrocyte ghosts for photolabeling by 3Bpa1c2-biotin ..... 118
Fig. 3.19. 3Bpa1c2-biotin selectively photolabels PMCA in erythrocyte ghosts. ..... 119
Fig. 3.20. Caloxin 1b2 inhibition of $Ca^{2+}$-$Mg^{2+}$ATPase activity of PMCA isoforms 1 and 4 measured in a coupled enzyme assay. ..... 122
Fig. 3.21. Selectivity of the phage pool from the 6$^{th}$ round of screening. ..... 125
Fig. 3.22. Caloxin 1a1 inhibition of PMCA activity in leaky human erythrocyte ghosts measured by monitoring the hydrolysis of [$\gamma$-$^{33}$P]-ATP. ..... 126

Fig. 3.23. Effect of DTT on caloxin 1a1 inhibition of PMCA activity in leaky human erythrocyte ghosts. ..... 128
Fig. 3.24. Effect of caloxin 1a1 (200 μM) and glutathione dimer GSSG (1 mM) on the $Ca^{2+}$-$Mg^{2+}$ATPase activity of SERCA and PMCA..... 129
Fig. 3.25. Effect of caloxin 1a1 on the 140-kDa acylphosphate intermediate of PMCA. ..... 129
Fig. 4.1. Comparison of affinities of caloxins. ..... 135
Fig. A1.1. Effect of caloxin 1b1 on $[Ca^{2+}]_i$ in cultured SMC and the EC. ..... 166
Fig. A1.2. Effect of caloxin 1b1 on $[Ca^{2+}]_i$ dynamics. ..... 167
Fig. A1.3. Effect of caloxin 1b1 on the de-endothelialized rat aortic rings..... 168
Fig. A1.4. Effect of caloxin 1b1 on the endothelium dependent relaxation of the rat aortic rings. ..... 168
Fig. A1.5. Effect of caloxin 1c2 on the basal tone of de-endothelialized pig coronary artery rings. ..... 170
Fig. A1.6. Effect of caloxin 1c2 on the contractility of de-endothelialized coronary artery rings. ..... 171
Fig. A1.7. Effect of caloxin 1a1 on cell $[Ca^{2+}]_i$ dynamics. ..... 172

Table number

Table 3.1. Testing small-scale Ph.D caloxin 1b1-like peptide library.....97
Table 3.2. Characterization of sample of Ph.D caloxin 1b1-like peptide library..97
Table 3.3. Characterization of phage clones selected after 4 rounds of screening of the Ph.D caloxin 1b1-like peptide library.....98
Table 3.4. Characterization of the phage clones selected after competition.....101

## LIST OF ABBREVIATIONS

| | |
|---|---|
| ATP | adenosine triphosphate |
| Bpa | p-Benzoyl-L-phenylalanine |
| BSA | bovine serum albumin |
| $Ca^{2+}$ | ionized calcium |
| $[Ca^{2+}]_i$ | cytosolic $Ca^{2+}$ concentration |
| cAMP | adenosine 3',5'-cyclic monophosphate |
| cGMP | guanosine 3',5'-cyclic monophosphate |
| DTT | 1-4-dithiothreitol |
| EC | endothelial cell |
| EDTA | (ethylenedinitrilo)-tetraacetic acid |
| EGTA | ethylene glycol-bis(β-aminoethyl ether)-N,N,N',N'-tetraacetic acid |
| Exdom | extracellular domain |
| HRP | horseradish peroxidase |
| IgG | immunoglobulin G |
| $IP_3$ | inositol 1,4,5-trisphosphate |
| $IP_3R$ | $IP_3$ receptor |
| $K_d$ | dissociation constant |
| KHLH | keyhole limpet hemocyanin |
| $K_i$ | inhibition constant |
| LB | Luria broth |
| MES | 2-[N-Morpholino] ethanesulfonic acid |
| mNCX | mitochondrial $Na^+/Ca^{2+}$exchanger |
| MOPS | 3-[N- Morpholino] propane sulfonate-NaOH |
| NADH | nicotinamide adenine dinucleotide (reduced form) |
| NCX | $Na^+/Ca^{2+}$exchanger |
| $P_i$ | inorganic phosphate |
| PBS | phosphate buffered saline |
| PEP | phospho(enol)pyruvate |
| Pfu | plaque forming unit |
| Ph.D | phage display peptide library |
| PIP2 | phosphatidylinositol 4,5-bisphosphate |
| PKA | protein kinase A |
| PKC | protein kinase C |
| PM | plasma membrane |
| PMCA | plasma membrane $Ca^{2+}$ ATPase |
| ROCC | receptor operated $Ca^{2+}$ channel |
| RyR | ryanodine receptor |
| SEM | standard error of the mean |
| SER | sarco/endoplasmic reticulum |
| SERCA | sarco/endoplasmic reticulum $Ca^{2+}$ ATPase |
| SMC | smooth muscle cell |

| | |
|---|---|
| SOCC | store operated $Ca^{2+}$ channel |
| TM | transmembrane |
| Tris | tris(hydroxymethyl)aminomethane |
| TRP | transient receptor potential |
| VOCC | voltage operated $Ca^{2+}$ channels |

# 1.0 INTRODUCTION

Plasma Membrane $Ca^{2+}$ ATPase (PMCA) is a high affinity system that transports $Ca^{2+}$ out of the cell[1-4]. Regulation of ionized calcium ($Ca^{2+}$) concentration in the cytosol ($[Ca^{2+}]_i$), is essential for cell survival and cellular signal transduction. There are a number of diseases associated with failed $Ca^{2+}$ homeostasis[5-14]. Lack of specific inhibitors of PMCA has limited the studies in understanding its role in $Ca^{2+}$ homeostasis and cell signaling. **The overall objective of this research was to obtain high affinity PMCA specific inhibitors called caloxins.** Before proceeding onto the details of the research proposal, a brief overview of $Ca^{2+}$ homeostasis, structure and regulation of PMCA, and limitations of the methods currently used to study PMCA are given below.

## 1.1 Overview of $Ca^{2+}$ Homeostasis

$Ca^{2+}$ is an important signaling messenger controlling the cellular processes ranging from fertilization to programmed cell death[15-17]. The high $Ca^{2+}$ signal sensitivity is achieved on a background of controlled low resting $[Ca^{2+}]_i$[18-20]. At rest, mammalian cells maintain $[Ca^{2+}]_i$ around 0.1 μM, thereby establishing a $Ca^{2+}$ concentration gradient of about 10,000 fold across the plasma membrane (PM)[21,22]. A rise in $[Ca^{2+}]_i$ controls a large number of cellular functions such as; modulation of metabolic routes, cell growth, cell cycle, syntheses and release of hormones, muscle and non-muscle motility, multiplicity of membrane-linked processes and apoptosis[15-20]. $[Ca^{2+}]_i$ is tightly regulated in time, space and

amplitude since cells extract specific information from these parameters[23,24]. The movement of $Ca^{2+}$ across the PM (between the cell and the extracellular space) plays a key role in the long term maintenance of $[Ca^{2+}]_i$ homeostasis. The short-term control of $[Ca^{2+}]_i$ varies from cell to cell, with cells such as neurons relying heavily on the PM as compared to the skeletal muscle cells, which rely mostly on their well-developed sarco/endoplasmic reticulum (SER)[25]. The SER can store up to 5-10 mM $Ca^{2+}$, most of which is buffered maintaining the free $Ca^{2+}$ in the lumen at levels around ~1 mM[26]. Thus, the cell has access to the supply of external $Ca^{2+}$ and a more finite internal $Ca^{2+}$ store sequestered within the SER, which can lead to an increase in $[Ca^{2+}]_i$ required for the signaling function[22]. Following the transient rise in $[Ca^{2+}]_i$, $Ca^{2+}$ has to be restored to lower levels and maintained at its resting concentration. The major mechanisms involved in removing $Ca^{2+}$ from the cytosol are outlined here followed by the systems regulating both the entry and release of $Ca^{2+}$ into the cytosol. Fig. 1.1 shows the major candidates involved in $[Ca^{2+}]_i$ homeostasis.

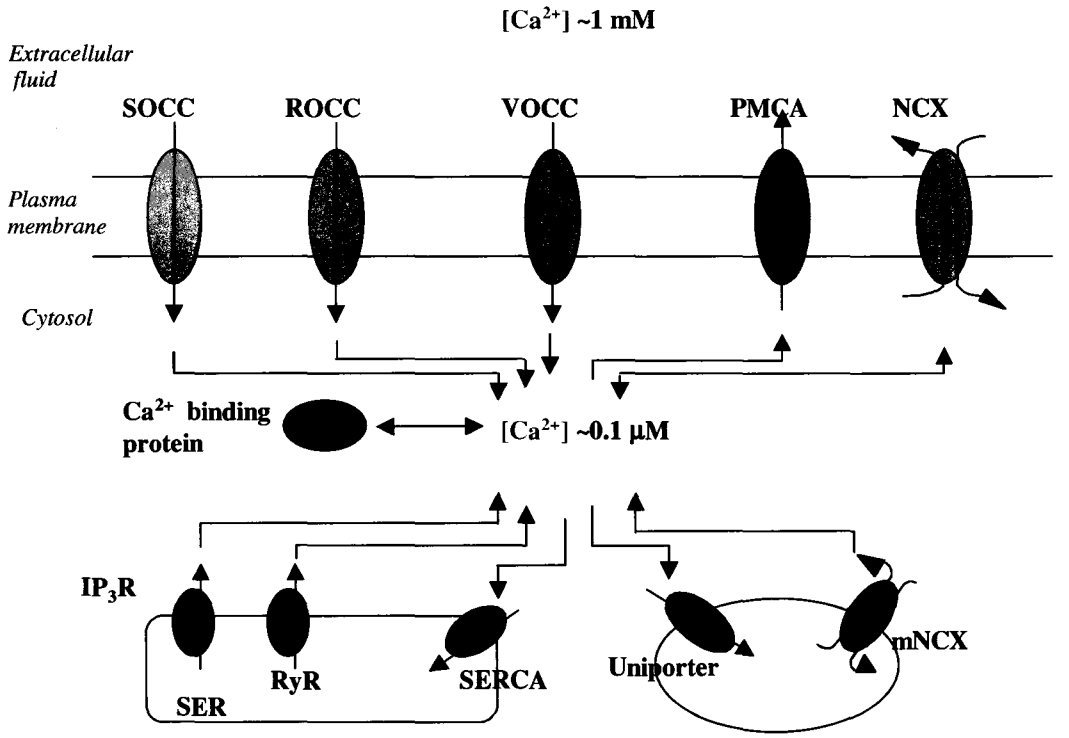


**Fig. 1.1 Major candidates in $Ca^{2+}$ homeostasis.**

$Ca^{2+}$ entry into the cells can occur through voltage operated $Ca^{2+}$ channels (VOCC) or receptor operated $Ca^{2+}$ channels (ROCC) or store operated $Ca^{2+}$ channels (SOCC). The receptor binding may activate phospholipase C to produce $IP_3$ (inositol 1,4,5-trisphosphate), which in turn releases $Ca^{2+}$ from SER via $IP_3$ receptor ($IP_3R$). $Ca^{2+}$ can induce $Ca^{2+}$ release from SER via activation of $Ca^{2+}$ induced $Ca^{2+}$ release channels/ryanodine receptors (RyR). $Ca^{2+}$ binding proteins can buffer $Ca^{2+}$ in the cytosol and in the SER lumen. Increase in $[Ca^{2+}]_i$ leads to cell specific response after which $Ca^{2+}$ is decreased to resting levels. $Ca^{2+}$ can be removed by PMCA and $Na^+/Ca^{2+}$ exchanger (NCX) or sequestered in SER by SER $Ca^{2+}$ ATPase (SERCA). Mitochondria may also sequester or release $Ca^{2+}$ via mitochondrial uniporter and mitochondrial $Na^+/Ca^{2+}$ exchanger (mNCX), respectively.

## 1.2 Mechanisms of maintaining low resting $[Ca^{2+}]_i$

The resting $[Ca^{2+}]_i$ is maintained primarily by the membrane $Ca^{2+}$ transport proteins that rapidly and efficiently lower $[Ca^{2+}]_i$ by transporting it across the membrane boundaries[16,19,27]. $Ca^{2+}$ can also be buffered by reversible complexation with $Ca^{2+}$ binding proteins within the cell[16,20,27]. The $Ca^{2+}$ transporters that remove $[Ca^{2+}]_i$ following cell stimulation include the $Ca^{2+}$ pumps and the ion exchangers. There are three families of the $Ca^{2+}$ pumps: the $Ca^{2+}$-$Mg^{2+}$-ATPase of the PM (PMCA) that extrudes $Ca^{2+}$ out of the cell and the $Ca^{2+}$-$Mg^{2+}$-ATPase of the SER (SERCA) and the golgi complex (SPCA) that pumps $Ca^{2+}$ into the lumen of the internal stores[28-33]. The $Ca^{2+}$ transporting ion exchangers include the $Na^+/Ca^{2+}$exchanger (NCX) or the $K^+$ dependent $Na^+/Ca^{2+}$exchanger (NCKX) in the PM[34-36]. Mitochondria can also transport $Ca^{2+}$ from the cytosol by an electrophoretic uniporter located in its inner membrane[37,38]. In general, the $Ca^{2+}$ pumps transport $Ca^{2+}$ with high affinity, whereas the ion exchangers and the mitochondrial uniporter are low $Ca^{2+}$ affinity systems. Due to the differences in their abundance and kinetic properties, the relative roles of the $Ca^{2+}$ transporters in removing $Ca^{2+}$ from the cytosol varies depending on the type of cell[39]. Since the focus of this thesis is on developing selective inhibitors of PMCA, this pump is described here in detail, followed by a brief description of the other transport mechanisms.

### 1.2.1 PMCA

PMCA are the $Ca^{2+}$-$Mg^{2+}$ ATPases that use the energy of ATP hydrolysis to pump $Ca^{2+}$ out of the cell against a large $Ca^{2+}$ electrochemical gradient[39-42]. The ATPase activity of PMCA was discovered in 1961[43], which was later shown to be associated with an uphill $Ca^{2+}$ transport in the resealed human red cell ghosts in 1966[44]. Since then, PMCA has been detected in all eukaryotic cells[31,45]. They have high affinity for $Ca^{2+}$, but their low abundance makes them a low capacity $Ca^{2+}$ extrusion system. For instance, PMCA represents less than 0.1 % of the total intrinsic PM proteins in erythrocytes[40]. There are 4 separate genes that encode PMCA isoforms 1 to 4[46,47]. Additional PMCA isoform variants are generated as a result of alternative splicing of the primary gene transcripts[48]. There are many known regulators of the $Ca^{2+}$ pump such as calmodulin, protein kinases and acidic phospholipids[25,49-51]. General properties, structural organization, regulation and the importance of PMCA are presented in detail in the following sections.

#### *1.2.1.1 General properties*

PMCA belongs to the family of P-type ion transport ATPases that generate essential ion gradients, which form the basis of diverse functions like signaling, secondary transport processes and energy storage[52,53]. The other members of the family include SERCA and the $Na^+$-$K^+$-ATPase[53,54]. The P-type ATPases are characterized by the formation of a reversible phosphorylated enzyme intermediate, which is intimately linked with the ion translocation process[52,53]. The reaction cycle of PMCA is based on the cyclical changes between two main

conformational states denoted as E1 and E2[55]. These conformational states have been documented in the recently solved crystal structures of the homologous $Ca^{2+}$ pump of the SER[56-61]. The similarity between the crystal structure of the E2 state of the $Na^{+}$-$K^{+}$ ATPase and SERCA emphasizes the similarity in the architecture shared by the members of P-type ATPases regardless of the size, charge or the number of ions they transport[62]. The intermediate steps involved in the reaction cycle of PMCA are formulated in a 4-step scheme: E1 $\leftrightarrow$ ($Ca^{2+}$) E1P $\leftrightarrow$ E2P $\leftrightarrow$ E2 $\leftrightarrow$ E1. $Ca^{2+}$ binds to the enzyme in the high affinity (E1) conformation and promotes its phosphorylation by ATP to form a high-energy phosphoenzyme intermediate. The pump relaxes to the low affinity E2P conformation with the release of the bound $Ca^{2+}$. The counter transport $H^{+}$ ion binds to the E2P, triggering its dephosphorylation. The E2 conformer relaxes to the E1 state with the release of the counter transport ion[57].

The partial reactions of the catalytic cycle of PMCA have been studied both in erythrocyte membranes as well as in PMCA protein purified from them[63,64]. The reaction cycle of PMCA can be reversed by phosphorylation with inorganic phosphate ($P_i$) to produce ATP[65]. The relative abundance of the two conformers of PMCA in the erythrocyte membranes has been determined by measuring the initial rate of phosphorylation, which is based on the hypothesis that only the E1 conformer catalyzes the phosphorylation by ATP. It was shown that in the absence of any ligands, PMCA exists mainly in the E2 conformation. $Ca^{2+}$ induces the E2 $\rightarrow$ E1 transition, which is accelerated by $Mg^{2+}$. $Ca^{2+}$ has been

shown to stabilize the E1 conformation of the pump[66]. Based on the kinetics of the enzyme phosphorylation, binding of $Ca^{2+}$ and ATP to E1 are not rate limiting[67]. However, the catalytic cycle of PMCA appears to be limited by the rate of dephosphorylation of the E2P and the E2→E1 transition. ATP at concentrations higher than that required for the phosphoenzyme formation, accelerates the dephosphorylation and the conversion of E2→ E1[68]. $Mg^{2+}$ dependent increase in the rate of dephosphorylation of the phosphoenzyme also requires the presence of high levels of ATP[69]. Consistent with its role as an intermediate in the reaction cycle, the formation of phosphoenzyme precedes the $P_i$ production in the ATPase activity of PMCA. The higher $Ca^{2+}$ dissociation constant of the phosphorylated PMCA as compared to the non-phosphorylated PMCA forms the basis of the mechanism coupling the catalysis and the $Ca^{2+}$ ion transport[63].

The Hill coefficients of 1 for the $[Ca^{2+}]_i$ and [ATP]-dependence of PMCA are consistent with a 1:1 stoichiometry, i.e. one $Ca^{2+}$ is translocated with hydrolysis of 1 molecule of ATP[1,40,70]. PMCA is suggested to operate as a $Ca^{2+}$: $H^+$ exchanger[1,41]. The $Ca^{2+}$: $H^+$ countertransport with net charge transfer has been demonstrated using PMCA protein purified from brain and reconstituted in liposomes[71]. However, similar studies with PMCA purified from erythrocytes showed an electroneutral exchange[72]. The coexistence of SERCA and PMCA that remove cytosolic $Ca^{2+}$, the transport channels that allow electrolyte leak in an intact cell, and the lack of specific inhibitors of PMCA has rendered it difficult to

directly characterize the electrogenic nature of the $Ca^{2+}$: $H^{+}$ exchange. Furthermore, there are inconsistencies in the results obtained by studies on the inside-out vesicles and the reconstituted proteoliposomes, where the presence of various detergents has different effects on the electrogenic properties of the $Ca^{2+}$ pump[41].

#### *1.2.1.2 Structural organization of PMCA*

The predicted amino acid sequences of P-type ATPases, domain organization of SERCA, hydropathy plots, and proteolytic digestion have been used to understand the membrane organization of PMCA[40-42,53]. Like other P-type ATPases, PMCA has 10 putative transmembrane (TM 1-10) spanning helices, with approximately 80% of the pump mass protruding into the cytosol. The TM domains of the $Ca^{2+}$ pump are connected on the extracellular side of the PM with very short loops called the extracellular domains (exdoms) (Fig. 1.2). The continuation of the polypeptide chain from the TM domains 1-5 projects into the cytosol as 'stalk' segments[41,42,53,73]. With both the N and C termini of PMCA being cytosolic, there are a total of 6 cytosolic domains[74]. In analogy to the structural features of SERCA obtained by X-ray crystallography, the cytosolic portion of PMCA protein can be divided into the following 3 main functional domains:

a). Actuator domain: This is a small cytosolic loop that connects the TM domains 2 and 3 and is proposed to couple the hydrolysis of ATP to the transport of $Ca^{2+}$.

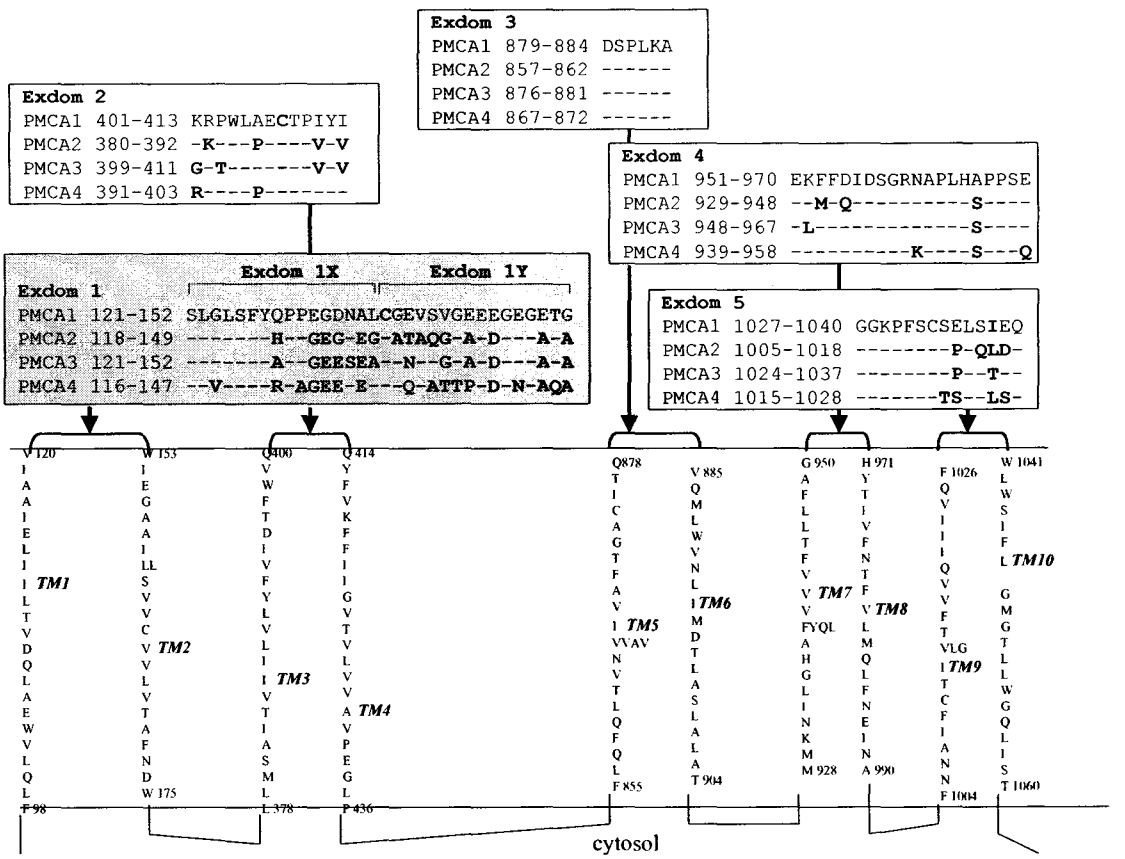


**Fig. 1.2. Extracellular domains (exdoms) in human PMCA1b protein.**

PMCA1b protein is based on sequence 20020 from Swiss Protein Bank. The exdoms will be used as targets to screen phage display (Ph.D) peptide libraries to obtain caloxins. Shown is the comparison of the exdom sequences between human PMCA isoforms 1-4. The exdom 1 sequence has cysteine (C) and is divided into exdom 1X and 1Y.

This domain contains a phospholipid responsive region, which is rich in basic amino acids and is involved in the regulation of PMCA by acidic phospholipids as described in *1.2.1.5*.

b). Catalytic domain: This is a large cytosolic loop connecting the TM domains 4 and 5 and contains both the 'N domain' (nucleotide binding site) and the 'P domain' (phosphoenzyme formation site). The ATP binding site in the N domain contains a sequence 'KGA' that is conserved in all P-type ATPases. Upstream of the N domain is the P-domain that contains the sequence 'CS**D**KTGTT', which is also conserved in all P-type ATPases. The aspartate (D) residue in the sequence forms the high-energy phosphoenzyme intermediate in the reaction cycle of PMCA. The P domain also contains a conserved sequence called the 'hinge' region, which is essential to bring the phosphorylation site close to the bound ATP during the reaction cycle of the ion pumping ATPases.

c). Regulatory domain: The last cytosolic unit that protrudes from the TM domain 10 is unique to PMCA and is involved in the multiplicity of its regulation due to the presence of calmodulin binding domain and consensus sequences for various protein kinases[39,42,73]. Calmodulin is the main regulator of PMCA (*1.2.1.5*). The calmodulin-binding domain of PMCA shares several structural features with other calmodulin binding proteins including: 1) predominance of lysine or arginine residues, 2) preponderance of hydrophobic residues in its N-terminal half and 3) presence of a conserved tryptophan[75]. The calmodulin-binding domain is flanked by two acidic domains, which are thought

to play a role in channeling $Ca^{2+}$ to its catalytic sites in the TM helices of PMCA[76].

In the unstimulated state, the regulatory domain of PMCA acts as an internal repressor leading to PMCA autoinhibition. The calmodulin binding domain and the region C-terminus to it is involved in PMCA autoinhibition and its cleavage by controlled proteolysis results in the production of a fully active pump[75]. Recent studies have provided evidence for the role of an aspartate residue upstream of the calmodulin-binding domain in stabilizing the autoinhibitory state of PMCA[77]. Thus, sequences both downstream and upstream of the calmodulin-binding domain are involved in PMCA autoinhibition. Crosslinking studies have shown that the N-terminus of the calmodulin-binding domain interacts with a region 70-amino acids downstream of the phosphoenzyme forming aspartyl residue in the catalytic domain, while its C-terminus interacts with the residues in the actuator domain of PMCA[78,79]. This autoinhibitory interaction may affect ATP binding, phosphorylation, access of $Ca^{2+}$ or the coupling of ATP hydrolysis to $Ca^{2+}$ transport in PMCA.

#### *1.2.1.3 PMCA isoforms*

The primary transcripts of the four PMCA genes can be alternatively spliced to increase the diversity of PMCA variants[48]. The primary transcripts contain two splice sites: splice site A in the actuator domain and splice site C in the C-terminal tail of PMCA. Of the large number of PMCA splice variants that are theoretically possible, over 20 have been detected at cDNA level[48]. The letters

(a,b,c,d) are used to describe the variants produced at splice site C while the letters at the end of the alphabet (w,x,y,z) designate the splices at site A. The alternative splicing at site A affects a small exon (36-42 bases) present in all four PMCA genes, which can be either inserted or excluded in the 'x' and 'z' splice variants, respectively. PMCA2 gene has in addition two more exons whose inclusion can produce the 'w' splice variant[48]. Since splice site A does not affect the regulatory domain of PMCA, earlier studies showed no functional differences among the splice A variants[80]. However, recent studies have shown a role for splice site A in the apical membrane targeting of PMCA2 in the polarized cells, regardless of the splicing pattern at site C[81,82]. The 'w' splice variant of PMCA2 is exclusively localized in the hair bundles of the vestibular auditory hair cells and in the apical membrane of epithelial cells in lactating mammary glands[82,83].

PMCA1 and 4 genes have a single large exon at splice site C, while PMCA2 and 3 contain an additional small exon. These exon(s) have multiple internal donor sites, which result in large number of possible splice variants. The insertion and exclusion of the alternatively spliced large exon in all PMCA genes results in the splice variants 'a' and 'b', respectively. The insertion of the large exon in the 'a' variant causes a shift in the reading frame leading to a stop codon, so that PMCAa variants are shorter than PMCAb variants. Due to the presence of splice site C in the middle of calmodulin-binding domain, only the N-terminal half of the domain is conserved in all PMCA isoforms. The alternative splicing at site C changes the C-terminal half of the calmodulin binding domain and the

region downstream from it[34,48]. Thus, site C splice variants of PMCA differ in their regulation by calmodulin and protein kinases. Since calmodulin is the major regulator of PMCA function, these differences in the regulation of PMCA variants by calmodulin are described in detail in *1.2.1.5.*

The last four C-terminal amino acids of the 'b' splice variants of PMCA conform to the minimal consensus sequence for binding to the PDZ domain of the proteins[34,48,84]. The PDZ domains are protein-protein interaction domains recognizing the C-terminal residues of their target proteins[48,85]. PMCA 'b' variants exhibit differential targeting to the PM domains and assemble into multiprotein complexes by interacting with other protein partners having the PDZ domains[48,84]. For example, interaction with PDZ domain containing $Ca^{2+}$/calmodulin dependent kinase may serve to cluster PMCA4b in the signaling complex in the presynaptic nerve terminals[86]. Different PMCA 'b' variants may interact with different PDZ proteins. For example, PMCA2b and not PMCA4b interacts with the $Na^{+}/H^{+}$ exchanger regulatory factor 2. This interaction is thought to be involved in the apical membrane targeting of PMCA2b[87]. The splicing at sites A or C however, does not affect the exdoms of PMCA[74].

### *1.2.1.4 Tissue distribution of PMCA isoforms*

The distribution of PMCA isoforms has been studied at both the mRNA and protein level[47,88]. PMCA isoforms show developmental, tissue and cell-specific patterns of expression. *In situ* hybridization studies on the developing mouse embryos showed that only PMCA isoform 1x/b was detected throughout

the embryo from the earliest time point analyzed (9.5 days post coitum)[48,84,89]. All other PMCA isoforms were detected from 12.5 day onwards. PMCA2 was confined mainly to the central nervous system through out the development. PMCA3, which is found mainly in the nervous system in the adult, was expressed widely during early days of development. PMCA4 showed lower expression than the other isoforms[89].

PMCA isoforms 1 and 4 have ubiquitous tissue distribution while PMCA2 and 3 are expressed almost exclusively in the brain and the striated muscle in the adult[47,48,88]. Some variants of PMCA2 are also found in the cardiac muscle in the adult[48]. Brain expresses all four PMCA isoforms in the highest amounts but shows differences in the regional distribution of individual PMCA isoforms and their splice variants[90,91]. Tissues with a wide diversity of cell types like the pancreas show cell specific expression of PMCA variants[92]. The beta cells of the pancreas express only PMCA4b, while the alpha and the gamma cells express both PMCA4a and 4b. The islets of Langerhans express only the 'b' variant of PMCA1 and 2[92]. Certain splice variants of PMCA are expressed in select cell types like PMCA2w/a, which is found only in the hair cells of the inner ear[48,82,84].

Although PMCA isoforms and their splice variants exhibit differential expression patterns, the mechanisms regulating their expression are not well understood. $Ca^{2+}$ has been shown to regulate the expression of genes involved in its homeostasis. Alteration of $Ca^{2+}$ homeostasis by inhibition of SERCA in cultured rat aortic endothelial cells increased the mRNA expression for both

PMCA and SERCA[93]. Another study showed $Ca^{2+}$ dependent regulation of the expression of PMCA isoforms and splice variants during the maturation of the rat cerebellar granule cells in culture. In these cells, the expressions of PMCA1a, 2 and 3 were increased both at the mRNA and protein level, while that of PMCA4a was down regulated during maturation under depolarizing conditions[94]. The down regulation of PMCA4a in cerebellar granule cells was mediated by changes in the activity of calcineurin, a $Ca^{2+}$/calmodulin sensitive phosphatase[95]. The alternative splicing in PMCA is also regulated in differentiation specific manner. For example, the undifferentiated L6 and H9c2(2-1) myoblasts, which express ubiquitous PMCA1b and 4b, were induced to express muscle specific variants PMCA1c, 1d and 4a upon myogenic differentiation. This differentiation specific switch was under the control of myogenic determination factor, myogenin. Fibroblasts, which express PMCA1b and 4b, could be induced to express muscle specific PMCA variants by constitutive expression of myogenin[96]. Similarly, neuronal differentiating factor could induce transformation of the pheochromocytoma (PC-12) cells into a neuronal phenotype, accompanied with an increase in the expression of neuronal specific PMCA variants[96,97]. However, the exact mechanism involved in mediating the switch in the expression of PMCA splice variants upon differentiation is not known.

#### *1.2.1.5 Regulation of PMCA*

The important property of PMCA that sets it apart from the other members of P-type ATPases is the presence of multiple regulatory sites in its long C-

terminal tail. The following sections briefly describe the role of calmodulin, protein kinases and phospholipids in the regulation of the $Ca^{2+}$ pump.

#### *1.2.1.5.1 Regulation by calmodulin*

Calmodulin is an acidic $Ca^{2+}$-binding protein that regulates PMCA by direct interaction[98,99]. The binding of calmodulin dissociates the autoinhibitory C-terminal domain to free the active site of PMCA resulting in an increase in both the $Ca^{2+}$ affinity of the pump and the rate of ion transport[49,73]. Calmodulin has 4 binding sites for $Ca^{2+}$ ($K_d$: 0.5-5 μM) and thus, PMCA activation by calmodulin is dependent on $[Ca^{2+}]_i$ concentration and exhibits positive cooperativity[100]. A two state model has been used to explain the calmodulin binding and activation of PMCA. According to the model, the pump exists in an inactive state with a non-dissociated autoinhibitory domain in the absence of calmodulin and in an active state with the dissociated autoinhibitory domain upon binding of calmodulin. However, recent studies with a single molecule polarization method using fluorescently labeled calmodulin have suggested that PMCA can exist in a third state. The third state of PMCA is the inactive state that exists under low $[Ca^{2+}]_i$ conditions in which calmodulin is bound to PMCA without the dissociation of the autoinhibitory domain[101]. Such a state may arise if only one of the two domains of calmodulin bind to PMCA or if calmodulin binds in a configuration that fails to dissociate the autoinhibitory domain. The existence of this third state with calmodulin bound to PMCA provides a mechanism for the rapid response of the pump to the subsequent $Ca^{2+}$ signaling events in the cell[102].

The effect of alternative splicing at site C, which affects the calmodulin-binding domain has been studied in more detail in PMCA isoforms 4a and 4b. Studies with the overexpressed variants showed that PMCA4a is less responsive to calmodulin, requiring about 7 fold higher concentration for half maximal activation as compared to PMCA4b. The lower calmodulin affinity of PMCA4a also decreases its $Ca^{2+}$sensitivity[103]. As compared to PMCA4b, the 4a variant has higher basal activity at any given concentration of $Ca^{2+}$ in the absence of calmodulin[104]. The contribution of the C-terminal residues to these differences in calmodulin regulation was confirmed experimentally by overexpressing PMCA4a mutants carrying different portions of its C-terminus[103,104]. In PMCA4a, the calmodulin-binding domain is long (49-amino acids) and contains within it the residues involved in pump autoinhibition. However, the 49-amino acid long domain is interrupted by a region, which is not involved in binding to calmodulin and may thus account for the lower calmodulin affinity and the less effective autoinhibition leading to its higher basal activity. In contrast, PMCA4b has a short contiguous calmodulin-binding domain (28-amino acids), which along with additional downstream residues is involved in pump autoinhibition[104]. This C-terminal structure of PMCA4b may be responsible for the observed high affinity for calmodulin and the more effective pump autoinhibition[103,104]. PMCA4b variant with its lower basal activity is expected to respond slowly to the increase in $[Ca^{2+}]_i$ and may be appropriately expressed in cells like erythrocytes that exhibit slower $Ca^{2+}$ decay (20-100 s)[105,106]. In contrast, PMCA4a with its lower

$Ca^{2+}$ sensitivity is found in tissues like brain and heart that experience large increases in $Ca^{2+}$[103-105]. The lower calmodulin affinity of PMCA4a than 4b may be a pattern followed by the 'a' and 'b' variants of all PMCA isoforms, as has been observed for PMCA2a and 2b[104,107].

Beyond the affinity of calmodulin for the $Ca^{2+}$ pump, its rate of binding and dissociation are also very important in determining the biological properties of PMCA. The differences in the rates of activation and inactivation of PMCA variants would lead to differences in their ability to respond to a sudden increase in $[Ca^{2+}]_i$ and in decoding the frequency of the repetitive $Ca^{2+}$ spikes[84]. Although PMCA4a has lower affinity for calmodulin, its rate of activation by calmodulin is faster ($t_{1/2}$ ~20 s) than that of PMCA4b ($t_{1/2}$ ~1 min). It also has a faster rate of inactivation ($t_{1/2}$ <1 min) by calmodulin removal as compared to PMCA4b ($t_{1/2}$ ~20 min)[105]. The two PMCA4 variants also differ in $[Ca^{2+}]_i$ dependence of their rate of inactivation by calmodulin removal. A given increase in $[Ca^{2+}]_i$ caused a 30-fold decrease in the rate of inactivation of PMCA4b as compared to a two-fold decrease in PMCA4a[108]. This suggests that $Ca^{2+}$ stabilizes the complex between calmodulin and PMCA4b in a much tighter manner than between calmodulin and PMCA4a, which is in line with the slower calmodulin off rate of PMCA4b. Fluorescently labeled calmodulin has been used to study the rate of calmodulin binding to PMCA4a and 4b. Both the N and C terminal lobes of calmodulin bound sequentially to PMCA4b, whereas calmodulin bound to PMCA4a through only one of its lobes, thereby allowing for its rapid rate of association and

dissociation[108,109]. Due to its higher rate of activation and inactivation by calmodulin, PMCA4a can thus react faster to $Ca^{2+}$ signals in the rapidly responding cells like nerves and muscles[105].

The calmodulin affinity of other PMCA isoforms has also been examined. PMCA2b has a 5-10 fold higher affinity for calmodulin than PMCA4b, while PMCA1b has similar calmodulin dependence as PMCA4b[80,107,110]. PMCA2b exhibits a fast rate of activation and a slow rate of inactivation by calmodulin, which may allow it to respond to $Ca^{2+}$ fluctuations in a cell in an integrative way[102]. Based on this property, a model has been proposed for the retention of the memory of recent activation of the $Ca^{2+}$ pump. According to the model, in the cells with repetitive $Ca^{2+}$ spikes, PMCA2b will remain preactivated and react faster to a new $Ca^{2+}$ signal. This may be important in PMCA2b expressing cells like neurons to maintain sensitivity to the signal frequency. PMCA3f has an unusual structure with a very short C-terminus and a high constitutive activity, which is only weakly stimulated by calmodulin[111]. A kinetic study revealed that the fast acting PMCA variants (3f, 2a) that are immediately activated by $Ca^{2+}$ are expressed in heart and skeletal muscle, in which the $Ca^{2+}$ signal decays rapidly (10-100 ms)[106]. Thus, the differences in the regulatory kinetics of different PMCA variants may be essential to meet $Ca^{2+}$ needs of different cell types[15]. However, studies using knockout mice are inconsistent with these conclusions since mice lacking PMCA2 do not show major cardiac or neuronal phenotypic defects (see 1.4).

### *1.2.1.5.2 Regulation by protein kinases*

The C-terminal domain of PMCA contains a high percentage of serine and threonine residues (17-31%) depending on the isoform. These residues are the targets of various kinases[39].

*Cyclic AMP dependent protein kinase (PKA):* PKA phosphorylates the serine residue in the sequence KRNSS which appears to fit with the PKA consensus sequence. This sequence is found only in PMCA 1b-d variants[50]. The PKA mediated phosphorylation of PMCA increases its affinity for calmodulin[112]. The phosphorylation increases the affinity of the pump for $Ca^{2+}$ and causes a two-fold increase in its maximum velocity. The stimulation of the $Ca^{2+}$ pump by calmodulin and PKA is non-additive[28,49]. Studies on the parotid acinar cells showed that PMCA is the target of cross talk between cAMP levels and $[Ca^{2+}]_i$. The agonists that increased the cAMP levels in the parotid acinar cells caused phosphorylation of PMCA and increased its sensitivity for $[Ca^{2+}]_i$. The PKA mediated modulation of PMCA activity was dependent on the agonist-evoked elevation of $[Ca^{2+}]_i$[113]. Although the parotid acinar cells express PMCA isoforms 1, 2 and 4, it was only PMCA1 that was phosphorylated. Furthermore, despite being expressed in all regions of the membrane, the apical PMCA1 was differentially regulated by PKA. Thus, PKA mediated increase in PMCA activity may shape the temporal kinetics of the $Ca^{2+}$signal, while the differential regulation of the apical PMCA by PKA may contribute to the spatial shaping of the signal[114].

*Cyclic GMP dependent protein kinase (G kinase):* G-kinase increases the maximum velocity and $Ca^{2+}$ affinity of the pump. To study the effect of cGMP-dependent regulation of PMCA, agents such as atrial natriuretic factor and sodium nitroprusside were used to increase the intracellular levels of cGMP in cultured vascular smooth muscle cells. The increase in cGMP levels within the vascular smooth muscle cells leads to relaxation. The treated cells showed an increase in PMCA mediated $Ca^{2+}$ efflux, which was faster than in the untreated cells at 0.1 μM $[Ca^{2+}]_i$, which is the threshold level for contraction[115]. The exact mechanism of cGMP dependent activation of PMCA is not known. Using PMCA protein purified from the smooth muscle of pig stomach and aorta, it was shown that cGMP dependent protein kinase may stimulate PMCA activity indirectly by phosphorylation of an associated phosphatidylinositol kinase, which in turn can phosphorylate phosphatidylinositol, which is a pump activator[116].

*Protein kinase C (PKC):* PKC increases the maximum velocity of PMCA. The individual PMCA isoforms show significant differences in their regulation by PKC[39]. The activation of PMCA4b by PKC has been shown both *in vivo* and *in vitro*[117,118]. The degree of phosphorylation and activation by PKC of PMCA4b constructs lacking various numbers of the C-terminus residues identified the phosphorylation site to lie in a region about 20 residues downstream of the calmodulin binding domain[117]. The activation of PMCA4b due to phosphorylation and calmodulin is non-additive. The phosphorylation is thought to relieve the partial inhibition due to the region downstream of the calmodulin-binding

domain[39,117]. This may allow for a graded activation of the $Ca^{2+}$ pump activity in a cell where the pump is partially stimulated by phosphorylation, followed by its complete activation by calmodulin[50]. In the absence of calmodulin, the splice variant 'a' of both PMCA2 and PMCA3 are phosphorylated by PKC without any effect on their activities. However, the phosphorylation prevents their stimulation by calmodulin, which can no longer bind to the pump[119]. PMCA2b splice variant is weakly phosphorylated by PKC, which does not phosphorylate PMCA3b variant[25,119]. Phosphorylation of other isoforms like PMCA4a is without any effect on its basal activity or calmodulin stimulation[120]. Thus different isoforms and variants of PMCA are regulated differently by various kinases and may be important to the unique $Ca^{2+}$homeostasis demands of the cell types expressing them.

#### *1.2.1.5.3 Regulation by acidic phospholipids*

The initial studies on the effects of phospholipids on PMCA activity were conducted in erythrocytes. The hydrolysis of phospholipids in the outer membrane leaflet of intact erythrocytes did not affect the $Ca^{2+}$-$Mg^{2+}$ ATPase activity of PMCA. However, treatment of leaky erythrocyte ghosts with phospholipases that degrade glycerophospholipids led to the inactivation of $Ca^{2+}$ pump[121]. The effect of phospholipids on PMCA activity was also studied on the purified PMCA reconstituted into liposomes of the specified phospholipid composition[40,99]. In general, the acidic phospholipids such as phosphatidylserine, phosphatidylinositol, phosphatidic acid and cardiolipin stimulate the pump by

increasing both its affinity for $Ca^{2+}$ and turnover rate[122,123]. They are more effective as activators as compared to calmodulin as they do not require $Ca^{2+}$ [123]. The neutral phospholipids and sphingomyelins are without any effect. Phosphatidylinositol 4,5 bisphosphate (PIP2) is one of the most potent stimulator of the pump and may keep PMCA partially active in the resting cells[124]. PIP2 can be phosphorylated or dephosphorylated and its phosphorylated derivatives are effective pump activators[73]. The turnover rate of these phospholipids is rapid and their breakdown products are not stimulatory[41,49,73]. Agonist mediated stimulation of phospholipase C (PLC) degrades PIP2 into diacylglycerol and 1,4,5-inositol trisphosphate ($IP_3$), thereby decreasing PMCA activity. A model has been presented in which PMCA co-localized in caveolae can share the common pool of PIP2 with PLC leading to its modulation by changes in the lipid composition of the membrane[41,49]. Although the exact mechanism of activation of PMCA by acidic phospholipids is not known, they have been shown to accelerate the dephosphorylation of the pump during its catalytic cycle[68].

The stimulation by phospholipids is partly based on their binding to $Ca^{2+}$ pump, which may occur through their polar head groups. Two regions in PMCA molecule have been identified to mediate the binding of acidic phospholipids[125]. One of the regions is found upstream of the third TM domain whose deletion results in a fully active PMCA with high affinity for $Ca^{2+}$, a characteristic of the pump activated by acidic phospholipids[126]. The second region involved in binding to phospholipids lies within the calmodulin-binding domain of PMCA[125]. The

regulation of PMCA by phospholipids is physiologically important since the concentration of acidic phospholipids in the membrane may be sufficient for half-maximal activation of the pump[40].

Thus, the combination of large diversity of PMCA variants and the multiplicity of their regulation provides functional versatility to fulfill tissue and cell specific roles in $Ca^{2+}$ handling.

#### *1.2.1.6 Potential role of PMCA*

Of the two $Ca^{2+}$ extrusion systems found in the PM, PMCA has higher affinity for $Ca^{2+}$ ($K_d$ ~0.2-0.5 μM) than NCX ($K_d$ ~1-10 μM)[4,28,127]. The extrusion of $Ca^{2+}$ in exchange for $Na^+$ depends on the electrochemical gradient of $Na^+$ that is maintained by the $Na^+$-$K^+$ ATPase. Thus, the $Na^+$ dependent $Ca^{2+}$ extrusion is limited by the activity of the $Na^+$-$K^+$ ATPase. Unlike PMCA that only extrudes $Ca^{2+}$, NCX can also facilitate $Ca^{2+}$entry depending on the electrochemical gradients of $Na^+$ and $Ca^{2+}$ [28,35]. Due to its high capacity, NCX may remove part of the excess $[Ca^{2+}]_i$ following stimulation of the cell, while PMCA may be responsible for the fine-tuning of $[Ca^{2+}]_i$ levels at all times[4,28]. The homeostatic role of PMCA was shown in neurons from the rat superior cervical ganglion, where its inhibition led to elevation of resting $[Ca^{2+}]_i$[127]. The exact roles of PMCA and NCX would also depend on their relative abundance and regulation in a tissue dependent manner[4]. In those cells, which lack NCX, PMCA is the only $Ca^{2+}$ extruding mechanism present e.g. in mature erythrocytes, hair bundles of the hair cells in the inner ear, Jurkat T cells and pancreatic acinar cells[39,82,114,130].

As compared to the internal SERCA pump, PMCA has a higher affinity for the substrate $MgATP^{2-}$ and the $Ca^{2+}$concentration dependence curve of PMCA fits well with a Hill coefficient of 1 versus 2 for SERCA[70]. Unlike SERCA activity, which decreases sharply with a change in pH, PMCA exhibits a much broader pH profile[70]. Also, SERCA is more susceptible to inactivation by reactive oxygen species than PMCA[128]. Based on these differences in the two $Ca^{2+}$pumps, PMCA may be active under conditions of low $[Ca^{2+}]_i$ and ATP when SERCA is inactive. The removal of $[Ca^{2+}]_i$ by SERCA is also limited by the $Ca^{2+}$ carrying capacity of the organelles that express them. Thus, due to the high affinity and ubiquitous expression, PMCA may play an important role in the long-term homeostasis of low $[Ca^{2+}]_i$[129].

In addition to their homeostatic role, PMCA have been shown to contribute to the generation and shaping of intracellular $Ca^{2+}$ signals. The contribution of PMCA to the intracellular $Ca^{2+}$ spikes has been easily demonstrated in human erythrocytes that lack SER and NCX. The stimulation of resealed human erythrocyte ghosts with $Ca^{2+}$ ionophore resulted in a $Ca^{2+}$ spike followed by a lower steady state level of $[Ca^{2+}]_i$. The delayed calmodulin activation of PMCA4b was responsible for the formation of a $Ca^{2+}$ spike, which was abolished in ghosts lacking calmodulin or containing the fully active PMCA made calmodulin insensitive by trypsin treatment[131]. Studies in the Jurkat human T cells that lack NCX provided the first evidence that due to a biphasic increase in its activity, PMCA increases the dynamics and stability of the $Ca^{2+}$ signals.

Following a rise in $[Ca^{2+}]_i$ in these cells, PMCA activity increased rapidly by direct binding of $Ca^{2+}$, followed by a slow $Ca^{2+}$ dependent modulation of PMCA, that further increased its $Ca^{2+}$senstivity and extrusion rate. The slow modulation of PMCA that could result from the binding of calmodulin persisted for several minutes after $[Ca^{2+}]_i$ had returned to basal levels. Thus, the rapid PMCA activation stabilizes $Ca^{2+}$ signals by matching the rate of $Ca^{2+}$ extrusion to $Ca^{2+}$ influx, while the slow onset of modulation and recovery after return of $[Ca^{2+}]_i$ to basal levels contributes to the magnitude and duration of the $Ca^{2+}$ spike[130]. The role of PMCA in shaping intracellular $Ca^{2+}$ signals has also been demonstrated in cells expressing NCX. PMCA played a prominent role in contributing to $Ca^{2+}$ signals evoked by capacitative $Ca^{2+}$ entry, while protecting against $Ca^{2+}$ overload in endothelial cells that express NCX[132].

NCX, which is abundant in excitable tissues is thought to play a major role in regulating $[Ca^{2+}]_i$. However, PMCA was shown to be the primary $Ca^{2+}$ extrusion system following a brief low-frequency activity in neurons, with no contribution from NCX or SERCA[127,133]. Immunocytochemistry showed that in astrocytes and neuronal somata, NCX is confined to the PM microdomains that overlie the sub-plasma membrane junctional SER. In contrast, PMCA protein had a more uniform distribution and may thus be involved in the regulation of bulk $[Ca^{2+}]_i$ while NCX may regulate the $Ca^{2+}$ sequestered in the junctional SER[134]. In the presynaptic nerve terminals, only PMCA is clustered at the active zones to maintain low $[Ca^{2+}]_i$ and 'reprime' the vesicular release mechanism[134]. The

importance of PMCA in neuronal function has also been confirmed by the studies in mice deficient in PMCA2 isoform, which led to the loss of hearing and balance[7].

PMCA appears to play an important role in the transcellular movement of $Ca^{2+}$ by the epithelia. In the epithelium of intestine and kidney, PMCA is localized in the basolateral membrane, the side towards which $Ca^{2+}$ is being moved after absorption[84]. On the other hand, PMCA2 has been shown to be expressed apically in the mammary epithelial cells where it is involved in secretion of $Ca^{2+}$into milk[83].

Recent studies based on two hybrid screens have identified numerous PMCA interacting proteins that may be involved in connecting PMCA to various signaling pathways in the cell[84,135]. The 'b' splice variants of PMCA contain a consensus sequence E-T/S-X-L/V in their C -terminus for interacting with many proteins with PDZ domain[48,136]. Various PDZ proteins serve as scaffolds for the assembly of multiprotein complexes that may be localized in caveolae, which are membrane structures important for signal transduction[48,85]. PMCA4b has been shown to interact with PDZ domain of neuronal nitric oxide synthase (nNOS) in caveolae and regulate its activity[137,138]. nNOS produces nitric oxide which is a major messenger molecule controlling diverse functions in the body including vascular relaxation[139]. This suggests that PMCA is a dynamic regulator of cellular $Ca^{2+}$ and may be locally regulated by various interacting protein partners.

However, the physiological effect of such protein interactions still needs to be determined in the native cellular environment of PMCA.

PMCA may be pivotal in the maintenance of low $[Ca^{2+}]_i$ during homeostasis in most tissues and also participate in additional roles in others. These additional roles may be in cell signaling, anchoring and transcellular $Ca^{2+}$ movements. The exact physiology of PMCA is thus tissue dependent.

### 1.2.2 $Ca^{2+}$ pumps of the intracellular organelles

SERCA use the energy of ATP hydrolysis to pump $Ca^{2+}$ from the cytosol into the SER lumen, which serves as an intracellular $Ca^{2+}$ storage organelle[32]. There are 3 genes that encode SERCA proteins in the mammals, which exhibit differential tissue expression[140]. SERCA1 isoform represents bulk of the SER protein in the fast twitch skeletal muscle and is the best-studied isoform in terms of its structure and function[32]. It consists of a single polypeptide chain of 110 kDa, which is arranged into 10 TM domains with a large part of the pump being cytosolic. The structure and membrane topology of SERCA1 has been confirmed by X ray crystallography[58]. SERCA has two $Ca^{2+}$ binding sites and transports two $Ca^{2+}$ ions for each molecule of ATP hydrolyzed. Recent studies on the crystals of SERCA have revealed the structural basis of the transport of the occluded $Ca^{2+}$ ions from the cytosol to the lumen of the SER vesicles. The ion transport process is achieved by altering the affinity and accessibility of the ion binding sites in the E1 and E2 conformations of the pump. SERCA in its E1 form binds two $Ca^{2+}$ ions ($2Ca^{2+}$• E1) with high affinity and forms acylphosphate using ATP, producing a

transition state with a high-energy aspartyl-phosphoanhydride bond with a conserved aspartate residue in its catalytic domain ($2Ca^{2+}$• E1~P). The transition state with occluded $Ca^{2+}$ ions is converted to low affinity E2P form. This transition is accompanied with the translocation of $Ca^{2+}$ ions due to the conformational change that opens a luminal exit pathway by separation of the TM domains 1 through 6. The partial neutralization of the charge of the luminally exposed cation-binding sites by protons in the E2P form is accompanied by the closure of the TM domains that leads the enzyme to the E2-P* transition state with occluded protons. The E2-P* state is dephosphorylated to E2 with the cytoplasmic pathway opening for the exchange of protons with $Ca^{2+}$ ions to complete the reaction cycle[57]. The $Ca^{2+}$ transport by SERCA is associated with pronounced conformational changes that can be transferred to all P-type ATPases[62]. Although SERCA belongs to the same family of P-type ATPases like PMCA and the more closely related SPCA, functionally, it can be easily distinguished due to its highly selective inhibitors such as thapsigargin and cyclopiazonic acid[28,32].

A secretory pathway $Ca^{2+}$ ATPase (SPCA) has been found in the Golgi complex of the cells. SPCA proteins share similarities with SERCA[30,32]. They are also a single subunit integral membrane protein with 10 TM domains and a large mass protruding into the cytosol. Unlike SERCA, SPCA contains only one $Ca^{2+}$ binding site, transporting one $Ca^{2+}$ for each ATP hydrolyzed. In addition to transporting $Ca^{2+}$, they also transport $Mn^{2+}$ with similar affinity. The Golgi

complex, like the SER influences the shape of the cytosolic $Ca^{+}$ transients. The expression of SPCA is upregulated in the lactating mammary gland and is thought to play an important role in the secretion of $Ca^{2+}$ into milk[83].

### 1.2.3 Other ion transporters in the PM

NCX is a $Ca^{2+}$extruding mechanism present in the PM. It has a low affinity for $Ca^{2+}$ but it may have a high transport capacity in some tissues. It exchanges 3 $Na^{+}$ for 1 $Ca^{2+}$ and is thus electrogenic. Unlike PMCA, NCX is non-vectorial and depending on the electrochemical gradients of $Na^{+}$ and $Ca^{2+}$, NCX can operate in $Ca^{2+}$ extrusion (forward) and $Ca^{2+}$ entry (reverse) modes[35]. There are three genes of NCX, of which NCX1 is most widely distributed. NCX1 shows high level of expression in heart, brain and kidney[16]. NCX1 contains several cryptic exons, which encode proteins containing 920-1000 amino acids. NCX1 is thought to contain 9 TM domains with a large cytosolic loop. The counter transport function of the exchanger is associated with the TM segments, while the intracellular loop is involved in its modulation by kinases, intracellular $Na^{+}$ and $Ca^{2+}$, and by the presence of an autoinhibitory exchange inhibitory protein (XIP) domain. There are two conserved regions in NCX, $\alpha 1$ and $\alpha 2$, which are responsible for binding and transporting ions. Due to its low affinity for $Ca^{2+}$, NCX operates only when $[Ca^{2+}]_i$ in its environment increases to micromolar levels[16,34,35].

Another type of exchanger found in the PM of mainly retina and brain is NCKX. NCKX co-transports $Ca^{2+}$ and $K^{+}$ in exchange for 4 $Na^{+}$. NCKX has

higher affinity for $Ca^{2+}$ as compared to NCX. Although NCKX shares low sequence homology, its suggested membrane topology is similar to that of NCX[34]. Five genes encoding NCKX have been cloned. The NCKX can mediate forward and reverse exchange of $Ca^{2+}$ and $K^+$ for $Na^+$ [34,36].

Mitochondria also plays a role in transporting cytosolic $Ca^{2+}$ by means of a low affinity, high-speed electrophoretic uniporter that is located in its inner membrane. The uniporter is coupled to oxidative phosphorylation, and uses the electropotential gradient across the inner mitochondrial membrane to drive $Ca^{2+}$ into the mitochondrion[19,37]. The mitochondrial uniporter has recently been identified as a $Ca^{2+}$selective ion channel, whose activity is regulated by $Ca^{2+}$itself[38]. The *in vitro* affinity of the uniporter for $Ca^{2+}$ ($K_d$: 10-20 μM) is low in comparison to the cytosolic $Ca^{2+}$ concentration found *in vivo* during physiological processes (0.01–2 μM). However, the close proximity of the mitochondria to the $Ca^{2+}$ release sites from the intracellular stores or $Ca^{2+}$ influx channels in the PM may create microdomains of high $Ca^{2+}$ concentration that is transported by mitochondria[19,37].

### 1.2.4 $Ca^{2+}$ binding proteins

$Ca^{2+}$ binding proteins in the cell cytosol are able to complex $Ca^{2+}$ with high affinity and specificity required for the regulation of its concentration in the cell. The most important and the best-understood class of $Ca^{2+}$ binding proteins belong to the family of EF hand proteins, which contain a helix-loop-helix $Ca^{2+}$ binding motif. The helix-loop-helix motif (EF hand $Ca^{2+}$ binding motif) consists

of two roughly orthogonal helices of about 10 amino acids, which flank a 12 amino acid loop involved in binding to $Ca^{2+}$ [16]. There are hundreds of members of the EF hand family, which differ in the organization of the EF hand motifs, kinetic properties and the expression patterns. The EF hand proteins may function as $Ca^{2+}$ buffers by protecting the cell against the increase in $[Ca^{2+}]_i$ and/or as $Ca^{2+}$ sensors as part of the $Ca^{2+}$ regulated pathway. Parvalbumin, calbindin-D28k, calbindin-D9k and calretinin are low molecular weight proteins that act as $Ca^{2+}$ buffers, and also limit the spatial spread of $Ca^{2+}$. Both calbindin-D28k and calbindin-D9k are regulated by vitamin D and are found in major $Ca^{2+}$transporting sites as intestine and kidney, respectively. $Ca^{2+}$ binding proteins like calmodulin, Troponin C, members of S100 proteins and neuronal $Ca^{2+}$ sensor proteins serve as $Ca^{2+}$ sensors while also buffering $Ca^{2+}$ [15,16,19,20].

The most studied $Ca^{2+}$ binding protein is calmodulin, which contains four $Ca^{2+}$ binding sites. These sites are arranged in pairs to form globular N- and C-terminal lobes connected by a long flexible central helix, conferring a dumbbell shaped appearance to the protein. The pair arrangement of the binding sites increases the affinity and cooperativity of the $Ca^{2+}$ binding sites of the calmodulin. In addition to buffering $Ca^{2+}$, calmodulin can decode $Ca^{2+}$ signal and transfer its information to the target proteins. The mechanism of the decoding process has been well studied in calmodulin, which undergoes conformational changes upon binding of $Ca^{2+}$ [16,27].

In addition to the cytosol, $Ca^{2+}$ binding proteins are also found in the SER lumen. A number of different acidic $Ca^{2+}$ binding proteins in the lumen of SER participate in buffering and storing $Ca^{2+}$ [141]. They are usually low affinity and high capacity proteins. Calsequestrin was the first such protein to be identified in the lumen of SER that can bind ~40 mol $Ca^{2+}$/mol protein[141]. A similar protein, calreticulin is found in many non-muscle cells. Other ubiquitous lumenal proteins include BiP, endoplasmin and calnexin all of which bind $Ca^{2+}$ with low affinity[26]. In addition to buffering $Ca^{2+}$, the $Ca^{2+}$ binding proteins in the SER lumen may also be involved in protein folding and post translational modifications[26,141].

The total soluble $Ca^{2+}$ binding proteins are present in the cell in finite amounts and may not be adequate to buffer the large $[Ca^{2+}]_i$ changes that occur in response to the physiological stimuli. Such quantitative limitations however, do not apply to the membrane bound proteins that can continually transport $Ca^{2+}$ across the membranes, thereby controlling and maintaining the resting $[Ca^{2+}]_i$.

## 1.3 Mechanisms of $Ca^{2+}$ elevation in the cytosol

Elevation of $[Ca^{2+}]_i$ is important in signaling pathways that regulate several functions of the cell. The increase in $[Ca^{2+}]_i$ can result either by influx from the extracellular fluid due to the large electrochemical gradient of $Ca^{2+}$ or by recruitment from the intracellular $Ca^{2+}$ pool in the SER as described below.

### 1.3.1 $Ca^{2+}$ entry channels

There are two main types of $Ca^{2+}$ entry channels found in the PM: voltage operated $Ca^{2+}$ channels (VOCCs) and non-voltage gated $Ca^{2+}$ channels. VOCCs

are found mainly in the excitable cells like muscle and neuronal cells, where they mediate $Ca^{2+}$ influx in response to membrane depolarization. VOCCs are classified as the high voltage activated channels (L, N, P/Q, R type) and the low voltage activated channels (T type). The former require strong depolarization, while the latter require weak depolarization for their activation. VOCCs play an important role in normal cell activation and their altered expression is implicated in various diseases including congestive heart failure[5,18,22,142].

There are two major subtypes of non-voltage gated $Ca^{2+}$ channels: receptor operated $Ca^{2+}$ channels (ROCCs), which are activated by second messengers generated by receptor activation and store operated $Ca^{2+}$ channels (SOCCs) that are activated in response to depletion of the intracellular $Ca^{2+}$ stores in the SER. ROCCs are non-specific cation channels with some degree of divalent specificity. They are particularly abundant in secretory cells and nerve terminals. They open as a result of binding of an agonist to a receptor, which is separate from the channel protein and may involve intracellular second messengers. The transient receptor potential (TRP) channels can form $Ca^{2+}$permeable channels and may function as ROCCs. The tetramers of TRP proteins forming the $Ca^{2+}$permeable channels activated downstream of the G-protein coupled receptor/ phospholipase C signaling pathway belong to the TRPC subfamily of the TRP genes[18,22,143].

SOCCs open in response to the depletion of SER $Ca^{2+}$ stores by a physiological $Ca^{2+}$ mobilizing messenger or pharmacological agents as

thapsigargin. SOCCs carry a highly selective $Ca^{2+}$ current that is called $Ca^{2+}$ release activated $Ca^{2+}$ current ($I_{CRAC}$). Although biophysically distinct SOCCs have been reported in different cell types, $I_{CRAC}$ is the best characterized and most widely distributed. A single gene identified to be crucial for $I_{CRAC}$ was named CRACM1 (CRAC modulator). CRACM1 encodes a small protein (32.7 kDa) with four predicted transmembrane domains whose multimers form the pore of SOCC responsible for $I_{CRAC}$. Stromal interaction protein, STIM 1, a single spanning transmembrane protein found in the SER may act as a $Ca^{2+}$ sensor, coupling the process of store depletion with $Ca^{2+}$ influx. However, the mechanism of communication between STIM 1 and CRACM1 is not known. Numerous models have been proposed to explain their action. These models are based on a diffusible messenger from $Ca^{2+}$ depleted stores, secretion like conformational coupling between the channels in the two membranes and vesicular fusion of SOCC into the PM upon depletion of $Ca^{2+}$ stores[143]. SOCCs may be one of the most ubiquitous PM $Ca^{2+}$channels[18,22].

### 1.3.2 $Ca^{2+}$ release channels

The SER is the primary $Ca^{2+}$ storage organelle that maintains its free $Ca^{2+}$ around ~1 mM. There are number of $Ca^{2+}$ buffering proteins in the SER lumen like calsequestrin, that have low affinity and high capacity for $Ca^{2+}$ binding. A steep $Ca^{2+}$ concentration gradient of more than four orders of magnitude across the SER membrane allows for a rapid localized release of $Ca^{2+}$ via $Ca^{2+}$ release channels. There are two types of channels in the SER that are voltage

independent: $Ca^{2+}$-induced $Ca^{2+}$-release channels (CICR, also termed ryanodine receptors (RyRs)) and $IP_3$ induced release channels ($IP_3$ receptors or $IP_3Rs$). The CICR is activated typically upon entry of $Ca^{2+}$ through the VOCC. The CICR channel may also be opened by protein-protein interactions with VOCC in a voltage sensitive manner. The CICR exhibits a bell shaped dependence on $[Ca^{2+}]_i$; they are activated by $[Ca^{2+}]_i$ in the range of 1-10 μM and inhibited by high $[Ca^{2+}]_i$ (1-10 mM). The luminal $Ca^{2+}$ also regulates the activity of CICR, which is increased at high luminal $Ca^{2+}$ concentrations (>1 mM). The CICR channels are modulated by caffeine and cyclic ADP ribose, which increases its activity. The cADP ribose is a $Ca^{2+}$ mobilizing metabolite of the coenzyme β-nicotinamide adenine dinucleotide (NAD) formed by the activation of the enzyme ADP ribosyl cyclase. It has been shown to cause release of $Ca^{2+}$ from the internal stores via the CICR. Nicotinic acid adenine dinucleotide phosphate (NAADP) has also been identified as a potent $Ca^{2+}$ mobilizing messenger. The levels of the NAADP change in the cell in response to extracellular stimuli that generates specific $Ca^{2+}$ signals. NAADP has a profound desensitizing mechanism unparalleled by any other second messenger. The activity of the CICR channel is altered by the plant alkaloid ryanodine and hence they are also termed RyRs. Ryanodine has complex effect on the activity of RyRs: at low concentration it opens the channel to a low conductance state and at high concentration it abolishes the ion conductance[15,16,18,22].

In the $IP_3$-$Ca^{2+}$ signaling pathway, the binding of an agonist to the receptor in the PM leads to the activation of PLC, which results in the formation of $IP_3$ and diacylglycerol. $IP_3$ is highly mobile in the cytosol and diffuses to encounter the $IP_3R$ in the SER. The binding of $IP_3$ to its receptor changes the conformation of $IP_3R$ to open an integral channel to allow $Ca^{2+}$ to be released into cytosol. The $IP_3R$ requires $IP_3$ to open but their activation is regulated by $[Ca^{2+}]_i$. $IP_3$ is metabolized rapidly[15,16,18,22].

Mitochondrial membranes contain NCX that runs at a slow rate and is involved in $Ca^{2+}$efflux into the cytosol. Both 2:1 and 3:1 $Na^+$: $Ca^{2+}$ exchange stoichiometry has been proposed for the mitochondrial NCX (mNCX). Transporters in the mitochondrial membrane can also export $Ca^{2+}$ in exchange for at least two $H^+$ [15,16,18,22].

### 1.4 Need for PMCA selective inhibitors

The specific inhibitors of the ion transporters have helped in understanding their structure and function in both physiology and pathophysiology. An example of the importance of inhibitors is provided by ouabain and digoxin both of which inhibit the $Na^+$ pump[144]. The $Na^+$ pump, which also belongs to the family of P-type ATPases, plays an important role in maintaining the gradients of $Na^+$ and $K^+$ ions across the PM. Its inhibitors have been used extensively to study the physiological roles of the pump and its mechanism of action. Digoxin is also used to treat congestive heart failure and

cardiac arrhythmias[144]. Another example of the selective inhibitor of an ion transporter is thapsigargin that inhibits SERCA activity[28].

Most of the biochemical studies on PMCA are carried out with the PM fractions isolated from cells or on the purified PMCA protein in isolation. Studies with the membrane preparations from different cells have an inherent limitation related to the absence of the native regulators and to the requirement of reproducing the exact physiological environment[28,145]. The membranes also contain high amount of non-PMCA ATPases whose activity makes it difficult to measure the $Ca^{2+}$ stimulated activity of PMCA[105]. To remove the interfering ATPases, PMCA is usually solubilized and reconstituted. However, the presence of detergents may alter the properties of the purified PMCA protein[146]. More importantly, such preparations do not allow for a study of the physiological role of PMCA. Therefore, PMCA specific inhibitors are required to study the role of PMCA under physiological conditions in an intact cell or in the tissue.

Vanadate and eosin inhibit PMCA activity and have been used to study the physiological role of PMCA. However, both the inhibitors are not selective for PMCA. Vanadate is a phosphate analog that inhibits various ATPases in its +5 oxidation state. It has a higher affinity for the $Na^+$ pump than for PMCA ($K_i$: 0.04 μM vs 100 μM)[74]. It also inhibits SERCA activity. Since it binds and inhibits at the cytosolic side of PMCA, its ability to be transported across the PM varies from cell to cell. Its reduction by glutathione inside the cell may affect its inhibitory potential thereby making it difficult to extrapolate the results obtained

in broken cell preparations to intact cells[74,147,148]. Eosin is routinely used as a probe for the conserved ATP binding site of various ATPases including SERCA and the $Na^+$ pump. It modulates their activities by interfering with the ATP binding[149]. Alteration of the $Na^+$ pump activity changes the $Na^+$ gradient and the electrical potential across the PM that affects the activity of NCX making it difficult to distinguish between the contributions of PMCA and NCX.

The other methods used to study the role of PMCA in cell function include its overexpression in cultured cells and the use of transgenic animals. PMCA is normally present in low levels across different cells and is difficult to overexpress at high levels with correct membrane targeting in cultured cells[145,150-152]. The overexpressed PMCA retained in the internal membranes has been shown to be active in some studies which then can influence the $Ca^{2+}$ homeostasis[150,152]. Their also exists tight regulation of $[Ca^{2+}]_i$, which is reflected in the plasticity and adaptability of the various $Ca^{2+}$ transporters and sensors in the cell[151]. For example, overexpression of PMCA1 in the rat aortic endothelial cells resulted in the down regulation of the expression and activity of SERCA and $IP_3R$, while increasing the rate of $Ca^{2+}$ influx. A similar decrease in the level of the phosphorylated intermediate of SERCA was observed in the cells overexpressing PMCA4b[153]. Interdependence between PMCA and SERCA gene expression has also been shown by down regulation of the endogenous SERCA and PMCA proteins in the rat aortic endothelial cells overexpressing SERCA[93]. Contrary to this interdependence observed in cells overexpressing PMCA, both PMCA and

SERCA protein levels are increased in the myometrium of women in labor[154]. Similarly, both SERCA and PMCA are upregulated in the mammary epithelial cells during lactation period in mice[83]. The cells overexpressing PMCA4b isoform had lower levels of resting $[Ca^{2+}]_i$ in line with the homeostatic role of PMCA[155]. However, at variance with this study, the overexpression of PMCA1a was without any effect on the resting $[Ca^{2+}]_i$, which was similar to that of control cells[156]. Thus, adaptations in $Ca^{2+}$ regulatory pathways in PMCA overexpressing cells, observed in one case and not in the others make it difficult to interpret the role of PMCA.

Studies with transgenic mice have shown that only PMCA1$^{-/-}$ null mutants are embryolethal, while other PMCA isoform specific null mutants appear to adapt by using alternative $[Ca^{2+}]_i$ regulating pathways[157]. Transgenic mice overexpressing PMCA4b in the arterial smooth muscle showed altered expression and activity of the endogenous regulators of $[Ca^{2+}]_i$ including SERCA and $IP_3R$[158]. Certain phenotypes as impaired portal vein smooth muscle contractions observed in PMCA4 ablated mice were dependent on the mice strain[157]. The transgenic mice overexpressing PMCA4 in the arterial smooth muscle showed that PMCA interacted with nNOS in the caveolae and down regulated its activity[159]. However, the transgenic mice overexpressing PMCA4 in the myocardium did not show any differences in the cardiac performance as compared to the wild type, even though a recent study has shown the existence of physical interaction between the endogenous PMCA4 and nNOS in the

heart[160,161]. PMCA2 isoform, which has faster kinetics, is expressed in heart[106]. However, PMCA2 deficient mice exhibited defects in balance, hearing and milk secretion in mammary glands, without any alteration in the contractile activity of the heart. This suggests that the mice may have adapted[7,83,106]. Thus, the results obtained from these studies are at best inconclusive.

The above mentioned limitations of the methods currently used to study the role of PMCA in $Ca^{2+}$ homeostasis and cell signaling emphasize the need for the specific inhibitors of PMCA.

## 1.5 The concept of Caloxins

Caloxins are defined as specific extracellular inhibitors of PMCA. We have obtained them as short peptides that bind to the exdoms of PMCA. The exdoms of PMCA do not share any significant homology with the other members of P-type ATPases and are therefore unique targets to obtain PMCA specific inhibitors. The exdom 1 that connects the TM domains 1 and 2 differs among PMCA isoforms 1-4 due to the large number of non-conservative amino acid substitutions. Since the exdoms of PMCA are not affected by alternative splicing, the exdom 1 can be used to obtain inhibitors specific for individual PMCA isoforms.

### 1.5.1 Screening the phage display (Ph.D) random peptide libraries

The Ph.D random peptide library is a selection technique based on the combinatorial library of random peptides displayed on the surface of the bacteriophage. Such Ph.D random peptide libraries provide an enormous diversity

of peptide sequences to identify a peptide ligand for a target[162-165]. An example is where random peptides are fused to the minor coat protein pIII of the bacteriophage M13[164]. The displayed peptide is expressed at the N-terminus of the pIII coat protein. The peptide is followed by a short spacer (GGGS), which continues into the wild type pIII coat protein. It provides a physical linkage between the vast library of the randomized peptides displayed on the bacteriophage surface by packaging the encoding DNA within the same virion. Three commercially available Ph.D peptide libraries express: 7-amino acid (PhD-7) or 12-amino acid (PhD-12) random linear peptides or disulfide constrained (PhD-C7C) random peptides, where an internal disulfide bond is formed by a pair of cysteines that flank the random 7-amino acid long peptides.

### 1.5.2 Properties of the known caloxins

The prototype caloxin 2a1 was obtained by screening the Ph.D-12 library for the peptide ligands that would bind to the exdom 2 of PMCA1. A synthetic peptide containing the sequence of the exdom 2 of PMCA protein was used as a target to screen the library. The exdom 2 in the native PMCA protein in the PM would form a loop with its two ends embedded in the membrane continuing into the TM domains 3 and 4. Therefore, a synthetic target peptide was designed with a cysteine residue added at one end of the exdom sequence for conjugation to a carrier protein, and an extra short TM sequence at the other end to form a loop like conformation with the carrier protein. While screening the Ph.D-12 library, the phage can also bind to the carrier protein molecule. Therefore, the synthetic

exdom 2 was conjugated to two different carrier proteins: KHLH and ovalbumin. The KHLH conjugate was used as a target, while its ovalbumin conjugate was used to elute the phage thereby, enriching the phage that bound only to the synthetic exdom 2 target. The screening using the synthetic exdom 2 of PMCA1 as a target resulted in the selection of a phage encoded peptide called caloxin 2a1. In the term caloxin 2a1, '2' denotes the exdom 2 of PMCA used as the target, 'a' denotes the method of screening the Ph.D library and '1' denotes first in the series of caloxins. Caloxin 2a1 selectively inhibited the $Ca^{2+}$-$Mg^{2+}$ ATPase activity of PMCA in the erythrocyte membranes but with a low affinity ($K_i$: 0.4 - 0.6 mM). Caloxin 2a1 had no effect on the other ATPases: $Na^+$-$K^+$ ATPase of the erythrocyte ghosts, $Mg^{2+}$ ATPase of the erythrocyte ghosts, $Ca^{2+}$-$Mg^{2+}$ ATPase of the SER of the fast twitch skeletal muscle. Since caloxin 2a1 was obtained by using the exdom 2 as a target, its inhibition of PMCA activity was non-competitive with respect to $Ca^{2+}$, ATP, and the activator calmodulin, all of which have their binding sites on the cytosolic domains of PMCA[166a]. Caloxin 2a1 inhibited the formation of $Ca^{2+}$-dependent acylphosphate intermediate of PMCA from ATP. It however, was without any effect on the acylphosphate intermediate of PMCA formed from $P_i$ in the reverse reaction of the transport cycle. Caloxin 2a1 produced endothelium dependent relaxation in the rat aortic rings precontracted with phenylephrine[166,166a].

The exdom 3 of PMCA is very short with only six residues, which are conserved among all four PMCA isoforms. It was used as a target to obtain

caloxin that would inhibit all PMCA isoforms. In an attempt to obtain caloxin with higher affinity than 2a1, the screening was carried out with increased stringency of washes to remove the phage binding loosely to the synthetic exdom 3 target. This resulted in caloxin 3a1, with two-fold higher affinity ($K_i$ of 0.2 mM) as compared to caloxin 2a1 ($K_i$ of 0.4-0.6mM). Caloxin 3a1 was also selective for PMCA inhibition, as it had no significant effect on the $Ca^{2+}$-$Mg^{2+}$ ATPase of the SER of the fast twitch skeletal muscle at a concentration, which produced more than 90% inhibition of PMCA activity. Unlike caloxin 2a1, caloxin 3a1 did not inhibit the $Ca^{2+}$-dependent acylphosphate intermediate formation of PMCA from ATP. When added extracellularly to the pig coronary artery cultured endothelial cells, caloxin 3a1 elevated $[Ca^{2+}]_i$ consistent with the decreased ability of cells to extrude $Ca^{2+}$ following inhibition of PMCA[167].

## 1.6 Objectives of the present study

Since caloxins 2a1 and 3a1 had low affinity for PMCA, it was rationalized that the synthetic exdoms used as targets to screen the Ph.D-12 library may differ in conformation from the exdoms in the native PMCA protein in the PM. Due to this difference in the conformation, the phage-encoded peptides that bind tightly to the synthetic exdom may fail to bind as tightly to the exdom in its native conformation in PMCA protein. Therefore, it was hypothesized that screening the Ph.D library using two targets, the synthetic exdom peptide and purified PMCA protein could result in obtaining caloxins with high affinity. Towards this end, the proposed study had following three Aims.

**Aim1:** Develop caloxins that have higher affinity and PMCA4 isoform selectivity by using the N-terminal half of the exdom 1 (exdom 1X) as a target.

***Hypothesis:*** The phage pool enriched for binding to synthetic exdom 1 of PMCA4 contains phage clones that bind preferentially to the exdom in the native PMCA protein.

***Rationale:*** The exdom 1 of PMCA differs among PMCA isoforms1-4 due to large number of non-conservative amino acid substitutions and can therefore be used as a target to obtain isoform selective caloxins. The exdom 1 is long and contains a cysteine in the middle that can produce uncertainties in the configuration by forming disulfide bridge. The exdom 1 was divided around the cysteine into exdom 1X and 1Y (Fig. 1.2). Human erythrocyte ghosts express mainly PMCA4, which can be purified by calmodulin affinity chromatography in which PMCA binds tightly to calmodulin only in the presence of $Ca^{2+}$. Following the initial few rounds of screening of the Ph.D-12 library with the synthetic exdom 1X of PMCA4, the phage pool will be screened for binding to the erythrocyte PMCA protein immobilized on the calmodulin-agarose column to select the phage clones that bind tightly to the exdom in its native conformation in PMCA.

**Aim2**: To determine that the high affinity PMCA4 selective caloxin obtained in Aim1 binds only to PMCA protein in human erythrocyte ghosts.

***Hypothesis:*** The high affinity PMCA4 selective caloxin inhibits PMCA activity by binding to the exdom 1X.

***Rationale:*** The exdom 1X of PMCA4 is the target used in screening the Ph.D-12 library to obtain the high affinity caloxin (Aim1). Therefore, the photoactivable derivative of the high affinity PMCA4 selective caloxin is expected to photolabel only PMCA protein in human erythrocyte ghosts. The synthetic exdom 1X peptide should compete for binding to the photoactivable derivative and therefore reduce the amount of photolabel incorporated at the specific site in the erythrocyte ghosts.

**Aim3:** To obtain caloxins using the C-terminal half of the exdom 1 (exdom 1Y) of PMCA4 as a target to screen Ph.D linear and cyclic peptide libraries.

***Hypothesis:*** The Ph.D libraries contain unique phage encoded sequences that bind selectively to the exdoms of PMCA protein.

***Rationale:*** The exdom 1X and 1Y can be used as targets to screen the Ph.D libraries to obtain high affinity caloxins that bind to the N and C-terminal half of the exdom 1 of PMCA4. The high affinity caloxin that binds to each half of the exdom 1 can be linked to form a bidentate caloxin that can attain a much higher affinity and PMCA4 isoform selectivity. Two molecules that bind to proximal sites on a protein can be optimally linked to make bidentate ligands with a much higher affinity and selectivity[168]. Unlike the linear Ph.D-12 library, the Ph.D-C7C library has random heptapeptides flanked by a pair of cysteine residues, which form a disulfide bridge during the phage assembly. This conformational strain in the peptides in the Ph.D-C7C library can lead to the

selection of ligands with higher affinity. The Ph.D-C7C and the Ph.D-12 libraries provide large complexity in the phage-expressed peptides that can lead to selection of high affinity caloxins for the exdom 1Y of PMCA4.

# 2.0 MATERIALS AND METHODS

## 2.1 Materials

Ph.D-12 library, Ph.D-C7C library and Ph.D cloning kit with the enzymes were purchased from New England Biolabs, Inc. (Mississauga, ON, Canada). Agar, trypticase peptone and yeast extract were obtained from Becton Dickinson, (Cockeysville, MD). [$\gamma$-$^{33}$P]-ATP was from Amersham (Piscataway, NJ). ATP, Bovine Serum Albumin (BSA), imidazole, ethylene glycol-bis(2-aminoethyl ether)-N,N,N',N'-tetra-acetic acid (EGTA), ethylenediamine tetra-acetic acid (EDTA), ouabain, NADH, Phospho (Enol) Pyruvate (PEP), pyruvate kinase-lactate dehydrogenase from rabbit muscle (~1000 units/ml lactate dehydrogenase; ~700 units/ml pyruvate kinase), calmodulin from bovine testes (>40,000 units/mg protein), 3-[N-Morpholino] Propane Sulfonate-Na (MOPS), 2-[N- Morpholino] Ethane Sulfonic acid (MES), Keyhole Limpet Hemocyanin (KHLH), ovalbumin, calmodulin-agarose (2.3 mg calmodulin from bovine testes/ml gel), soyabean phosphatidyl serine, egg yolk phosphatidyl choline, protein A agarose (2 mg protein A/ml gel; ≥10mg/ml IgG binding capacity), dithiothreitol (DTT), Tween, polyethylene glycol–8000 and tetracycline were obtained from Sigma Aldrich (St Louis, MO). Acrylamide, agarose and NZ amine were obtained from GibcoBRL (Grand Island, NY). Complete Mini EDTA-free protease inhibitor cocktail tablets (broad spectrum of serine and cysteine proteases) were from Roche Diagnostics, IN. USA. Antibodies JA9 and 5F10 were from Bioaffinity Reagents. Streptavidin and anti-mouse IgG conjugated to horseradish peroxidase (HRP) were from GE

Healthcare. All other chemicals were purchased from the standard commercial sources. QIAGEN maxiplasmid purification kit, QIAprep miniplasmid purification kit, MinElute PCR Purification Kit and QIAquick gel extraction kit were from QIAGEN Inc. Mississauga, Canada. The non-competent XL1-Blue *E. coli* cells and XL2-Blue Ultracompetent cells were from Stratagene (La Jolla, USA). The synthetic exdom peptides were synthesized by Dalton Pharma Services (Toronto, ON, Canada). Conjugation of the synthetic exdom peptides to keyhole limpet hemocyanin and ovalbumin was carried out by Bio-synthesis, Inc U.S.A. Dr E.E. Escher, Sherbrooke University, Canada, synthesized the two photoreactive derivatives of caloxin 1c2, 3Bpa1c2-biotin and 16Bpa1c2-biotin. All peptides were greater than 95 % pure by HPLC and verified by mass spectroscopy.

## 2.2 Two-step screening of Ph.D-12 library with PMCA4 exdom 1X as target

The exdom 1 of human PMCA4 consists of residues 116-147 (SLVLSFYRPAGEENELCGQVATTPEDENEAQA, GenBank accession no: NM_001684). The exdom 1 was divided around the cysteine in the middle to synthesize two peptides corresponding to the sequence of the exdom 1X (116-131) and the exdom 1Y (132-147). The exdom 1X was used as a target to screen the Ph.D-12 combinatorial library of random 12-amino acid peptides. A synthetic peptide corresponding to the exdom 1X sequence was synthesized with a cysteine added at the N-terminus (CSLVLSFYRPAGEENEL). The cysteine was used to

conjugate the synthetic exdom 1X to a carrier protein Keyhole Limpet Hemocyanin (KHLH) or ovalbumin.

The two-step screening of the Ph.D-12 library consisted of: a) screening using the synthetic exdom 1X as a target in the first step and, b) affinity chromatography with PMCA protein purified from human erythrocyte membranes in the second step[169].

### 2.2.1 Screening Ph.D-12 library using the synthetic exdom 1X target

The Ph.D-12 library provides a large diversity (>$10^9$) of 12-amino acid peptide sequences fused to the minor coat protein (pIII) of the bacteriophage M13. The phage can infect *Escherichia coli* cells containing the F' factor. The phage initially replicates as a double stranded plasmid DNA in the cells and then synthesizes its coat proteins. These pack the single stranded DNA, which is liberated non-lytically from the cells into the growth medium[164]. The Ph.D-12 library was screened using the synthetic exdom 1X of PMCA4 as a target. The screening was carried out for 3 rounds to enrich the phage pool in sequences that bind to the synthetic exdom 1X. Each round of screening consisted of the following steps:

- Day1: Two wells of the 96 well microtiter plate (96-Well Cell Culture Plates, BD Falcon) were each coated with 100 µl of the target peptide solution which was a mixture of 0.1 mg/ml each of the synthetic exdom 1X and its KHLH conjugate dissolved in sterile phosphate-buffered saline (PBS) containing 1 mM

sodium azide. PBS contained in mM: 137 NaCl, 2.7 KCl, 8 $Na_2HPO_4$ and 1.5 $KH_2PO_4$ (pH 7.4).

- The microtiter plate with the coated wells was covered with Saran Wrap and left overnight at 4°C.

- Day2: The excess target peptide solution was poured off from the wells of the microtiter plate, which was then firmly slapped face down on a clean paper towel to remove residual solution.

- The remaining binding sites in the coated wells were blocked for 1 h at 4°C with 200 µl blocking buffer containing 5 mg/ml BSA in sterile PBS with 1 mM sodium azide.

- The excess blocking buffer was discarded and the coated wells were washed 6x with chilled sterile PBS. The microtiter plate was firmly slapped face down on a clean paper towel after each wash. All the remaining steps were carried out at 22-24°C.

- $2x10^{11}$ plaque forming units (pfu) of the original Ph.D-12 library were diluted in 200 µl of a solution containing BSA, Ovalbumin and KHLH (BOK solution: 5 mg/ml BSA and 0.5 mg/ml each of ovalbumin and KHLH in sterile PBS). 100 µl of the phage solution was then added to each coated well. The microtiter plate was rocked gently for 1 h.

- The unbound phage was pipetted out carefully without touching the surface of the wells. The wells were washed once with chilled sterile PBS. The non-specific phage was removed by washing the wells sequentially with 10 min

incubation on the rocker with the following solutions: a) BOK solution, b) 5 % carnation milk in PBS and, c) PBS. The wells were washed 1x with chilled sterile PBS after each 10 min incubation. The last incubation was followed by quick 10x washes with chilled sterile PBS. The microtiter plate was firmly slapped face down on a clean paper towel after each PBS wash.

- The phage from each well was eluted for 24 h with 100 µl of the synthetic exdom 1X-ovalbumin conjugate at a concentration of 0.1 mg/ml in PBS with 10 µg/ml of tetracycline.

- The eluted phage was amplified, titered and subjected to next cycle of screening at a constant input of $10^{11}$ pfu.

#### *2.2.1.1 Amplification and precipitation of the eluted phage*

Luria Broth (LB: 85.6 mM NaCl, 0.5 % yeast extract, 1 % trypticase peptone) was used to culture non-competent XL1-Blue *E. coli* cells. All culture media and pipette tips were autoclaved for 40-60 min at 120°C before use. The XL1-Blue cells were first streaked on an LB-agar-tetracycline (1.5 % agar in LB with 10 µg/ml tetracycline) plate (sterilized disposable plastic petri dishes, Fischer Scientific) and cells from a single colony were allowed to grow in LB-tetracycline (LB with 10 µg/ml tetracycline) for 16-18 h in an environmental shaker (225-250 rpm) at 37°C. The culture was diluted 1:100 in fresh 6 ml LB and grown again for 2 h. The eluted phage (100 µl) was added to 0.9 ml of the culture and incubated at 37°C for 4.5 h with shaking. The amplified phage was centrifuged at 16000 g for 2 min and the supernatant was transferred to fresh tubes containing 300 µl of

PEG/NaCl (20 % (w/v) polyethylene glycol–8000, 2.5 M NaCl) to precipitate the phage overnight at 4°C. The amplified phage was stored at 4°C and its titer determined before use.

#### *2.2.1.2 Determining phage titers*

- The LB-agar plates were prewarmed to 37°C.
- An overnight culture started with a single colony of XL1-Blue cells in LB-tetracycline was diluted 1:500 in 100 ml LB-tetracycline and grown at 37°C for 4 h with shaking.
- Cells were harvested by centrifugation at 23,000 g at 4°C for 5 min and then suspended in 3-6 ml fresh LB.
- The agarose top (0.6 % agarose in LB) was melted and equilibrated in a water bath at 48°C.
- Amplified phage was serially diluted over a wide range in LB containing Eppendorf tubes.
- 100 µl cells were dispensed into 15 ml plastic round bottom tubes (BD Falcon), one for each phage dilution.
- 100 µl of the diluted phage was added to the corresponding 15 ml tube with cells.
- One at a time, 4 ml of 0.6 % agarose at 48°C was added to the tubes containing the cells and the contents were poured immediately onto the prewarmed LB-agar plates.

- After cooling for 20 min at 22-24°C, the plates were inverted and incubated at 37°C for 16-18 h. The plaques were counted and multiplied with the dilution factor to get the titers in pfu/100 µl.

#### *2.2.1.3 Picking phage clones and amplification*

The enriched phage pool at the end of screening was titered at a dilution to get well-spaced 50-100 plaques per plate. Each plaque was picked with a sterile plastic stick (inoculating needles, VWR) and transferred to a 15 ml sterile tube containing 500 µl early log phase culture of XL1-Blue cells. The individual phage clones were amplified at 37°C with shaking at 250 rpm for 4.5 h. The amplified phage for each clone was centrifuged at 16,000 g for 2 min and the supernatant was transferred to fresh tubes and stored at 4°C.

For the phage DNA sequencing, 200 µl of the amplified phage clone was added to 1.3 ml of early log culture of XL1-Blue cells and amplified at 37°C for 4.5 h with shaking. The cells were pelleted by centrifugation at 16,000 g for 2 min. The amplified phage in the supernatant was transferred to fresh tubes and stored at 4°C. The cell pellet was used for isolation of the plasmid DNA.

#### *2.2.1.4 Isolation of plasmid DNA*

The plasmid DNA for each clone was purified from the pelleted XL1-Blue *E. coli* cells (*2.2.1.3*) by using the Plasmid Mini Purification Kits. Briefly, the cells were lysed under alkaline conditions in the presence of RNase A. The lysate was neutralized and centrifuged at high speed to remove the debris. Cleared lysate was then loaded for adsorption of the plasmid DNA to the silica resin. After

washing the resin with ethanol, the plasmid DNA was eluted. The DNA was quantified on agarose gel using known amounts of DNA molecular weight markers or using a Beckman DU640 spectrophotometer. The plasmid DNA was then sequenced by MOBIX (McMaster University, Hamilton, Canada) using the downstream –96 primer (5'-CCCTCATAGTTAGCGTAACG-3') provided in the Ph.D-12 library kit. The reliability of sequencing was confirmed by using a second downstream –28 primer (5'-GTATGGGATTTTGCTAAACAAC-3') for sequencing the plasmid, which gave the same insert sequence.

### 2.2.2 Screening Ph.D-12 library using PMCA affinity chromatography

PMCA has a calmodulin-binding domain at its C-terminal end and can bind calmodulin in the presence of $Ca^{2+}$. This property of PMCA has been used previously to purify it[99]. Here it was used to screen the phage by affinity chromatography with PMCA using immobilized calmodulin.

An aliquot of the calmodulin deficient human erythrocyte ghosts prepared as described in section 2.11 was centrifuged at 500,000 g at 4°C for 15 min. The pellet was resuspended and solubilized at a protein concentration of 8 mg/ml in 0.8 % Triton X-100 (w/v), 260 mM KCl, 40 mM HEPES pH 7.4, 1 mM $MgCl_2$, 0.1 mM $CaCl_2$, 2 mM DTT, protease inhibitor cocktail (Complete Mini EDTA-free) at 4°C, for 10 min. The non-solubilized material was removed by centrifugation for 30 min at 500,000 g at 4°C. A suspension of phosphatidylserine and phosphatidylcholine (2 % in 1 % (w/v) Triton X-100) was prepared by sonication on ice and stored under $N_2$ at -80°C until use. The phospholipid

suspension was added to the supernatant to a final concentration of 0.05 % and allowed to mix by slow rotation at 4°C for 10 min. The calmodulin-agarose suspension was packed in a column (Bio-Spin disposable chromatography columns, Bio-Rad, CA) to a bed volume of 200 µl and washed with 10x bed volume of wash buffer composed of (mM): 130 KCl, 20 HEPES pH 7.4, 1 $MgCl_2$, 0.1 $CaCl_2$, 2 DTT, 0.05 % of phospholipid suspension, 0.4 % Triton X-100 (w/v) and the protease inhibitor cocktail. The supernatant was applied to the calmodulin-agarose column. The unbound flow through from the column was discarded and the column was plugged at the bottom. The phage eluted from the third round of screening with the synthetic exdom 1X was amplified and used for PMCA affinity chromatography. The phage ($2x10^8$ pfu) was diluted in the wash buffer and applied to the calmodulin-agarose column. The column was capped and the phage was allowed to bind to PMCA immobilized on the calmodulin-agarose by rotation at 4°C for 1 h. The column was washed with 20x bed volume of wash buffer to remove any unbound phage. The traces of wash buffer were removed by a quick centrifugation step. PMCA with the phage bound to it was eluted from the calmodulin-agarose column by adding 400 µl $Ca^{2+}$ free elution buffer composed of (mM): 130 KCl, 20 HEPES pH 7.4, 1 $MgCl_2$, 5 EGTA, 2 DTT, 0.05 % of phospholipid suspension and 0.4 % Triton X-100 (w/v). The phage was dissociated from PMCA at 0°C by addition of 100 µl of 0.2 M glycine-HCl (pH 2.2), which was neutralized within 10 min with 75 µl of 1 M Tris-HCl

(pH 9.1). The phage was amplified as described in *2.2.1.1* and used at $2x10^8$ pfu for the next round of affinity chromatography.

In a preliminary experiment, to test the binding of PMCA protein to the calmodulin-agarose column, PMCA was eluted from the column in a $Ca^{2+}$ free elution buffer and tested for its $Ca^{2+}$-$Mg^{2+}$ ATPase activity using the coupled enzyme assay described in 2.13.

## 2.3 Assay for selectivity of phage binding to the exdom target

Following the rounds of screening, the enrichment of the phage that bound selectively to the target was determined. The assay was carried out by the method similar to that used for screening the phage as described in 2.2.1. There were two coating targets: a) a mixture of the synthetic exdom and its KHLH conjugate as the selective target and, b) KHLH as a negative control. The target peptide solutions were made at a concentration of 0.1 mg/ml in sterile PBS with 1 mM sodium azide. The binding to the two targets was tested in parallel using $10^{10}$ pfu of either the phage enriched after screening or the original random Ph.D-12 library. After extensive washing, the phage bound to the selective target was eluted for 24 h with ovalbumin conjugate of the synthetic exdom at a concentration of 0.1 mg/ml in sterile PBS containing tetracycline (10 μg/ml). Ovalbumin, at the same concentration was used to elute the phage bound to the negative control. Titers of the eluted phage were determined.

## 2.4 Two-step screening of Ph.D-12 library with PMCA4 exdom 1Y as target

A synthetic peptide corresponding to residues 132-147 of the exdom 1Y of human PMCA4 was synthesized (CSLVLSFYRPAGEENEL). The cysteine at the N-terminus of the synthetic exdom 1Y was used to conjugate the peptide to a carrier protein KHLH or ovalbumin. The two-step screening of the Ph.D-12 library was carried out as described in 2.2 using the exdom 1Y as a target.

## 2.5 Screening a cysteine bridge constrained Ph.D-C7C library

The Ph.D-C7C library expresses random heptapeptides flanked by cysteine residues that form an internal disulfide bridge. The library was screened for binding to the synthetic exdom 1Y (CSLVLSFYRPAGEENEL) of PMCA4. The protocol and the conjugates used were similar to those in 2.2.1 except that the screening was repeated for 6 rounds. The C7C-phage pool from the last round of screening was subjected to selectivity assay as described in 2.3.

## 2.6 Construction of the Ph.D caloxin 1b1-like peptide library

A Ph.D library was constructed which expressed caloxin 1b1-like peptides. In the phage encoding caloxin 1b1, the 12-amino acid sequence unique to caloxin 1b1 is fused at its N-terminus to the leader peptide sequence and at its C-terminus is followed by a short spacer that continues into the minor coat protein pIII of the bacteriophage M13. During phage assembly, the leader peptide sequence is cleaved off so that caloxin 1b1 is positioned directly at the N-terminus of the coat protein pIII. The 12-amino acids unique to caloxin 1b1 are

encoded by an oligonucleotide duplex of 36 bases. To construct the Ph.D caloxin 1b1-like peptide library, limited mutagenesis was carried out in the 36 bases that encode caloxin 1b1. It was computed that retaining 91 % of the original base at each of the 36 base positions and replacing the remainder with equal percent of the other three bases would be optimum. Therefore, a mixture of oligonucleotides with partially randomized caloxin 1b1 encoding domain, flanked by conserved bases in the minus strand of the phage DNA were synthesized by W.M. Keck Facility, Yale University, USA (Fig. 2.1). The flanking conserved bases contained the restriction sites *Kpn1/EagI* required for cloning. This caloxin 1b1 biased single stranded oligonucleotide mixture was then used in constructing a library in the M13KE vector, which is a derivative of M13 bacteriophage with cloning sites *Kpn1/EagI* inserted in the 5' end of the gene encoding pIII coat protein. The steps involved in the library construction are briefly described below.

### 2.6.1 Synthesis of a duplex from single stranded oligonucleotides

The caloxin 1b1 biased single stranded oligonucleotides were dissolved in Tris-EDTA (10 mM Tris-HCl pH 8, 1 mM EDTA), aliquoted and precipitated using 0.3 M Na-acetate and 2.5 volumes of ethanol. An aliquot of the precipitated oligonucleotides was dissolved in 100 µl Tris-EDTA and quantified with a spectrophotometer by measuring the optical density ($OD_{260}$) at 260 nm (1 absorbance unit at 260 nm = 20 µg/ml single stranded DNA). A 5 µg aliquot of the mixture of single stranded oligonucleotides was annealed with 3 molar equivalents (approximately 4.2 µg) of the universal extension primer

(5'CATGCCCGGGTACCTTTCTATTCTC3' purchased from New England Biolabs, Fig. 2.1) in a total volume of 50 µl of Tris-EDTA buffer containing 100 mM NaCl. The extension primer has a sequence complementary to the 3' end of the single stranded oligonucleotides. The annealing reaction was heated to 95°C for 10 min and the tube was then placed in a beaker filled with boiled water that was allowed to cool to approximately 37°C. The annealed duplex was extended by adding 30 units of Klenow fragment, 1x NEB3 reaction buffer (100 mM NaCl, 50 mM Tris-HCl, 10 mM $MgCl_2$, 1 mM DTT, pH 7.9 at 25°C) and 0.4 mM each of dATP, dCTP, dGTP and dTTP in a final reaction volume of 200 µl. The extension reaction was carried out at 37°C for 10 min and then at 65°C for 15 min. The duplex was checked on 12 % polyacrylamide gel electrophoresis. Molecular masses of the bands were estimated using a GeneRuler™ 50 bp DNA Ladder (Fermentas, Burlington, Canada).

### 2.6.2 Digestion of the oligonucleotide duplex

The oligonucleotide duplex was digested with 100 units each of *Eag1* and *Acc651* in the NEB3 reaction buffer in a final volume of 400 µl. (*Acc651* has the same recognition site as *Kpn1* and it can be used with *Eag1* in the buffer NEB3). The digestion was carried out by incubation at 37°C for 3 h. The digested product was purified using MinElute PCR Purification Kit and tested using 12 % polyacrylamide gel electrophoresis.

### 2.6.3 Preparation of the M13KE vector

The M13KE vector (20 μg) was digested at 37°C for 3 h with 200 units each of *Eag1* and *Acc651* in a total volume of 800 μl of 1x NEB3 reaction buffer with 0.1 mg/ml BSA. The digested DNA was dephosphorylated at 37°C for 1 h by 10 units of alkaline phosphatase in the same buffer. The digested M13KE vector was tested on 1 % agarose in Tris-acetate-EDTA (40 mM Tris acetate/1 mM EDTA) buffer and the molecular mass was determined using the O'GeneRuler™ 1 kb DNA ladder (Fermentas, Burlington, Canada). The digested M13KE vector was gel purified using QIAquick Gel Extraction Kit.

### 2.6.4 Ligation of digested oligonucleotide duplex and M13KE vector

The ligation conditions were optimized using different proportions of the digested vector and the digested oligonucleotide duplex mixture. The ligation was carried out with 200 units of T4 DNA ligase in 20 μl volume of 1x ligase reaction buffer (50 mM Tris-HCl, 10 mM $MgCl_2$, 1 mM ATP, 10 mM DTT, 25 μg/ml BSA pH 7.5 at 25°C) for 16-18 h at 16°C. After its completion, the reaction was stopped by heating at 65°C for 15 min. The ligated product from each reaction was then used to transform XL2-Blue Ultracompetent cells following the protocol provided by the manufacturer. The tubes containing the transformed cells were incubated with 0.9ml NZY+ broth (1 % NZ amine, 0.5 % yeast extract, 85.5 mM NaCl, pH 7.5 (NaOH) with 20 mM glucose and 12.5 mM each of $MgCl_2$ and $MgSO_4$ added prior to use) at 37°C for 30 min with shaking at 225-250 rpm. The transformation mixture was centrifuged at 16,000 g for 2 min and the supernatant

containing the phage was titered using the mid log phase culture of non-competent XL1-Blue cells to determine the efficiency of each ligation reaction. Plaques were picked from the ligation reaction that gave the highest titer to determine the complexity of the library. The phage DNA in the plaques was characterized as described in *2.2.1.3* and *2.2.1.4*. The ligation of 40 ng of the digested M13KE vector with 1.25 molar excess of the insert gave the highest titer. This titer was >100 fold higher than the control without the oligonucleotide duplex mixture. This ligation reaction was scaled up 10-fold.

### 2.6.5 Transformation of XL2-Blue Ultracompetent cells

The large-scale ligation reaction was divided into 10 tubes to transform the ultracompetent cells as above. After growing the transformed cells at 37°C for 30 min with shaking at 225-250 rpm, the transformation mixture was centrifuged and the supernatant containing the phage was pooled. The phage was precipitated for 16-18 h by adding 1/3 volume of PEG/NaCl. The precipitated phage was resuspended in 100 µl Luria Broth and amplified by infecting the early log culture of non-competent XL1-Blue cells as described in *2.2.1.1*. This resulted in an amplified library containing $7.5x10^9$ pfu/µl. The amplified Ph.D caloxin 1b1-like peptide library was precipitated by addition of PEG/NaCl with glycerol and stored at –20°C.

## 2.7 Construction of the Ph.D caloxin 1b2-like peptide library

A Ph.D caloxin 1b2-like peptide library with the M13KE vector was prepared following the protocol described in 2.6 for the construction of the Ph.D

caloxin 1b1-like peptide library. Mutations were made in the minus strand (5'CCACGCATACAAAGACTGATAATTAATCCAACCATG3') of the caloxin 1b2 as described for caloxin 1b1.

## 2.8 Photolabeling reaction

The photoreactive derivatives of caloxin 1c2, 3Bpa1c2-biotin and 16Bpa1c2-biotin, were freshly prepared as 1 mM stocks in 1 % ethanol in tubes covered with foil. Routinely, ghosts (0.5 μg protein/μl, see 2.11 for preparation) and 3Bpa1c2-biotin or 16Bpa1c2-biotin in presence of 2 mM fresh DTT in a tube covered with a foil were incubated for 20 min by slow rotation at 4°C. A 96-well flat bottom plate (Sarstedt) was placed on ice water in an ice bucket with a magnetic stir bar at the bottom. Aliquots (50 μl containing 25 μg protein) of the incubation mixture were transferred into wells of this plate. The plate was covered with a foil and the ice bucket was taken to the dark room and placed on top of a magnetic stirrer. The foil was removed and a hand held UV lamp (Model UVLS-28, Upland, CA) was placed on the plate directly over the samples. The samples were irradiated at 365 nm for 30 min. The irradiated samples were pooled and stored at –80°C until use. Several variations of this method were used in which the ghost protein, the probe concentration, or the length of the UV irradiation time were varied or the competing peptides were added.

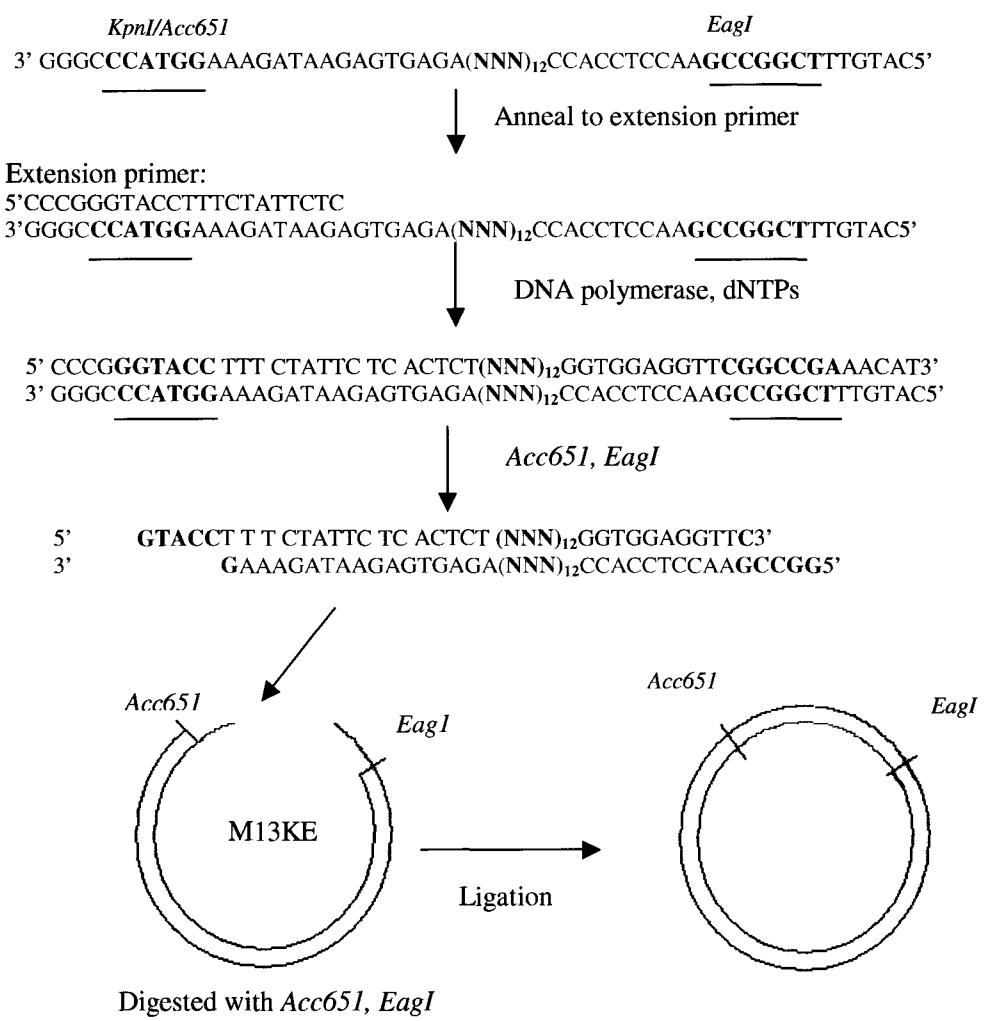


**Fig. 2.1. Construction of Ph.D caloxin 1b1-like peptide library.**

$(NNN)_{12}$ is the partially randomized nucleotide sequence biased towards caloxin 1b1.

## 2.9 PMCA immunoprecipitation from human erythrocyte ghosts

Immunoprecipitation of PMCA was carried out using the antibody 5F10 that binds to all four PMCA isoforms. Protein A-agarose was added to the Bio-Rad spin columns to get a bed volume of 200 µl and washed with 5 bed volumes of the buffer IPA (0.02 M $NaH_2PO_4$, 0.15 M NaCl, pH 8.0). The antibody 5F10 (5 µg) in 200 µl volume of buffer IPA was added to the column to allow its binding to protein A by slow rotation at 4°C for 5-6 h. The unbound antibody was removed by washing the column with 5 bed volumes of buffer IPA. The photolabeled erythrocyte ghosts were concentrated in a centrifuge at 4°C and resuspended in PBS to a final concentration of 2.5 µg/µl. The ghost protein was solubilized in an equal volume of solubilization buffer (150 mM NaCl, 10mM $Na_2HPO_4$, pH 7.2, 1 % sodium deoxycholate, 0.1 % sodium dodecyl sulfate (SDS), 1 % Triton X-100, and a protease inhibitor cocktail tablet) by incubation for 1 h at 4°C. The non-solubilized material was removed by centrifugation at 95,000 g in an Airfuge. The solubilized protein was added to the 5F10-protein A-agarose and incubated for 16-18 h by rotation at 4°C. The column was washed with 20 bed volumes of buffer IPA. The traces of the buffer IPA were removed by a quick centrifugation step. The captured PMCA was eluted from the protein A-agarose column in a minimum volume of 4x Laemmli SDS sample buffer (0.25 M Tris-HCl pH 6.8, 8 % SDS, 30 % glycerol, 0.4 M DTT, 0.02 % bromophenol blue) at 95°C for 10 min, followed by a quick centrifugation to collect the eluate.

The elution was repeated again to elute any PMCA not eluted in the first round. The eluted protein was then subjected to Western blotting as described in 2.10.

**2.10 Western blotting**

The immunoprecipitated PMCA or the photolabeled ghosts were diluted in 4X Laemmli SDS sample buffer and the proteins were separated on SDS-polyacrylamide (7.5 %) gel electrophoresis at 80 V as described previously[170]. The proteins were electroblotted to the nitrocellulose membrane (Pall Corp.) at 100 V for 2 h using an ice-cold low methanol transfer buffer (25 mM Tris base, 150 mM glycine, 4 % methanol; pH 8.3). The nitrocellulose membrane (blot) was then blocked with rocking for 1 h at 22-24 °C with 5 % skim milk powder in TBS-Tween (10 mM Tris/HCl, 140 mM NaCl, 0.1 % (v/v) Tween 20; pH 7.5). The blot was then incubated with rocking for 1 h with streptavidin conjugated to horseradish peroxidase (HRP-streptavidin; 1:5000) for binding to biotinylated proteins. The blot was given 3-4 quick washes and then washed 4 times for 15 min with TBS. The blot was then developed with ECL Western blotting detecting reagents following their recommended protocol (GE Healthcare) and exposed to X-ray film. The molecular mass of the bands was determined using PageRuler™ Prestained Protein Ladder Plus (Fermentas, Burlington, Canada). The quantitative band intensity analysis was carried out with Multi Gauge v 3.0 software (Fujifilm).

## 2.11 Preparation of the leaky human erythrocyte ghosts

The leaky human erythrocyte ghosts were prepared as described previously[171]. Briefly, 25-30 ml of human blood in acid citrate dextrose (2.5 % trisodium citrate, 1.4 % citric acid, 2 % dextrose, pH 4.5) was obtained and centrifuged at 3,000 g for 5 min. The clear buffy layer containing platelets and plasma were siphoned off. These steps were carried out in another lab by a person who routinely works with blood. The lower layer of erythrocytes was then transferred to four 250 ml centrifuge bottles and mixed with 10 volumes of 172 mM Tris-HCl (pH 7.6 at 4°C). The samples were centrifuged at 4,000 g for 5 min and the clear supernatant was removed. The erythrocytes were washed 4 times in 172 mM Tris-HCl. The red blood cells were then lysed by vigorous shaking in 14 volumes of chilled distilled water and centrifuged at 14,000 g for 10 min. The red supernatant was removed, leaving behind a tight and loose pellet. The pellets were then washed in 14 volumes of imidazole-EDTA (10 mM imidazole-HCl, 1 mM EDTA, pH 7.0 at 23°C) by centrifugation at 14,000 g for 10 min. This washing was repeated about 8 times and the pale loose pellet was transferred to new 250 ml tube and washed in 14 volumes of imidazole-HCl (40 mM imidazole-HCl, pH 7.0 at 23°C). Finally, the loose pellets were pooled and washed in storage buffer (in mM: 130 KCl, 20 HEPES, 0.5 $MgCl_2$, 0.05 $CaCl_2$ and 2 DTT). The ghosts were then concentrated and stored in small aliquots at –80°C.

## 2.12 Protein estimation

Protein estimation was done with Bradford reagent (Bio-Rad, Hercules, CA) using bovine serum albumin to make the standard curve. Absorbance was measured at 595 nm.

## 2.13 Coupled enzyme ATPase assay

In this assay the ATP hydrolyzed by an ATPase to ADP is regenerated using the energy of oxidation of NADH which can be monitored using a spectrofluorometer (excitation at 340 nm and emission at 460 nm[99,166]. All the ATPase activities were determined at 37°C. The basal $Mg^{2+}$ ATPase activity was measured as a slope for the disappearance of NADH in a 135 µl assay solution containing the following in mM: 0.1 ouabain, 1 sodium azide, 0.005 thapsigargin, 100 NaCl, 20 KCl, 6 $MgCl_2$, 30 imidazole-HCl (pH 7.0), 0.5 EDTA, 0.5 EGTA, 0.2 NADH, 1 phosphoenol pyruvate, along with 0.006-0.02 mg ghost protein, excess pyruvate kinase-lactate dehydrogenase, 0.5 mM ATP, and 4 µg/ml calmodulin. After 6-7 min, 10 µl $CaCl_2$ was added to attain a final concentration of 0.55 mM and the disappearance of NADH monitored for another 13-14 min. The slope after the addition of $Ca^{2+}$ gave a measure of total ATPase activity. The difference in the ATPase activity in saturating (6 mM) $Mg^{2+}$ with and without $Ca^{2+}$ is defined as the $Ca^{2+}$-$Mg^{2+}$ATPase activity of PMCA. SERCA activity of 0.02-0.04 mg/ml fast twitch skeletal muscle microsomes was measured in the same assay solution in the absence of thapsigargin. The $Na^{+}$-$K^{+}$ ATPase activity

was measured in the same assay solution used to measure the basal $Mg^{2+}$ ATPase activity, except that ouabain, $Ca^{2+}$ and calmodulin were not added.

To test the effects of caloxins on the ATPase activity of PMCA, SERCA and the $Na^{+}$ pump, the membranes were incubated with different concentrations of the peptides on ice for 30 min before adding it to the assay solution in the cuvette. The $Ca^{2+}$-$Mg^{2+}$ATPase activity of PMCA in the absence of caloxin was taken as 100 % and the decrease in the activity in its presence was used to compute the percent inhibition.

To study the effect of caloxin on different PMCA isoforms, the ghost protein in the assay was replaced by membrane preparation of specific PMCA isoform. The microsomes from the insect cells overexpressing PMCA2 and 3 were kindly given by Dr. Filoteo[102]. The PM enriched fraction from the rabbit duodenal mucosa and the HEK-293 cells was obtained according to published protocol[128].

**2.14 ATPase assay based on hydrolysis of radioactive ATP**

This assay measures the inorganic orthophosphate $^{33}P_i$ released by hydrolysis of [$\gamma$-$^{33}$P]-ATP[172]. The 55 µl assay solution contained in mM: 30 imidazole–HCl pH 7.1, 0.4 EDTA, 0.33 EGTA, 3 $MgCl_2$, 0.2 ATP with trace amount of [$\gamma$-$^{33}$P]-ATP with 0 and 0.5 $CaCl_2$ plus 4 µg/ml calmodulin and 0.004-0.01 mg of ghost protein. The samples were incubated in a shaking water bath for 60 min at 37°C and then placed on ice. Then 10 µl of chilled solution of bovine serum albumin (1 mg/ml) and 100 µl of trichloroacetic acid-ATP solution (10 %

trichloroacetic acid solution, 50 mM unlabelled ATP) were added to each sample. The samples were vortexed and then centrifuged for 10 min at 10,000 g at 4°C. 100 µl of supernatant from each sample was transferred to new tubes and each sample was mixed with 200 µl of a solution containing 1 % (w/v) ammonium molybdate and 3.2 % (v/v) sulfuric acid. Butyl acetate (800 µl) was added to each tube and mixed. The tubes were then centrifuged at 14,000 g for 2 min. Supernatant from each tube was transferred to a scintillation vial and mixed with 5 ml of scintillation cocktail (Ready safe, Beckman). The samples were counted in the scintillation counter and the counts obtained after 3-4 h were used to determine the $Ca^{2+}$-$Mg^{2+}$-ATPase activity. To test the effects of caloxins on the ATPase activity, the ghost protein was incubated with different concentrations of caloxins on ice for 30 min before the start of the assay. The $Ca^{2+}$-$Mg^{2+}$-ATPase activity of PMCA was defined as the difference in the $^{33}P_i$ released in the presence and absence of $Ca^{2+}$. The $Ca^{2+}$-$Mg^{2+}$ATPase activity of PMCA in the absence of a caloxin was taken as 100 % and the decrease in the activity in its presence was used to compute the % inhibition.

While testing the effect of the photoreactive derivatives of caloxin 1c2 on PMCA activity in human erythrocyte membranes, 3Bpa1c2-biotin and 16Bpa1c2-biotin were found to interfere with the extraction of $^{33}P$ following the [$\gamma$-$^{33}P$]-ATP hydrolysis. Therefore, these peptide inhibitors were added to all the samples following the [$\gamma$-$^{33}P$]-ATP hydrolysis step to attain the same final concentration.

## 2.15 Phosphatase assay

The *p*-nitrophenylphosphate is a substrate for the phosphatases that catalyze its hydrolysis to *p*-nitrophenol, a chromogenic product that absorbs light at 405 nm. The $K^+$-$Mg^{2+}$-phosphatase activity was measured in an assay solution containing in mM: 100 imidazole-HCl pH 7.8, 5 *p*-nitrophenylphosphate, 5 $MgCl_2$, and 0 or 5 KCl, plus 0.02-0.05 mg of protein. The difference in the absorbance monitored at 405 nm in the presence and absence of $K^+$ is the $K^+$-$Mg^{2+}$-dependent phosphatase activity. The $Mg^{2+}$-phosphatase activity was measured in the same solution without KCl and in the presence and absence of 5 mM $MgCl_2$. The difference in the absorbance with and without $MgCl_2$ gave the $Mg^{2+}$-phosphatase activity[169].

## 2.16 Acylphosphate assays

The formation of the acid stable $Ca^{2+}$-dependent 140 kDa acylphosphate was determined with SDS-PAGE at pH 4.0 as previously described[128]. Human erythrocyte ghosts were incubated for 30 min at 0°C with given concentration of caloxin. The ghosts were then added to the reaction mixture, which had 100 mM KCl, 30 mM imidazole-HCl (pH 6.8 at 20-23°C), 0.05 mM $CaCl_2$, 4 μg/ml calmodulin, 0.4-0.7 mg/ml membrane protein and 0.005 mM ATP with trace amounts of [$\gamma$-$^{33}$P]-ATP in a volume of 0.2 ml. The reaction was run for 60 sec and then quenched with 0.25 ml of ice-cold stopping solution (TCAP) containing 10 % tricholoroacetic acid, 50 mM phosphoric acid and 0.5 mM unlabelled ATP. The proteins were precipitated after centrifugation at 4°C, the supernatant

discarded and the pellet washed again with TCAP. The proteins were then resuspended in MEDS buffer, pH 5.5, (10 mM MOPS, 1 mM EDTA, 10 % sucrose, 3 % SDS, 10 mM DTT and 0.01 % methyl green) and electrophoresed using 7.5 % SDS-PAGE at pH 4.0. The acylphosphate was quantified using PhosphorImager (Molecular Dynamics) to determine the intensity of each band after subtracting the background intensity.

### 2.17 Contractility studies and Cytosolic $Ca^{2+}$ measurements

Other researchers in our lab carried out studies to test the effects of caloxins 1b1 and 1c2 on the contractility of the arterial tissues[169]. The effects of caloxins 1b1 and 1a1 on the $[Ca^{2+}]_i$ in the cultured smooth muscle and endothelial cells were also studied as described[169,173].

### 2.18 Data Analysis

The values given are mean ± SEM. For non-competitive inhibition by caloxins in the presence of saturating substrates, the data were analyzed by non-linear regression using the equation: percent inhibition = 100 x [inhibitor]/($K_i$ + [inhibitor]). The curve fitting was done with FigP software (Biosoft Corporation, Ancaster, Ontario). Where applicable Student's t-test was used and values of $p < 0.05$ were considered to be statistically significant. The acyphosphates were quantified using a phosphorImager. The quantitative band intensity analysis in Western blot was carried out with Multi Gauge v 3.0 software (Fujifilm).

## 3.0 RESULTS

The present study had three aims. Aim 1 was to obtain a high affinity PMCA4 isoform selective caloxin using the N-terminal half of the exdom 1 (exdom 1X) of PMCA4 as a target, Aim 2 was to determine experimentally that the caloxin binds PMCA protein, and Aim 3 was to develop caloxins using the C-terminal half of the exdom 1 (exdom 1Y) of PMCA4 as a target.

### 3.1 Aim 1: Developing high affinity caloxins using the exdom 1X as target

The first caloxin, caloxin 2a1, was obtained by screening the Ph.D-12 library for binding to the synthetic peptide based on the sequence of exdom 2 of PMCA. Caloxin 2a1 selectively inhibited PMCA activity in human erythrocyte ghosts with an inhibition constant ($K_i$) value of 0.5 mM. The same method was used to obtain caloxin 3a1 for binding to the synthetic exdom 3 peptide of PMCA. Caloxin 3a1, like the prototype caloxin 2a1, selectively inhibited the PMCA activity in human erythrocyte ghosts with a $K_i$ of 0.2 mM. Thus, both caloxins 2a1 and 3a1 were selective for PMCA inhibition but had a low affinity. It was hypothesized that the synthetic exdom peptides used as targets to screen the Ph.D-12 library may differ in conformation from the exdoms in the native PMCA protein, thus, resulting in the low affinity of the caloxins. Furthermore, the exdom 2 and 3 are quite similar in PMCA isoforms 1, 2, 3 and 4 and cannot be used to obtain caloxins with isoform selectivity. However, the exdom 1 sequence differs considerably between these PMCA isoforms. Therefore, the exdom 1 of PMCA4 was chosen as a target to obtain high affinity caloxins with PMCA4 isoform

selectivity. However, the exdom 1 (amino acids 116-147) is long and contains a cysteine in the middle that can produce uncertainties in configuration of the exdom. Therefore, it was decided to use the N-terminal half of the exdom 1 (exdom 1X) of PMCA4 (amino acids 116-131) as a target. The overall rationale behind the strategy was: a) to develop a screening process to select the phage encoded 12-amino acid peptide that will recognize the exdom in PMCA protein and inhibit its activity with a high affinity, b) to construct and screen a Ph.D library based on the limited mutagenesis of the selected peptide to further increase its affinity and isoform selectivity without altering the inhibitory potential.

### 3.1.1 Screening of the Ph.D-12 library

The Ph.D-12 library was screened to select the phage encoded 12-amino acid peptide that would bind selectively to the exdom 1X of PMCA4. A method was developed to screen the library in two-steps. In the first step, the Ph.D-12 library was screened in 3 rounds using the synthetic peptide based on the sequence of the exdom 1X of PMCA4 as a target. This step would result in the enrichment of the phage pool with a bias towards the synthetic exdom 1X. In the second step, the screening was carried out with purified PMCA protein to allow for the selection of the phage-encoded peptide that recognizes the exdom 1X in the conformation present in PMCA protein. Human erythrocyte ghosts that express mainly PMCA4 were used as a source of purified PMCA[47]. The ability of PMCA to bind calmodulin only in the presence of $Ca^{2+}$ formed the basis of the second step of screening. The phage selected after the two-step screening was

tested for its ability to bind to synthetic exdom 1X and then the corresponding phage encoded peptide was synthesized. The peptide was tested for the inhibition of PMCA activity and for its effects on cultured cells and tissues.

### *3.1.1.1 Two-step screening of Ph.D-12 library using PMCA4 exdom 1X*

The exdom 1 of human PMCA4 is long and consists of residue 116-147 (SLVLSFYRPAGEENELCGQVATTPEDENEAQA). The presence of cysteine in the middle produces an uncertainty in the conformational differences between the synthetic peptide target and the exdom as a target in PMCA protein. Therefore, the exdom 1 was divided into exdom 1X and 1Y around the cysteine. The synthetic exdom 1X (SLVLSFYRPAGEENEL) was used as a target for the first step of screening. The peptide was synthesized with a cysteine added at the N-terminus to conjugate it to KHLH or ovalbumin. The mixture of the synthetic exdom 1X and its KHLH conjugate was used as the binding target while its ovalbumin conjugate was used for the elution as described in the Experimental Methods. The screening was started with $10^{11}$ pfu of the Ph.D-12 library and the phage eluted after each round was amplified to keep the input pfu constant for the next round. The phage pool enriched after three rounds of screening with the synthetic target was used in the second step of screening by 2 rounds of affinity chromatography with PMCA protein purified from human erythrocyte ghosts, which express mainly PMCA4[47]. The input pfu for affinity chromatography was kept constant with $2x10^8$ pfu. After two rounds of affinity chromatography, the phage pool was subjected to another round of screening with the synthetic exdom

1X target, which was followed by the last round of screening using PMCA affinity chromatography.

The phage from the last round of the screening was titered, 45 phage clones were picked and amplified, and the phage DNA was sequenced. Out of a total of 45 clones, 44 encoded for the consensus 12-amino acid peptide sequence TAWSEVLHLLSR.

### *3.1.1.2 Selectivity of the obtained phage clone for the exdom 1X*

The phage clone encoding the consensus peptide sequence in *3.1.1.1* was obtained by two-step screening of the Ph.D-12 library using the exdom 1X of PMCA4 as a target. The selectivity of the obtained phage clone for binding to the exdom 1X of PMCA4 was tested using the synthetic exdom 1X. The phage clone or an equal titer ($10^{10}$ pfu) of the PhD-12 random library were allowed to bind to two coating targets: a) the mixture of synthetic exdom 1X and its KHLH conjugate as the selective target and, b) KHLH alone as the negative control. The phage bound to the selective target was eluted with ovalbumin conjugate of the synthetic exdom 1X and those for the negative control with ovalbumin. The titer of the eluted phage was highest when the binding was carried out with the phage clone using the selective target (Fig. 3.1). Thus, as expected the phage clone bound selectively to the synthetic exdom 1X target and the binding was much higher with this clone than for the random Ph.D-12 library.

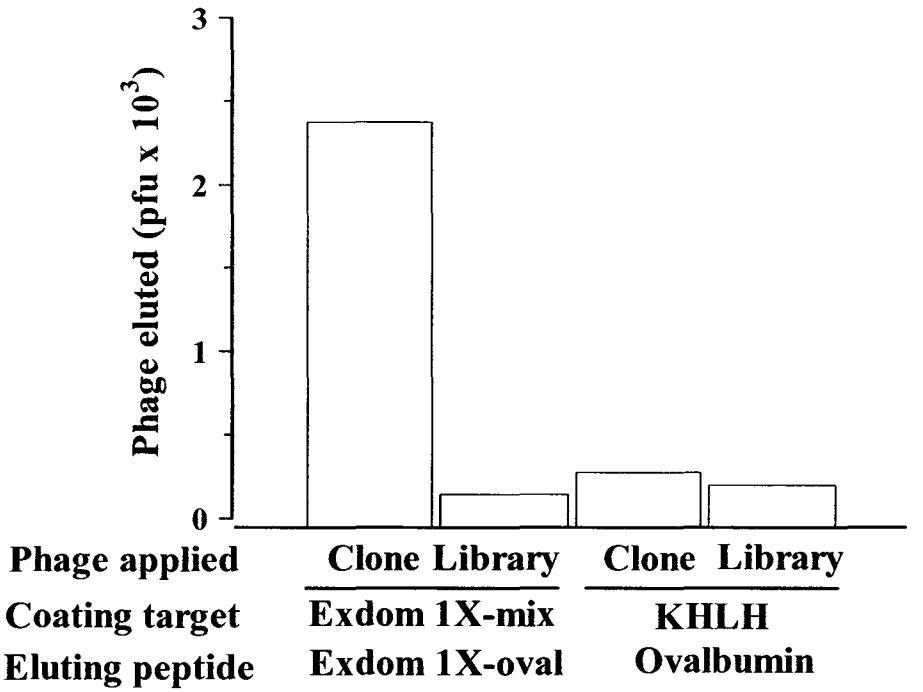


**Fig. 3.1. Selectivity of phage clone.**

Mixture of the synthetic exdom 1X and its KHLH conjugate (Exdom 1X-mix) or KHLH alone was used as the coating target with $10^{10}$ pfu of the phage clone obtained in *3.1.1.1* or the Ph.D-12 library. The phage bound to the Exdom 1X-mix and KHLH was eluted with ovalbumin conjugate of the exdom 1X (Exdom 1X-oval) and ovalbumin, respectively. Shown are titers of the eluted phage.

### *3.1.1.3 Caloxin 1b1 modulates the $Ca^{2+}$-$Mg^{2+}$ ATPase activity of PMCA*

In the phage, the displayed 12-amino acid peptide sequence continues into GGGS spacer and then the remainder of the pIII coat protein. The phage-encoded peptide (*3.1.1.1*) was synthesized with inclusion of the GGG spacer at its C-terminus and termed caloxin 1b1 (TAWSEVLHLLSRGGG-amide). P-type ATPases are expected to involve long-range conformational interactions to couple the processes of ATP hydrolysis in the cytosolic domain to the ion transport in the TM domains[174]. Therefore, it was hypothesized that caloxin 1b1 would modulate the $Ca^{2+}$-stimulated $Mg^{2+}$ ATPase activity of PMCA by binding to its exdom 1X.

PMCA activity was measured in an ATPase assay by isotopic determination of inorganic phosphate released from [$\gamma$-$^{33}$P]-ATP or in an ATP regenerating coupled enzyme assay where ATP hydrolysis is coupled to the oxidation of NADH as described in the Experimental Methods. The assay solution for measuring PMCA activity contained thapsigargin, ouabain and sodium azide to inhibit SERCA, the $Na^+$-$K^+$ ATPase and the mitochondrial $Ca^{2+}$ ATPase, respectively.

In an initial experiment, it was determined that caloxin 1b1 did not affect the coupled enzyme assay by itself. The formation of ATP by addition of excess ADP (1 mM) causes a rapid decrease in the NADH fluorescence in the coupled enzyme assay (not shown). This rapid decrease was observed even in the presence of caloxin 1b1 at a concentration as high as 200 μM (Fig. 3.2A). Therefore, the

subsequent results obtained with caloxin 1b1 are not the artifacts of its effects on the assay system.

Next, the effect of caloxin 1b1 on the $Ca^{2+}$-$Mg^{2+}$ATPase activity of PMCA was tested using leaky human erythrocyte ghosts, which contain mostly PMCA4. The difference in the $Ca^{2+}$-$Mg^{2+}$ATPase activity decreased markedly in the presence of 200 μM caloxin 1b1 (Fig. 3.2B). Thus, caloxin 1b1 inhibited the $Ca^{2+}$-$Mg^{2+}$ATPase activity of PMCA in human erythrocyte ghosts. Caloxin 1b1 also inhibited the $Ca^{2+}$-$Mg^{2+}$ATPase activity of PMCA protein purified from human erythrocyte ghosts by affinity chromatography using calmodulin-agarose. This suggested that the inhibition was likely due to the direct action on PMCA rather than due to interaction with other proteins present in the ghosts. Human erythrocyte ghosts mainly express PMCA4, while the pig aortic smooth muscle PM expresses both PMCA1 and 4, although the relative amount of these proteins in the smooth muscle is not known. Caloxin 1b1 also inhibited the $Ca^{2+}$-$Mg^{2+}$ATPase activity in the PM enriched fraction isolated from the pig aortic smooth muscle (Fig. 3.2B). The inhibition with 200 μM caloxin 1b1 in the aortic smooth muscle PM preparation (82 ± 10 %) was similar to that obtained with human erythrocyte ghosts (79 ± 8 %).

#### *3.1.1.4 Inhibition constant of caloxin 1b1 for PMCA in erythrocyte ghosts*

The effect of different concentrations of caloxin 1b1 on the $Ca^{2+}$-$Mg^{2+}$ATPase activity of PMCA in leaky human erythrocyte ghosts was tested first

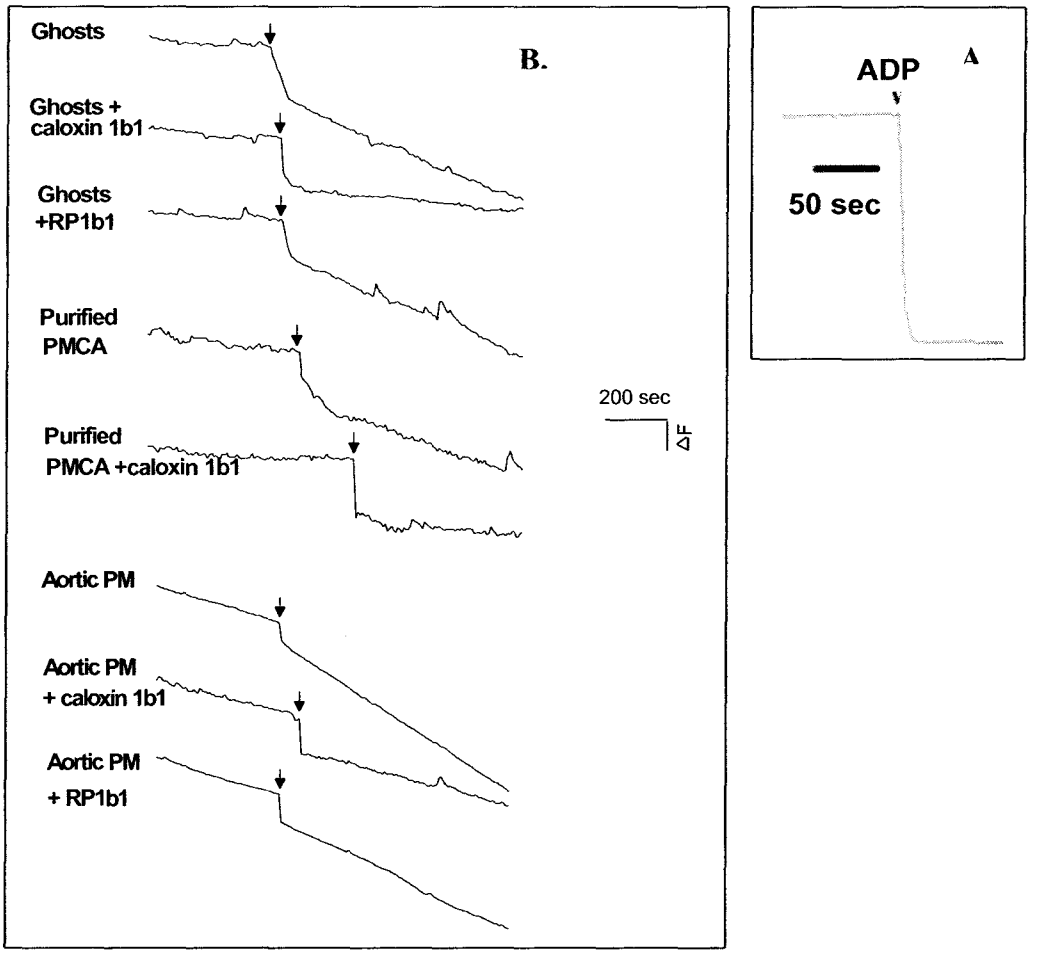


**Fig. 3.2. Traces showing the coupled enzyme assay for ATPase.**

**A**. 200 μM caloxin 1b1 did not inhibit the rapid disappearance of NADH fluorescence by 1 mM ADP. **B**. PMCA activity measured as the difference in the slopes of the NADH fluorescence in the presence and absence of $Ca^{2+}$. The scale △F indicates the change in the fluorescence corresponding to 1 nmole NADH for ghosts, 0.8 nmole for purified PMCA and 2.4 nmole for PM enriched fraction. The arrow indicates the time of addition of $Ca^{2+}$. The rapid decrease in the slope at the time of addition of $Ca^{2+}$ is due to the dilution effect. The amino acid sequence of caloxin 1b1 was randomized using random number generator on Lotus 123 and a randomized peptide (RP1b1: GAETLSHGLRLGSVW-amide) was synthesized. The RP1b1 was used as a control peptide to test for the sequence specificity of caloxin 1b1. Modified from reference 169.

in the coupled enzyme assay and then by following the hydrolysis of [$\gamma$-$^{33}$P]-ATP. Caloxins are obtained for binding to the exdoms of PMCA and hence are expected to be non–competitive with respect to its various substrates, which bind to the cytosolic domains of the pump. The non-competitive nature of the inhibition has been demonstrated for caloxin 2a1. Therefore, the effect of caloxin 1b1 on PMCA activity was tested under saturating substrate concentrations. Fig. 3.3 shows the inhibition using 0, 20, 40, 60, 80, 100, 200 and 500 μM caloxin 1b1 on the $Ca^{2+}$-$Mg^{2+}$ATPase activity of PMCA. Using these data points and assuming 100 % inhibition, the data were fitted into the inhibition curve described in the Experimental Methods. Caloxin 1b1 produced 50 % inhibition of PMCA activity ($K_i$) at a concentration of 46 ± 5 μM. Fig. 3.4 shows a similar experiment in which PMCA activity was determined by monitoring the hydrolysis of [$\gamma$-$^{33}$P]-ATP. This assay gave results similar to those obtained with coupled enzyme assay with a $K_i$ of 48 ± 4 μM (Fig. 3.4).

#### *3.1.1.5 PMCA isoform preference of caloxin 1b1*

The phage encoding caloxin 1b1 was selected for binding to the synthetic exdom 1X (PMCA4) and to PMCA protein from human erythrocyte ghosts (mainly PMCA4). There are few conservative and non-conservative differences in the exdom 1X amongst PMCA isoforms 1-4 (Fig. 1.2). Therefore, two hypotheses were tested: a) there are sufficient similarities in the exdom 1X of PMCA isoforms 1-4 so that caloxin 1b1 will inhibit the activity of PMCA1-3 and b) due

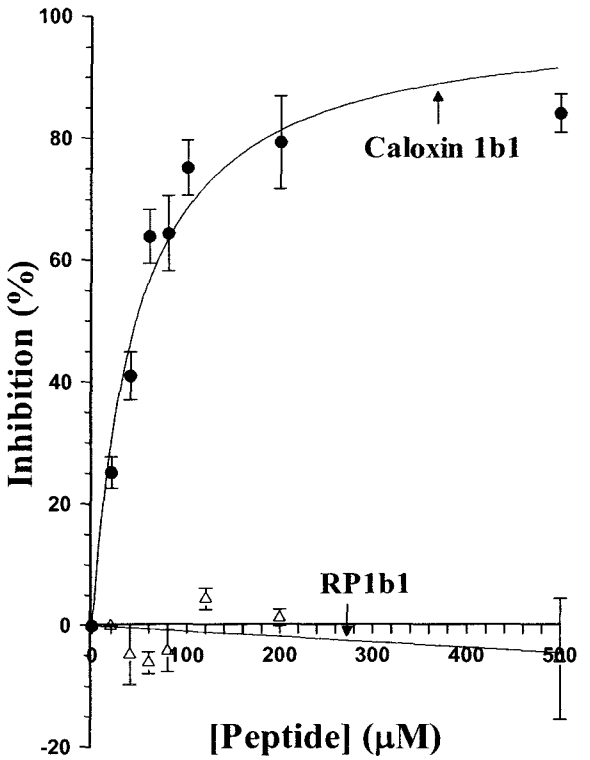


**Fig. 3.3. Caloxin 1b1 inhibition of PMCA activity in leaky human erythrocyte ghosts measured by coupled enzyme assay.**

The difference between the slopes of the NADH fluorescence in the presence and absence of $Ca^{2+}$ is the $Ca^{2+}$-$Mg^{2+}$ATPase activity of PMCA. For each experiment, the data were normalized with the mean value of the $Ca^{2+}$-$Mg^{2+}$ATPase activity in the absence of caloxin 1b1 taken as 100 %. Each value is mean ± SE from 3-4 experiments. The data for caloxin 1b1 fit best ($r^2 = 0.9657$) with the $K_i$ (inhibition constant) of 46 ± 5 μM. RP1b1: randomized caloxin 1b1 peptide. Modified from reference 169.

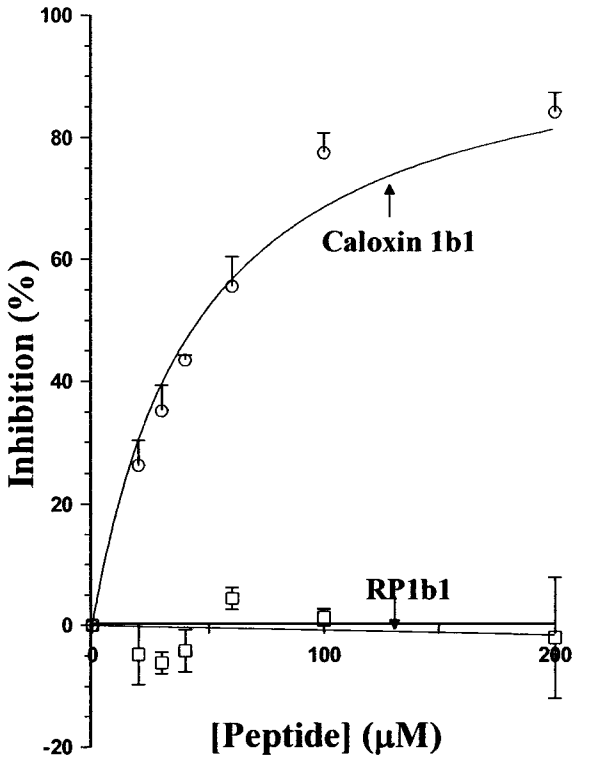


**Fig. 3.4. Caloxin 1b1 inhibition of PMCA activity in leaky human erythrocyte ghosts measured by hydrolysis of [γ-$^{33}$P]-ATP.**

The difference in the activity with and without the addition of $Ca^{2+}$ is the $Ca^{2+}$-$Mg^{2+}$ATPase activity of PMCA. The experiment was carried out on 2 different days. For each day, the data were normalized with the mean value of the $Ca^{2+}$-$Mg^{2+}$ATPase activity in the absence of caloxin 1b1 taken as 100 %. Each value is mean ± SE from 8-12 replicates for caloxin 1b1 and 4 replicates for RP1b1. The data for caloxin 1b1 fit best ($r^2$ = 0.9875) with the $K_i$ of 48 ± 4 μM. RP1b1: randomized caloxin 1b1 peptide.

to the differences in the sequence of the exdom 1X in PMCA isoforms 1-4, caloxin 1b1 will inhibit PMCA4 with higher affinity as compared to PMCA1-3. The hypotheses were tested by comparing the effects of caloxin 1b1 on leaky human erythrocyte ghosts (mainly PMCA4), the PM enriched fractions from the HEK-293 cells and the rabbit duodenal mucosa (mainly PMCA1), and microsomes from the SF9 insect cells overexpressing PMCA2 and 3 isoforms respectively (Fig. 3.5). ATP and $Ca^{2+}$ access PMCA on the cytosolic side, while caloxin 1b1 is expected to bind on the extracellular side. Therefore, to make PMCA accessible from both the sides, the PM vesicles were permeabilized by preincubation with 0.1 % Triton X-100 for 30 min. The HEK-293 PM preparation had high basal $Mg^{2+}$ATPase, which also decreased following the preincubation with 0.1 % Triton X-100 for 30 min. In the control experiment, the detergent at the same concentration had no effect on caloxin 1b1 inhibition of the $Ca^{2+}$-$Mg^{2+}$ATPase in human erythrocyte ghosts.

Caloxin 1b1 inhibited PMCA isoforms 1, 2, 3 and 4. However, the inhibition required higher concentrations of caloxin 1b1 with the PM enriched fraction from the HEK-293 cells than with the ghosts. Caloxin 1b1 inhibited PMCA1 in the PM enriched fraction from the HEK-293 cells with a 2 fold lower affinity ($K_i$: 105 ± 11 μM) than in the erythrocyte ghosts (PMCA4, $K_i$: 46 ± 5 μM). Caloxin 1b1 also inhibited PMCA2 ($K_i$: 167 ± 67 μM) and 3 (274 ± 40 μM with a lower affinity than PMCA4. Thus, caloxin 1b1 inhibited all the isoforms of

PMCA but it showed slightly higher affinity for PMCA4 than for other three PMCA isoforms.

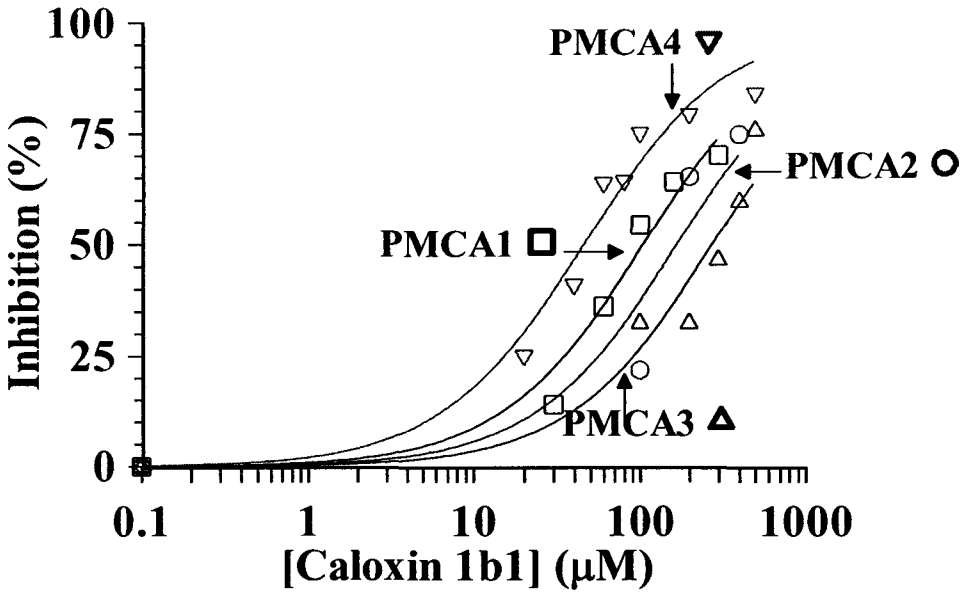


**Fig. 3.5. Caloxin 1b1 inhibition of $Ca^{2+}$-$Mg^{2+}$ATPase activity of PMCA1-4 measured by coupled enzyme assay.**

The sources of PMCA isoforms are: PMCA1 (PM enriched fraction of HEK293 cells), PMCA2 and 3 (PM enriched fraction of SF9 insect cells overexpressing PMCA isoforms 2 and 3 respectively), PMCA4 (leaky human erythrocyte ghosts). Each value is the mean of 3-4 experiments done on 2-4 different days. For each day, the data were normalized with the mean value of the activity in the absence of caloxin 1b1 taken as 100 %. The data fit best with the $K_i$ values of 105 ± 11 μM (PMCA1), 167 ± 67 μM (PMCA2), 274 ± 40 μM (PMCA3) and 46 ± 5 μM (PMCA4). Modified from reference 169a.

### *3.1.1.6 Inhibition by caloxin 1b1 and its randomized peptide*

The Ph.D-12 library contains 2.7 x$10^9$ independent electroporated sequences that provide sufficient diversity to encode a peptide that would bind to a given target. Caloxin 1b1 encoding phage dominated the clones selected after two-step screening of the Ph.D-12 library for binding to the exdom 1X of PMCA4. The inhibition of the $Ca^{2+}$-$Mg^{2+}$ATPase activity of PMCA by caloxin 1b1 is thus expected to be dependent on its amino acid sequence (TAWSEVLHLLSRGGG). A randomized peptide RP1b1 (GAETLSHGLRLGSVW) with the same amino acid composition as caloxin 1b1, but in a different sequence was used to test this hypothesis.

A representative tracing of the NADH fluorescence in the coupled enzyme assay is shown in Fig. 3.2. In the absence of any peptide, the difference in the slopes in presence and absence of $Ca^{2+}$ is large for both leaky human erythrocyte ghosts and the PM enriched fraction isolated from the pig aortic smooth muscle. This difference in the slopes did not change in the presence of 200 μM RP1b1, in contrast to the marked decrease in the presence of 200 μM caloxin 1b1. The effect of different concentrations of both caloxin 1b1 and RP1b1 on PMCA $Ca^{2+}$-$Mg^{2+}$ATPase in leaky human erythrocyte ghosts was tested in a coupled enzyme assay (Fig. 3.3) and by following the [γ-$^{33}$P]-ATP hydrolysis (Fig. 3.4). Caloxin 1b1 inhibited PMCA $Ca^{2+}$-$Mg^{2+}$ATPase in human erythrocyte ghosts in both the assays while RP1b1 at concentrations as high as 500 μM had no effect on PMCA

activity. Thus, the amino acid sequence of caloxin 1b1 is essential for the inhibition.

### *3.1.1.7 PMCA selectivity of caloxin 1b1 over other ATPases*

PMCA belongs to the family of P-type ATPases whose other members include the $Na^+$-$K^+$-ATPase, the $H^+$-$K^+$ ATPase and SERCA. During the ion transport process, all the members of the P-type ATPases form a phosphorylated intermediate involving a few conserved residues that reside within their cytosolic domains[53]. The exdoms of PMCA, however, do not share any significant homology with the other members of P-type ATPases. Therefore, it was hypothesized that the effects of caloxin 1b1 is specific for PMCA over other ATPases.

The fast twitch skeletal muscle microsomes from rabbit were used to study the effect of caloxin 1b1 on the $Ca^{2+}$-$Mg^{2+}$ATPase activity of SERCA1. Thapsigargin was omitted from the assay solution since it inhibits SERCA activity, which was monitored by following the hydrolysis of [$\gamma$-$^{33}$P]-ATP. Caloxin 1b1 did not affect the $Ca^{2+}$-$Mg^{2+}$ ATPase activity of SERCA at any given concentration (Fig. 3.6A). The effect of caloxin 1b1 on SERCA activity was also tested using the coupled enzyme assay. Even at concentrations as high as 500 μM, caloxin 1b1 did not cause any significant inhibition as 97 ± 3 % (4 replicates) of SERCA activity still remained.

The effect of caloxin 1b1 on the $Na^+$-$K^+$-ATPase in human erythrocyte ghosts was tested using the coupled enzyme assay solution that did not contain

ouabain, the specific inhibitor of this enzyme (Fig. 3.6B). The effect of caloxin 1b1 on the $K^+$-$Mg^{2+}$ phosphatase, which is a partial reaction of the $Na^+$-$K^+$-ATPase, was determined by following the hydrolysis of *p*-nitrophenylphosphate in the absence of ouabain. The difference in the extent of hydrolysis of *p*-nitrophenylphosphate monitored by the absorbance at 405 nm in the presence and absence of KCl is the $K^+$-$Mg^{2+}$ phosphatase activity (Fig. 3.6C). At concentrations as high as 200-500 μM, caloxin 1b1 did not inhibit the $Na^+$-$K^+$-ATPase or the $K^+$-$Mg^{2+}$ phosphatase in leaky human erythrocyte ghosts.

The effect of different concentrations of caloxin 1b1 on the $Mg^{2+}$ ATPase activity in leaky human erythrocyte ghosts and the PM enriched fraction of HEK-293 cells was tested using the coupled enzyme assay in the absence of $Ca^{2+}$. At any given concentration, caloxin 1b1 did not inhibit the $Mg^{2+}$ ATPase activity of human erythrocyte ghosts or the PM enriched fraction of HEK-293 cells (Fig. 3.6E,F). The effect of different concentrations of caloxin 1b1 on the $Mg^{2+}$ phosphatase in leaky human erythrocyte ghosts was determined by following the hydrolysis of *p*-nitrophenylphosphate. The difference in the extent of hydrolysis of *p*-nitrophenylphosphate monitored by the absorbance at 405 nm in the presence and absence of $MgCl_2$ is the $Mg^{2+}$ phosphatase activity. At concentrations as high as 500 μM, caloxin 1b1 did not have any effect on the $Mg^{2+}$ phosphatase of human erythrocyte ghosts (Fig. 3.6D). Thus, caloxin 1b1 did not have any effect on the activity of various ATPases and phosphatases tested. Therefore, caloxin 1b1 is a specific inhibitor of PMCA.

### *3.1.1.8 Effect of caloxin 1b1 on PMCA acylphosphate levels*

PMCA like other members of P-type ATPases forms a high-energy acylphosphate intermediate during its reaction cycle. These ATPases cycle between two conformational states, E1 and E2. ATP phosphorylates the E1 conformation at a conserved aspartate residue in the cytosolic domain during the ion transport process[53]. Thapsigargin, a specific inhibitor of SERCA that binds to its luminal loops, inhibits the formation of acylphosphate intermediate during its reaction cycle[175]. Thus, it was hypothesized that caloxin 1b1 may affect the steady state level of acylphosphate intermediate formed during the reaction cycle of PMCA.

PMCA forms a $Ca^{2+}$dependent acid stable 140 kDa phosphorylated intermediate from ATP during its reaction cycle[128]. Caloxin 2a1, which was selected for binding to exdom 2, inhibited the formation of the acylphosphate intermediate from ATP. Caloxin 3a1, selected for binding to exdom 3, which is conserved in all the four PMCA isoforms, did not have any effect on the formation of the acylphosphate. Thus, different exdoms may play a different role in PMCA function. The effect of caloxin 1b1 was tested on the acylphosphate intermediate formation in the reaction cycle of PMCA (Fig. 3.7).

The acylphosphate intermediate formed by [$\gamma$-$^{33}$P]-ATP in human erythrocyte ghosts gave only one band at ~140 kDa (lane 1). The acylphosphate

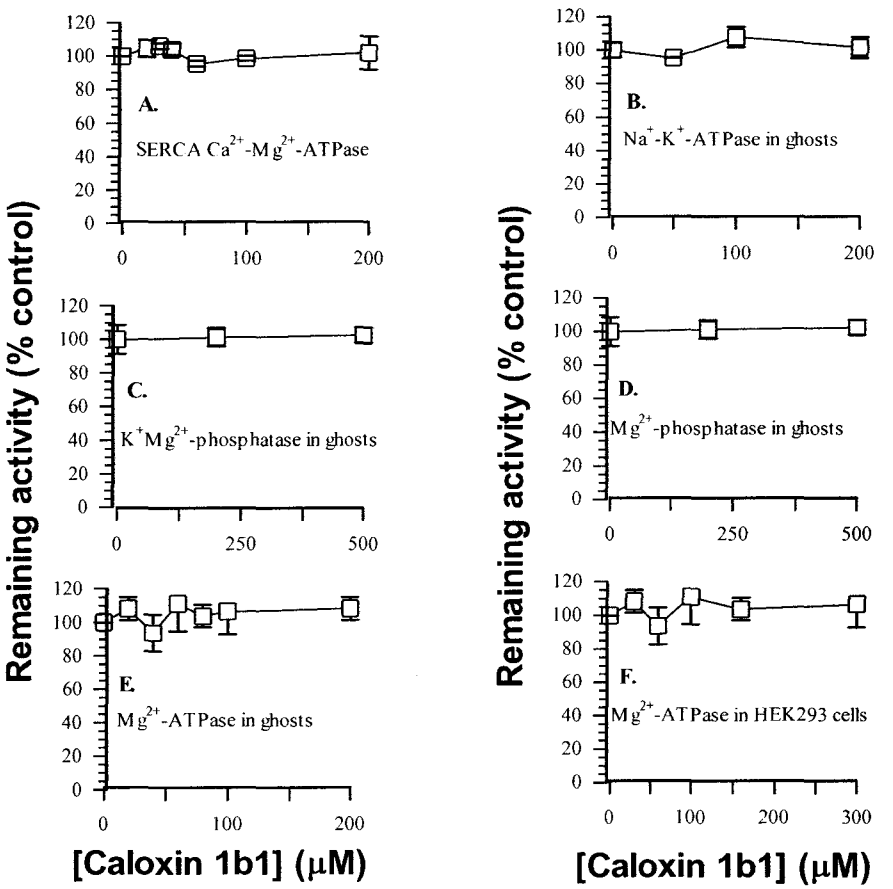


**Fig. 3.6. Effect of caloxin 1b1 on various ATPases.**

The activity in the absence of caloxin 1b1 was taken as 100 % and the activity in its presence was used to compute the % activity remaining. **A.** SERCA in the fast twitch skeletal muscle microsomes. The values are mean ± SE from 4 replicates. **B.** $Na^+$-$K^+$ ATPase in human erythrocyte ghosts. The values are mean ± SE of 2 replicates at each concentration of caloxin 1b1 and 5 replicates in the absence of caloxin 1b1. **C.** $K^+$- $Mg^{2+}$ phosphatase in human erythrocyte ghosts. The values are mean ± SE of 4 replicates. **D.** $Mg^{2+}$ phosphatase in human erythrocyte ghosts. The values are mean ± SE of 4 replicates. $Mg^{2+}$ ATPase activity in human erythrocyte ghosts (**E**), and the HEK-293 microsomes (**F**). The values are mean ± SE of 2-4 replicates at each concentration of caloxin 1b1 and 4 replicates without caloxin 1b1. Modified from reference 169.

formation was $Ca^{2+}$dependent and disappeared in the presence of the $Ca^{2+}$ chelator EGTA (lane 4). Preincubation of the erythrocyte ghosts with 500 μM caloxin 1b1 before the phosphorylation reaction increased the intensity of the band at 140 kDa by 48 ± 7 % ($P < 0.05$) as measured in 14 gels (lane 3). RP1b1 did not have any effect on the intensity of the band at 140 kDa (lane 2).

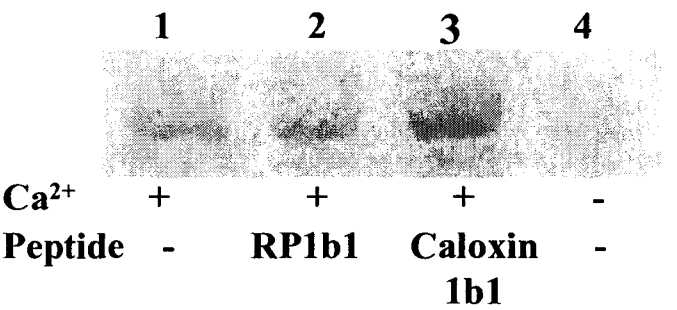


**Fig. 3.7. Effect of caloxin 1b1 on the 140-kDa acylphosphate intermediate of PMCA.**

Human erythrocyte ghosts were preincubated with caloxin 1b1 or RP1b1. The acylphosphate formation was carried out with [γ-$^{33}$P]-ATP and the samples analyzed by acid gel electrophoresis. The final concentration of peptides was 500 μM. Lane 4 contained 1 mM EGTA, the $Ca^{2+}$chelator.

#### *3.1.1.9 Physiological effects of caloxin 1b1*

Caloxin 1b1 increased the sensitivity of de-endothelialized rat thoracic aortic rings for contraction to phenylephrine but did not affect endothelium dependent relaxation in response to carbachol. The effect of caloxin 1b1 was also tested on the smooth muscle and endothelial cells cultured from pig coronary artery. Caloxin 1b1 increased basal $[Ca^{2+}]_i$ in both smooth muscle that expresses PMCA isoform 1 and 4, and endothelial cells that express mainly PMCA1, but the effect was more pronounced on the smooth muscle cells. These effects of caloxin 1b1 are presented in detail in App. 1.

### 3.1.2 Limited mutagenesis of caloxin 1b1 to obtain caloxin 1c2

Caloxin 1b1 ($K_i$: 46 ± 5 μM) has a 10-fold higher affinity for PMCA in leaky human erythrocyte ghosts than the prototype caloxin 2a1 (529 ± 109 μM). It was obtained by screening the Ph.D-12 library using the exdom 1X (PMCA4) as a target. The Ph.D-12 library contains 2.7 $x10^9$ independent electroporated sequences. While this allows for a large diversity, it also means that only a limited number of copies of each peptide sequence would be present in the $10^{11}$ pfu used for screening. The clones not selected in the initial rounds of screening, particularly because the initial screening was carried out with the synthetic exdom 1X, they would not be present in the subsequent rounds of screening. This presents the possibility that a caloxin 1b1-like sequence that may have higher affinity for the exdom in PMCA may not have been selected during the initial

rounds of screening. It was hypothesized that a caloxin 1b1-like peptide may have higher affinity and selectivity for PMCA4. Such a peptide may differ from caloxin 1b1 in one, two or three amino acids and may increase its affinity and selectivity without affecting the inhibitory potential. The overall strategy to obtain caloxin 1c2 involved constructing Ph.D caloxin 1b1-like peptide library, followed by its screening by affinity chromatography using PMCA protein purified from human erythrocyte ghosts to select peptides with a affinity higher than that of parent caloxin 1b1.

#### *3.1.2.1 Construction of Ph.D caloxin 1b1-like peptide library*

The 12-amino acid caloxin 1b1 sequence is encoded by a 36 base long oligonucleotide $(NNN)_{12}$ that is fused via short spacer to the pIII coat protein encoding DNA of the M13 bacteriophage. It was computed that retaining 91 % of the original base at each of the 36 base positions in $(NNN)_{12}$ and replacing the remainder with equal percent of the other three bases would be optimum to maximize the proportion of the peptides that differ from caloxin 1b1 by 1, 2 or 3 amino acid changes. Altering a smaller proportion of residues in $(NNN)_{12}$ would bias the resulting peptide library towards the original caloxin 1b1 sequence, while changing a larger proportion of residues would result in higher number of phage clones encoding peptides with >3 amino acid substitutions. The mixture of oligonucleotides with the optimum substitutions for encoding caloxin 1b1-like peptides was synthesized as shown in Fig. 3.8. The plus and minus strand of caloxin 1b1 encoding oligonucleotide $(NNN)_{12}$ is bolded. At its 5' end, the

$(NNN)_{12}$ is preceded by conserved bases that encode the leader sequence, which is cleaved upon secretion, thereby expressing the first residue of the random peptide at the N-terminus of the pIII coat protein. At the 3' end, $(NNN)_{12}$ is flanked by conserved bases encoding a short spacer (GGGS) and part of the pIII coat protein of the M13 bacteriophage. The bolded sequence encoding caloxin 1b1 was altered for the construction of the Ph.D caloxin 1b1-like peptide library. A mixture of single stranded oligonucleotides retaining 91 % of the original base and replacing the remainder with equal percent of other three bases in the minus strand of caloxin 1b1 encoding oligonucleotide was synthesized (Fig. 3.8).

The mixture of oligonucleotides was first used to construct a small-scale Ph.D caloxin 1b1-like peptide library. A sample of 42 clones from the small-scale library was sequenced (Table 3.1). The statistical analysis showed that there was no difference in the observed and the expected frequencies of the peptides with 0, 1, 2, 3 or >3 amino acid substitutions in the small-scale library (Table 3.2). A large-scale Ph.D caloxin 1b1-like peptide library was constructed by scaling up the ligations used to construct the small-scale library. The Ph.D caloxin 1b1-like peptide library had a diversity of $7x10^5$ pfu.

### *3.1.2.2 First screening of Ph.D caloxin 1b1-like peptide library*

The Ph.D caloxin 1b1-like peptide library was amplified once and then $2x10^8$ pfu were used for screening by 4 rounds of affinity chromatography with PMCA protein purified from human erythrocyte membranes. Since amplification may introduce bias due to differential amplification efficiencies of individual

phage clones, the phage pool was not amplified in between the 4 rounds of screening by affinity chromatography. The titers of the phage decreased with each round of screening until only 315 pfu remained after the 4th round. Of these, 104 phage clones were sequenced and they encoded 33 different types of peptides as shown in Table 3.3. There were 22 copies of the parent caloxin 1b1 peptide with no amino acid change. Most of the phage encoded peptides selected after 4 rounds of affinity chromatography differed from the parent caloxin 1b1 by 1 or 2 amino acids only. These amino acid differences were restricted to the first two or last five residues in 12-amino acid peptides. Caloxin 1b1 contained residues WSEVL at position 3-7. These amino acids or their conservative substitutions (WS(E/D)V(L/V) appeared at the given positions in 88 % of the total 104 clones sequenced.

**A.** Caloxin 1b1 (TAWSEVLHLLSR) encoding oligonucleotide $(NNN)_{12}$ in the phage genome is bolded.

Plus strand: 5'-

CATGCCCGGGTACCTTTCTATTCTCACTCT**ACTGCTTGGAGTGAGGT**

**TTTGCATCTTTTGTCGAGG**GGTGGAGGTTCGGCCGAAACATG-3'

Minus strand: 5'

CATGTTTCGGCCGAACCTCCACC**CCTCGACAAAAGATGCAAAACCTC**

**ACTCCAAGCAGT**AGAGTGAGAATAGAAAGGTACCCGGGCATG-3'

**B.** Substitution of bases in the minus strand of caloxin 1b1 oligonucleotide by retaining 91 % of the original base at each position.

5'CATGTTTCGGCCGAACCTCCACC**778765755556586755557787578 77**

**5567568**AGAGTGAGAATAGAAAGGTACCCGGGCATG-3' where

5= **A**:G:C:T **91**:3:3:3

6= A:**G**:C:T 3:**91**:3:3

7= A:G:**C**:T 3:3:**91**:3

8= A:G:C:**T** 3:3:3:**91**

**Fig. 3.8. Mixture of oligonucleotides encoding caloxin 1b1-like peptides.**

**A.** The caloxin 1b1 encoding oligonucleotide duplex (bold) is flanked by conserved sequences of the M13 phage. **B.** The oligonucleotide mixture was synthesized by retaining 91 % of the original base in the minus strand of the caloxin 1b1 oligonucleotide. 5 = 91 % A (and 3 % of other 3 bases), 6 = 91 % G, 7 = 91 % C and 8 = 91 % T.

| | | |
|---|---|---|
| TAWSEVL**P**LLSR | TAW**TD**VLHL**WW**R | **NA**SSEVLHLLSR |
| **S**AWS**A**VLH**IS**SR | TAWS**QD**LHL**F**SR | **TTC**SE**AWP**L**W**SR |
| TA**L**SEV**MN**LLSR | TA**C**SEVL**YL**V**S**T | TAWSEVLH**QF**SR |
| TAW**C**EVLHLLS**L** | TA**PR**EVLH**P**LSR | **TS**WSEVLHL**M**SR |
| TAC**S**EV**SDLFSK** | TAWSEV**SR**LLSR | TAWSE**D**LHLLSR |
| TA**R**SEVLHLLSR | TAWSEVLHL**V**S**M** | TAWSEVLH**QF**SR |
| TAWSEVLHLLSR | T**G**WSEV**S**HLLSR | TAWS**QD**LHL**F**SR |
| TA**R**SEVLHLLSR | TA**SSEHLLL**LSR | TA**PR**EVLH**P**LSR |
| TSWSEVLHL**M**SR | TAWSE**D**LHLLSR | TAWSEVLHLLSR |
| TA**R**SEVLHLLSR | TAWSEVLH**P**LSR | TAWS**D**VLHLLSR |
| **NAWHEVSHPSSR** | TA**S**SEV**W**HL**MA**R | **I**AWSEVLHLLS**K** |
| TAWS**D**VLHLLSR | TA**C**SEVL**PP**LSR | TAWS**K**VLHLLSR |
| TAWS**D**VLHLLSR | T**PR**SE**D**LH**F**LSR | TAWSEVLHLLSR |
| TAWS**V**VL**N**LL**P**R | T**PCN**EVLHLLSR | TAWS**D**VLHLLSR |

**Table 3.1. Testing small-scale Ph.D caloxin 1b1-like peptide library.** The library was constructed by retaining 91 % of the original base and replacing the remainder with 3 % of the other three bases in the caloxin 1b1 encoding oligonucleotide. A total of 42 phage clones were sequenced. The sequence of the parent caloxin 1b1 is TAWSEVLHLLSR. The amino acids substituted in the caloxin 1b1-like peptides are bolded.

| Number of amino acid substitutions | Expected frequency | Observed frequency in 42 phage clones |
|---|---|---|
| 0 | 2.9 | 3 |
| 1 | 9.2 | 12 |
| 2 | 12 | 10 |
| 3 | 9.6 | 10 |
| >3 | 7.9 | 7 |

**Table 3.2. Characterization of the sample of Ph.D caloxin 1b1-like peptide library**. A total of 42 phage clones from the Ph.D caloxin 1b1-like peptide library were sequenced. Shown is the expected and observed frequency of phage clones encoding peptides with a given number of amino acid substitutions. Chi square value test showed that the two distributions are not significantly different ($p > 0.1$).

| Sequence | Observed frequency | Sequence | Observed frequency |
|---|---|---|---|
| **AS**WSEVLHLLSR | 10 | TAWSEVLHLLSR | 22 |
| TAWSEVL**D**LL**R**R | 26 | T**G**WSEVLHLLSR | 5 |
| TAWSEVL**T**LL**A**R | 2 | TA**S**SEVLHLLSR | 1 |
| TAWS**D**V**F**HLLSR | 1 | TAWS**D**VLHLLSR | 4 |
| TAWSE**A**LHL**V**SR | 1 | **S**AWSEVLHLLSR | 1 |
| T**P**WS**D**VLHLLSR | 1 | TAWSEVL**D**LLSR | 1 |
| TA**R**S**D**VLHLLSR | 1 | **A**AWSEVLHLLSR | 1 |
| **AS**WS**D**VLHLLSR | 8 | T**S**WSEVLHLLSR | 1 |
| **AS**WSEVLHLLS | 1 | TAWS**K**VLHLLSR | 1 |
| TAWSE**DFN**LLSR | 1 | TAWSEVLH**H**LSR | 1 |
| T**T**WS**AD**LHLLSR | 1 | TAWSEVLHL**M**SR | 1 |
| **N**AWSEVLHLL | 2 | TAWSEVLH**D**LSR | 1 |
| **I**AW**I**EVL**D**LLSR | 1 | TAWSEV**V**HLL**A**R | 1 |
| T**T**WSEV**V**H**R**LSR | 1 | TA?**KED**LHL**MTT** | 1 |
| **I**AWSEV**Y**HLLS**K** | 1 | TA**R**SE**AM**HLLSR | 1 |
| **AA**WS**D**VL**Q**LLSR | 1 | TA**GGEFPHH**LSR | 1 |
| T**V**R**S**EVL**S**VLSR | 1 | | |

**Table. 3.3. Characterization of the phage clones selected after 4 rounds of screening of the Ph.D caloxin 1b1-like peptide library**. After the last round of affinity chromatography, a total of 104 phage clones were sequenced, which encoded 33 different types of peptide sequences. Given is the observed frequency of the phage encoding a unique peptide. The amino acids different from the original parent caloxin 1b1 sequence are bolded.

### *3.1.2.3 Competition between phage clones selected in the first screening*

The Ph.D caloxin 1b1-like peptide library had a diversity of $7x10^5$ pfu. In spite of this diversity, the first screening resulted in enrichment of only 33 different types of phage-encoded peptides out of a total of 104 clones sequenced. However, it is noted that the Ph.D caloxin 1b1-like peptide library was biased. The copy number of the phage clone encoding caloxin 1b1 would be highest in the library. There would be roughly equal frequency of phage encoding peptides with one, two or three substitutions (Table 3.2). However, the number of possibilities for unique peptides that can exist with three substitutions >> the number of possibilities for unique peptides that can exist with two substitutions >> the number of possibilities for unique peptides that can exist with only one substitution. Therefore, in this library there would be significantly fewer copies of a phage encoding an individual peptide with three substitutions than for two or one substitutions. The degeneracy in the codons for individual amino acids and the differential amplification efficiency of the phage expressing different peptides can also lead to bias in the copy number of a given phage clone. Thus, to ensure the selection of phage based on its binding affinity to PMCA, equal number of each of the 33 phage clones selected after first screening were allowed to compete in 4 rounds of affinity chromatography using PMCA protein purified from human erythrocyte membranes. Frequencies of the phage encoding unique caloxin 1b1-like peptides are given in Table. 3.4. The sequences with the highest frequencies

were termed caloxin 1c1, 1c2 and 1c3. Probabilities of obtaining the observed frequencies of the three peptides purely by chance were less than 0.0005.

The phage encoding the parent caloxin 1b1 peptide, which appeared with a copy number of 22 after the first screening was absent after competition. The (WS(E/D)V(L/V) moiety at position 3-7 in the selected 12-amino acid peptide appeared in 88 % of the clones sequenced after the first screening and in 96 % of the clones sequenced after competition. This moiety was conserved in caloxins 1b1, 1c1, 1c2 and 1c3.

#### *3.1.2.4 Inhibition of PMCA by caloxins 1c1, 1c2 and 1c3*

Based on sequences in Table 3.4, the peptides caloxin 1c1 (TTWSEVVHRLSRGGGSK-amide), 1c2 (TAWSEVLDLLRRGGGSK-amide) and 1c3 (ASWSEVLHLLSRGGGSK-amide) were synthesized. Lysine (K) was added at the C-terminus to increase the solubility of the peptides and to potentially use its Є-amino group for labeling them. These caloxins differ in 2 or 3 amino acids from the parent caloxin 1b1. It was hypothesized that caloxins 1c1, 1c2 and 1c3 would inhibit the $Ca^{2+}$-$Mg^{2+}$ATPase activity of PMCA with higher affinity than caloxin 1b1. The effects of different concentrations of caloxins 1c1, 1c2, and 1c3 on PMCA $Ca^{2+}$-$Mg^{2+}$ATPase in leaky human erythrocyte ghosts was tested. $K_i$ values obtained for caloxins 1c1, 1c2 and 1c3 were 20 ± 3 μM, 2.3 ± 0.3 μM and 18 ± 3 μM, respectively (Fig. 3.9). For comparison, the data obtained with parent caloxin 1b1 ($K_i$ = 46 ± 5 μM) is also shown. Thus, the three caloxin 1b1 mutants have higher affinity for PMCA than the parent caloxin 1b1. Caloxin

1c2 had the highest affinity for PMCA ($K_i$ : 2.3 ± .3 μM) which was 20-fold of the parent caloxin 1b1 ($K_i$ : 46 ± 5 μM).

**Table. 3.4. Characterization of the phage clones selected after competition.**

| Sequence | Observed frequency | |
|---|---|---|
| NAWSEVLHLL | 4 | |
| ASWSEVLHLLSR | 7 | Caloxin 1c3 |
| TTWSEVVHRLSR | 17 | Caloxin 1c1 |
| TGWSEVLHLLSR | 3 | |
| TAWSEVLDLLRR | 8 | Caloxin 1c2 |
| TAWSEVLTLLAR | 2 | |
| SAWSEVLHLLSR | 1 | |
| TSWSEVLHLLSR | 1 | |
| ASWSDVLHLLSR | 2 | |
| TAWSKVLHLLSR | 2 | |
| AAWSEVLHLLSR | 1 | |

Equal number ($3x10^3$ pfu) of each of the 33 phage clones selected in the first screening were allowed to compete for binding to PMCA by affinity chromatography. The phage was not amplified in between the 4 rounds. After the last round of affinity chromatography, a total of 48 phage clones were sequenced. Given is the copy number of each phage encoding a unique peptide. The probability of appearance of a clone at a given frequency at random was computed as: combination (n,r)*(1/r^j)*((r-1/r)^(n-j)). Here n (48) is the number of clones sequenced, j is the observed frequency for a sequence and r (33) is the number of possible choices, which equals the number of types of clones used. The probabilities of the observed frequencies are: caloxin 1c1 ($2.5 \times 10^{-14}$), caloxin 1c2 (0.00008) and caloxin 3 (0.0005).

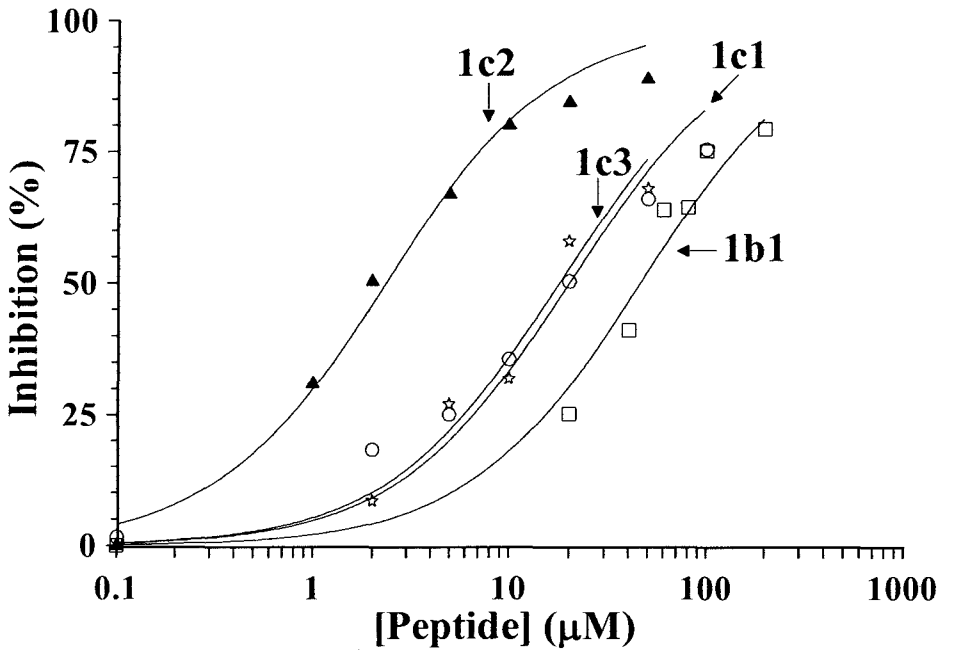


**Fig. 3.9. Inhibition of PMCA activity in leaky human erythrocyte ghosts by caloxin 1b1 and its mutants.**

PMCA activity was measured in a coupled enzyme assay. The activity in the absence of any peptide was taken as 100 % and the decrease in the activity in its presence was used to compute the % inhibition. Each value is the mean from 3-4 experiments carried out on 2-4 different days. The data fit best with the $K_i$ value of 46 ± 5 μM (caloxin 1b1), 20 ± 3 μM (caloxin 1c1), 2.3 ± 0.3 μM (caloxin 1c2), and 18 ± 3 μM (caloxin 1c3). Modified from reference 169a.

### *3.1.2.5 PMCA isoform preference of caloxin 1c2*

Caloxin 1b1 showed preference for PMCA4 over the other isoforms of PMCA. Caloxin 1c2 differs from the parent caloxin 1b1 by two amino acid substitutions and has a twenty fold higher affinity. Since caloxin 1c2 was obtained by using PMCA4 rich erythrocyte ghosts for screening, it was hypothesized that caloxin 1c2 would have higher affinity for PMCA4 than PMCA isoforms 1-3. Fig. 3.10 shows the effects of different concentrations of caloxin 1c2 on the $Ca^{2+}$-$Mg^{2+}$ATPase activity of the four PMCA isoforms. It inhibited the activity of the different PMCA isoforms with a $K_i$ of 21 ± 6 μM (PMCA1), 40 ± 10 μM (PMCA2), 67 ± 8 μM (PMCA3), and 2.3 ± 0.3 μM (PMCA4). Thus, caloxin 1c2 has higher affinity for PMCA4 than PMCA isoforms 1-3. Caloxin 1c2 has a 10-fold higher affinity for PMCA4 over PMCA1 as compared to caloxin 1b1, which had only 2 fold higher affinity for PMCA4 over PMCA1 (Fig. 3.5).

### *3.1.2.6 Physiological studies with caloxin 1c2*

The pig coronary artery smooth muscle contains both PMCA4 and PMCA1 while the endothelium is rich in PMCA1. Caloxin 1c2 has a preference for PMCA4. Therefore, the effects of caloxin 1c2 on the contraction of smooth muscle in the absence of endothelium were examined. Caloxin 1c2 increased the basal tone of the pig coronary artery rings and the effect of 10, 20 and 50 μM caloxin 1c2 was similar suggesting that mainly PMCA4 was involved in this increase. Caloxin 1c2 (20 μM) also increased the sensitivity of the coronary artery to extracellular $Ca^{2+}$. Details of these experiments are presented in App. 1.

### *3.1.2.7 Caloxin 1c2 inhibition of PMCA in different species*

The exdom 1X of human PMCA4 was used as a target to obtain caloxin 1b1. The exdom 1X of PMCA4 has few amino acid differences amongst human, pig and rabbit. Therefore, the effect of caloxin 1c2 was tested on leaky erythrocyte ghosts from different species. Fig. 3.11 shows that caloxin 1c2 inhibited PMCA activity in leaky erythrocyte ghosts from human, pig and rabbit with similar $K_i$ values of 2.3 ± 0.3 μM, 2.6 ± 0.6 μM and 2.73 ± 0.5 μM respectively. Caloxin 1c2 can thus be used to study the tissue distribution, biochemistry and physiology of PMCA4 isoform in different experimental species.

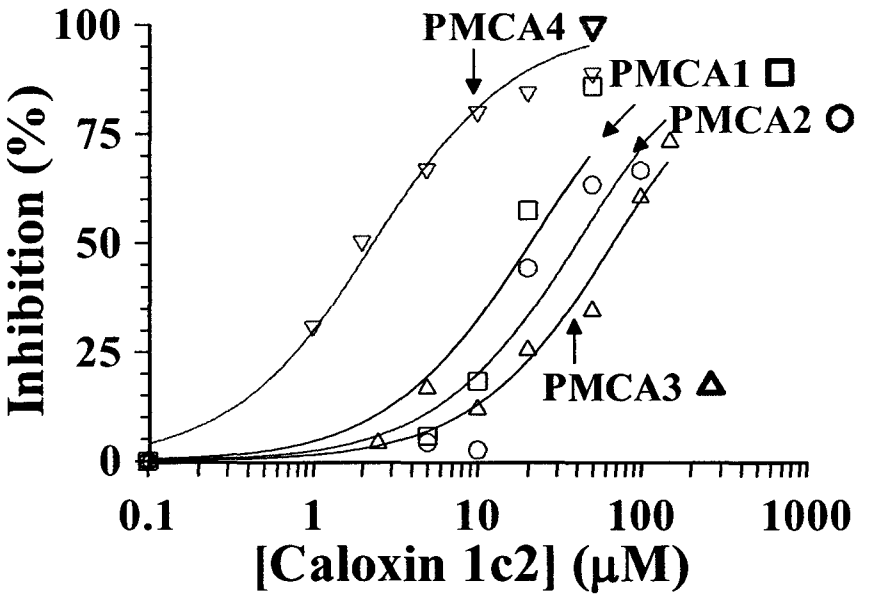


**Fig. 3.10. Caloxin 1c2 inhibition of $Ca^{2+}$-$Mg^{2+}$ATPase activity of PMCA isoforms 1-4 measured in a coupled enzyme assay.**

The sources of different PMCA isoforms are: PMCA1 (PM fraction of rabbit duodenal mucosa), PMCA2 and 3 (microsomal fraction of SF9 insect cells overexpressing PMCA isoforms 2 or 3), PMCA4 (leaky human erythrocyte ghosts). Each value is the mean of 3-4 experiments done on 2-4 different days. For each day, the data were normalized, with the mean value of the activity in the absence of caloxin 1c2 taken as 100 %. The data fit best with the $K_i$ values of 21 ± 6 μM (PMCA1), 40 ± 10 μM (PMCA2), 67 ± 8 μM (PMCA3), and 2.3 ± 0.3 μM (PMCA4). Modified from reference 169a.

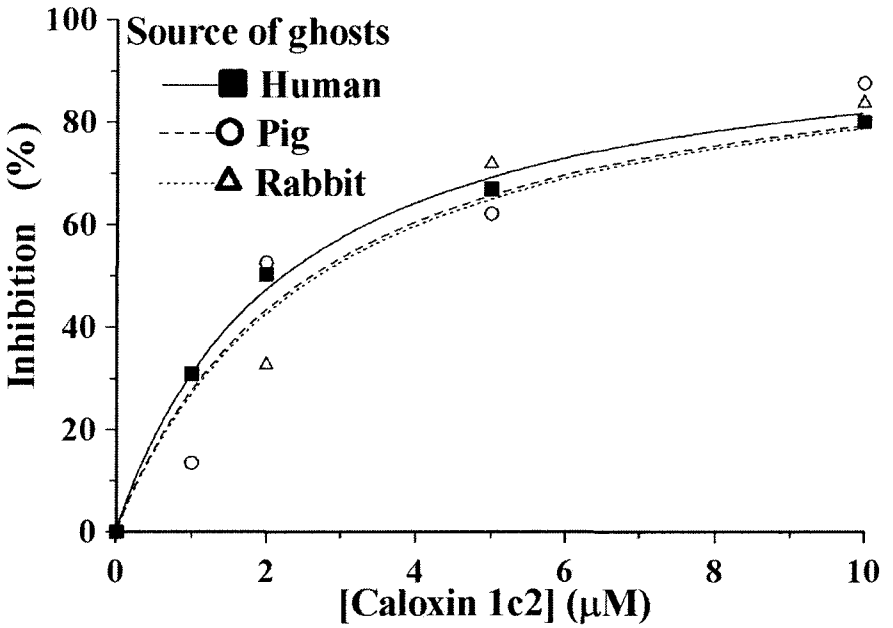


**Fig. 3.11. Caloxin 1c2 inhibition of $Ca^{2+}$-$Mg^{2+}$ATPase activity of PMCA in leaky erythrocyte ghosts from different species.**

PMCA activity was measured in a coupled enzyme assay. Each value is the mean of 3-4 experiments done on 2-4 different days. For each day, the data were normalized, with the mean value of the activity in the absence of caloxin 1c2 taken as 100 %. The data fit best with the $K_i$ values of 2.3 ± 0.3 μM (human), 2.6 ± 0.6 μM (pig), and 2.73 ± 0.5 μM (rabbit). Modified from reference 169a.

## 3.2 Aim 2: Determine the caloxin 1c2-binding domain on PMCA protein

Caloxin 1b1 was selected by two-step screening of the Ph.D-12 library using the exdom 1X of PMCA4 as a target and caloxin 1c2 was obtained by screening a library of caloxin 1b1-like peptides. Therefore, it was hypothesized that the mechanism of inhibition by caloxin 1c2 involves its selective binding to the exdom 1X of PMCA4. The overall strategy included: a) synthesizing a photolabel, which is a photoactivable derivative of caloxin 1c2 with a biotin tag for tracking; b) determining PMCA inhibitory potential of the photolabel using leaky human erythrocyte ghosts; c) photolabeling the erythrocyte ghosts; d) determining the selectivity of the photolabeling site on the erythrocyte ghosts; e) confirming PMCA photolabeling in the erythrocyte ghosts by immunoprecipitation of PMCA followed by tracking the photolabel.

Two photoactivable derivatives of caloxin 1c2 were synthesized with a C-terminal biotin tag. Caloxin 1c2 (TAWSEVLDLLRRGGGSK-amide) sequence has a tryptophan (W) at position 3, which appeared in 95 % of the clones sequenced after the first screening of the library of caloxin 1b1-like peptides (Table 3.3) and in 100 % of the clones selected after competition (Table 3.4). Therefore, W may be an essential part of the moiety that binds to the exdom 1X of PMCA4. A photoactivable group p-benzoyl-L-phenylalanine (Bpa) has been used as a conservative substitution for W in literature and forms a covalent bond to amino acid groups in its vicinity upon UV-irradiation[176]. Bpa has several advantages over other photophores: it can be directly incorporated at the defined

position during peptide synthesis; it is inert towards water, facilitating greater photoinsertion; it is stable in ambient light; it is activated at longer wavelengths and reacts with a broad range of C-H bonds[176]. W at position 3 in caloxin 1c2 sequence was replaced by Bpa to synthesize photolabel 3Bpa1c2-biotin (TA**Bpa**SEVLDLLRRGGGSK(biotin)-amide) in which biotin was added to the Є-amino group of K at the C-terminus. A second photolabel 16Bpa1c2-biotin (TAWSEVLDLLRRGGG**Bpa**K(biotin)-amide) was synthesized by substituting serine (S) at position 16 with Bpa and biotinylation of the C-terminal K to test if the C-terminal domain of caloxin 1c2 plays a role in binding to PMCA.

### 3.2.1 Caloxin 1c2 derived photolabels inhibit PMCA activity

The effects of 3Bpa1c2-biotin, 16Bpa1c2-biotin and caloxin 1c2 on PMCA $Ca^{2+}$-$Mg^{2+}$-ATPase activity in leaky human erythrocyte ghosts were compared. The routinely used ATP regenerating coupled enzyme assay to measure the $Ca^{2+}$-$Mg^{2+}$-ATPase activity of PMCA could not be used as it monitors the change in fluorescence of NADH, which is excited at 340 nm wavelength. At this wavelength, Bpa can be activated to covalently crosslink the photolabels to the protein. Therefore, the hydrolysis of [$\gamma$-$^{33}$P]-ATP in the reaction medium was used to measure the $Ca^{2+}$-$Mg^{2+}$-ATPase activity of PMCA. The derivatives 3Bpa1c2-biotin and 16Bpa1c2-biotin inhibited the $Ca^{2+}$-$Mg^{2+}$-ATPase activity of PMCA in human erythrocyte ghosts with $K_i$ of 50 μM and 5.1 μM, respectively (Fig. 3.12). In 3Bpa1c2-biotin, the substitution of W by Bpa resulted in a 20-fold decrease in the affinity of the photolabel for PMCA. W at

position 3 is part of the moiety (WS(E/D)V(L/V) within the selected 12-amino acid sequence of caloxin 1c2 that is conserved in caloxins 1b1,1c1,1c2 and 1c3. The decrease in the affinity of the photolabel suggests that W in the moiety (WS(E/D)V(L/V) plays an important role in inhibiting PMCA activity. The substitution of S at position 16 by Bpa and the addition of a biotin moiety to K in the C-terminus did not greatly affect the affinity of the photolabel for PMCA. Both S and K residues lie outside the selected 12-amino acid sequence of caloxin 1c2 and are separated from it by three glycine spacers suggesting that the substitution of residues in the C-terminus and addition of bulky groups like biotin do not affect the inhibitory potential of caloxin 1c2.

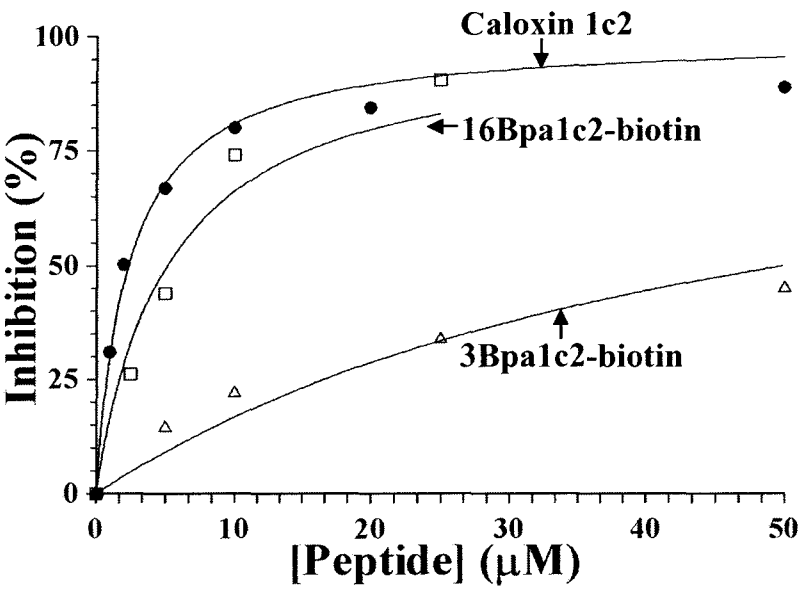


**Fig. 3.12. Effect of caloxin 1c2-derived photolabels on PMCA activity in leaky human erythrocyte ghosts measured by the $Ca^{2+}$ stimulated hydrolysis of [$\gamma$-$^{33}$P]-ATP.**

The activity in the absence of any peptide was taken as 100 % and the decrease in the activity in the presence of peptide was used to compute the % inhibition. Each value is the mean from 3-4 experiments. The data fit best with a $K_i$ of 2.3 ± 0.3 μM (caloxin 1c2), 5.1 ± 0.8 μM (16Bpa1c2-biotin) and 50 ± 6 μM for (3Bpa1c2-biotin). Modified from reference 169a.

### 3.2.2 Photolabeling erythrocyte ghosts with caloxin 1c2-derived photolabels

The photolabels 3Bpa1c2-biotin and 16Bpa1c2-biotin contain the photoreactive group Bpa that forms a radical pair upon exposure to long wavelength ultraviolet light (320-365 nm). This radical reacts with a broad range of C-H bonds to form covalent cross-links. The reaction conditions for crosslinking the photolabels to human erythrocyte ghosts were optimized with respect to: a) concentration of the photolabel; b) concentration of the ghost protein; c) time of UV-irradiation.

In an initial experiment, the yield of the photoadduct formed by crosslinking 8 μg erythrocyte ghosts with 50 μM 3Bpa1c2-biotin or 16Bpa1c2-biotin in a 50 μl reaction volume was compared. The photoadduct was detected in a Western blot by chemiluminescence with HRP-streptavidin (Fig. 3.13). Both photolabels formed a photoadduct, which appeared as a high molecular weight doublet at 250-270 kDa. However, 3Bpa1c2-biotin gave a more intense photoadduct doublet as compared to 16Bpa1c2-biotin even though the latter inhibits PMCA activity in the erythrocyte ghosts with a higher affinity. Since 3Bpa1c2-biotin gave a higher yield of the photoadduct, it was used in all the future experiments of crosslinking.

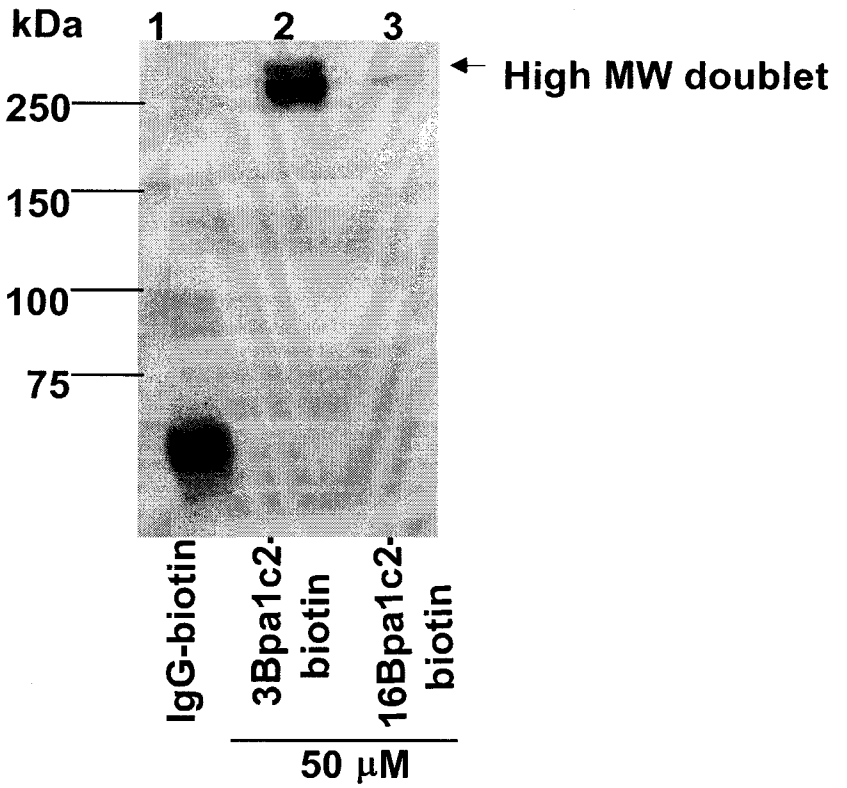


**Fig. 3.13. Photolabeling of erythrocyte ghosts by caloxin 1c2-derived photolabels.**

The photolabeling was carried out with 50 μM each of 3Bpa1c2-biotin and 16Bpa1c2-biotin. 15μg of the ghost protein photolabeled with 3Bpa1c2-biotin (*lane 2*) and 16Bpa1c2-biotin (*lane 3*) was used. The biotinylated proteins were detected in Western blots as described in the Experimental Methods. *Lane 1:* 50 ng control IgG-biotin. The arrow shows a doublet at 250-270 kDa. Positions of the markers and their molecular weights in kDa are shown. The experiment was repeated 3 times with similar results.

### *3.2.2.1 3Bpa1c2-biotin concentration dependence of photolabeling*

The effect of different concentrations of 3Bpa1c2-biotin on the formation of the photoadduct doublet in human erythrocyte ghosts was determined. Increasing the concentration of 3Bpa1c2-biotin in the photolabeling reaction with 25 μg of ghost protein in 50 μl volume increased the amount of biotin at 250-270 kDa observed in a Western blot (Fig. 3.14). The yield of the photoadduct doublet formed with 50 μM and 100 μM 3Bpa1c2-biotin was 8 % and 20 % respectively of that formed with 400 μM 3Bpa1c2-biotin. At higher concentrations of the photolabel, biotin was also detected as a faint diffuse band corresponding to approximately 100 kDa.

### *3.2.2.2 Ghost protein concentration dependence of photolabeling*

The effect of varying protein concentration of human erythrocyte ghost in the photolabeling reaction carried out with 400 μM 3Bpa1c2-biotin is shown in Fig. 3.15. The yield of the photoadduct doublet at 250-270 kDa increased with the increase in the protein concentration, becoming constant at ~20μg of the ghost protein in the photolabeling reaction volume of 50 μl. Shown in Fig. 3.15 are the different time exposures of the same Western blot. At any given protein concentration, the intensity of the diffuse lower molecular weight band was always fainter than the 250-270 kDa doublet as seen in the short exposure of the Western blot (Fig. 3.15A).

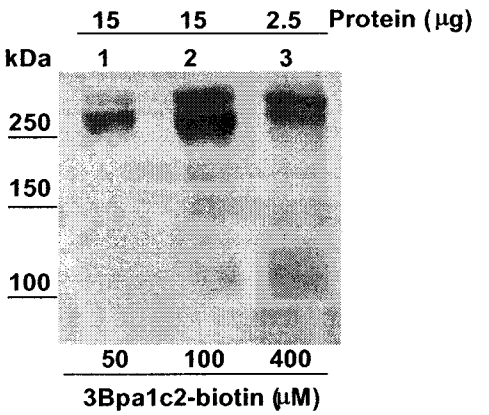


**Fig. 3.14. 3Bpa1c2-biotin concentration dependence of photolabeling.**

The photolabeling of 25 μg ghost/50 μl reaction volume was carried out with increasing concentration of 3Bpa1c2-biotin (μM): 50 (lane 1), 100 (lane 2), 400 (lane 3). Given amount of protein (μg) was used to detect biotin-containing bands in a Western blot.

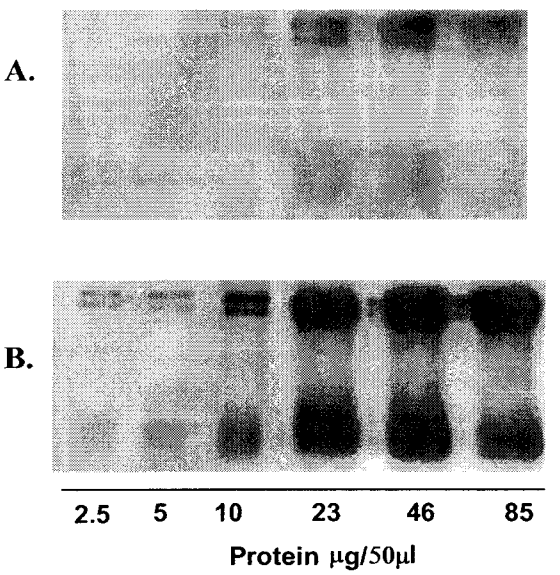


**Fig. 3.15. Erythrocyte ghost protein concentration dependence of photolabeling.**

Increasing amounts of ghost protein/50 μl reaction volume were photolabeled with 400 μM 3Bpa1c2-biotin for 30 min. Equal volume of photolabeled ghosts (5.5 μl) were used for detection of biotin containing bands in Western blot. The same immunoblot was exposed for 10 sec (**A**) and 60 sec (**B**).

### *3.2.2.3 UV-irradiation time dependence of photolabeling*

The effect of increasing length of UV-irradiation (365 nm) on the photolabeling of 25 μg of erythrocyte ghosts/50 μl reaction volume with 100 μM 3Bpa1c2-biotin was determined. The yield of the photoadduct doublet at 250-270 kDa increased with the increase of UV-irradiation time from 1 min to 15 min (Fig. 3.16). In another experiment, it was determined that irradiation for longer periods did not result in further increase in the photolabel incorporation (data not shown). The intensity of the diffuse low molecular weight band also increased with the increasing time of UV-irradiation.

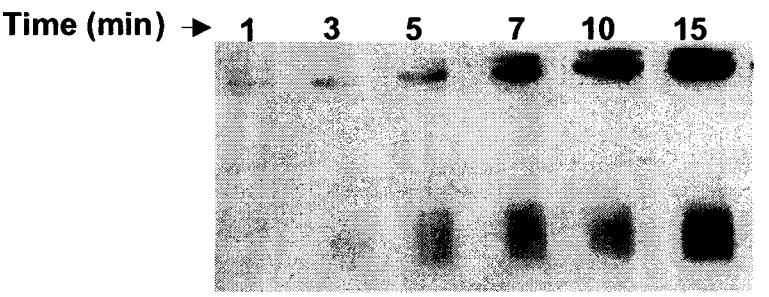


**Fig. 3.16. The effect of increasing length of UV irradiation on photolabeling.**
The ghosts (25 μg)/50 μl were photolabeled with 100 μM 3Bpa1c2-biotin with increasing UV-irradiation time. An equal amount of protein (1 μg) was used for detection of biotin containing bands in Western blot.

### 3.2.3 Selectivity of the photolabeling site in erythrocyte ghosts

It was hypothesized that caloxin 1c2 would compete with its derivative 3Bpa1c2-biotin for binding to PMCA as they were expected to bind at the same site. The photolabeling of human erythrocyte ghosts was carried out with 50 μM 3Bpa1c2-biotin, which forms the photoadduct doublet at 250-270 kDa (Fig. 3.17). The photolabeling with 50 μM 3Bpa1c2-biotin in the presence of increasing concentrations of caloxin 1c2 (0 to 500 μM) decreased the yield of this doublet (Fig. 3.17). The intensity of the doublet decreased by 36 % and 63 % in the presence of 200 μM and 500 μM caloxin 1c2, respectively. The presence of caloxin 1c2 during photolabeling with 100 μM 3Bpa1c2-biotin also decreased the yield of the photoadduct at 250-270 kDa (data not shown). No such trend was observed with the diffuse lower molecular weight band at ~100 kDa which was always fainter than the high molecular weight doublet in the absence or presence of any given concentration of caloxin 1c2.

Caloxin 1c2 was obtained by screening a Ph.D caloxin 1b1-like peptide library, and exdom 1X of PMCA4 was used as the target to obtain caloxin 1b1. Caloxin 1c2 is the high affinity mutant of caloxin 1b1. Therefore, it was hypothesized that the exdom 1X peptide (CSLVLSFYRPAGEENEL) could bind to 3Bpa1c2-biotin and hence compete in the photolabeling of PMCA. The synthetic exdom 1X peptide was synthesized with an added N-terminal cysteine, which was used for conjugation to the carrier proteins. A control peptide of similar length with N-terminal cysteine and with 71 % of its amino acids similar

to those of the synthetic exdom 1X peptide was used as a negative control. The photolabeling of human erythrocyte ghosts with 50 μM 3Bpa1c2-biotin was carried out in the presence and absence of the synthetic exdom 1X peptide or the control peptide. The presence of 1 mM synthetic exdom 1X peptide decreased the intensity of the 250-270 kDa biotinylated band by 76 % (Fig. 3.18). The control peptide had no effect.

Thus, excess caloxin 1c2 and the exdom 1X peptide decrease the photolabeling by 3Bpa1c2-biotin, verifying the doublet (250-270 kDa) as the specific site of crosslinking to PMCA.

### 3.2.4 Immunoprecipitation to establish that PMCA was photolabeled

It was hypothesized that 3Bpa1c2-biotin crosslinks specifically with PMCA protein in the erythrocyte ghosts which migrates as a doublet at 250-270 kDa in the SDS-PAGE. Erythrocyte ghosts were photolabeled and immunoprecipitated using an anti-PMCA antibody and then examined in Western blots for biotin. Human erythrocyte membranes express mainly PMCA4[47]. However, in initial experiments it was determined that the PMCA4 specific monoclonal antibody JA9, is IgG1 isotype that did not bind efficiently to protein A, which was to be used to capture the antigen-antibody complex during immunoprecipitation. The PMCA specific antibody 5F10, which recognizes all PMCA isoforms, has been used for immunoprecipitation of PMCA from different tissues. It binds to protein A agarose and was used to immunoprecipitate PMCA from the photolabeled erythrocyte ghosts. The immunoprecipitate was examined

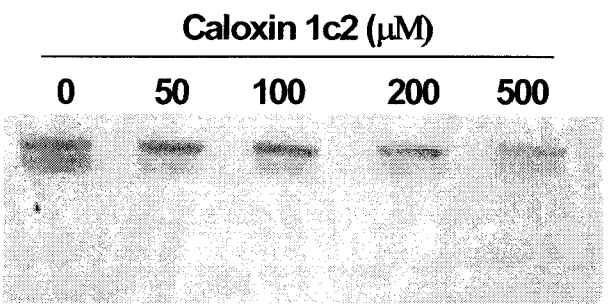


**Fig. 3.17. Caloxin 1c2 competes with 3Bpa1c2-biotin for photolabeling of the erythrocyte ghosts.**

Ghosts (25 μg/50 μl) were photolabeled with 50 μM 3Bpa1c2-biotin for 30 min either in the absence (0 μM) or presence of increasing concentrations of caloxin 1c2 (50 – 500 μM). 2.5 μg of the photolabeled protein was used for detection of biotin in Western blot.

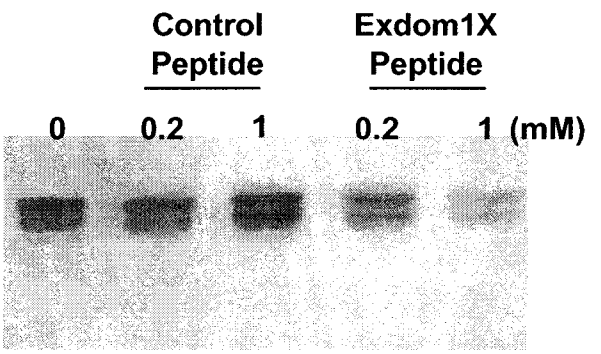


**Fig. 3.18. The synthetic exdom 1X peptide of PMCA4 competes with the erythrocyte ghosts for photolabeling by 3Bpa1c2-biotin.**

Ghosts (25 μg/50 μl) were photolabeled with 50 μM 3Bpa1c2-biotin for 30 min either in the absence (0 mM) or presence of 0.2 and 1 mM exdom 1X peptide or the control peptide. 4.6 μg of the photolabeled protein was used to detect biotin in Western blot. The experiment with exdom 1X peptide was repeated 2 times and the figure of a representative experiment is shown here.

for biotin in Western blot. The photoadduct doublet observed at 250-270 kDa in the photolabeled erythrocyte ghosts was also detected at the same position in PMCA protein immunoprecipitated from the photolabeled erythrocyte ghosts (Fig. 3.19).

The results conclude: a) caloxin 1c2 is the high affinity selective inhibitor of PMCA, b) the photoreactive derivative, 3Bpa1c2-biotin, crosslinks specifically to PMCA protein in the erythrocyte ghosts, c) the exdom 1X is the binding domain of caloxin 1c2 on PMCA protein.

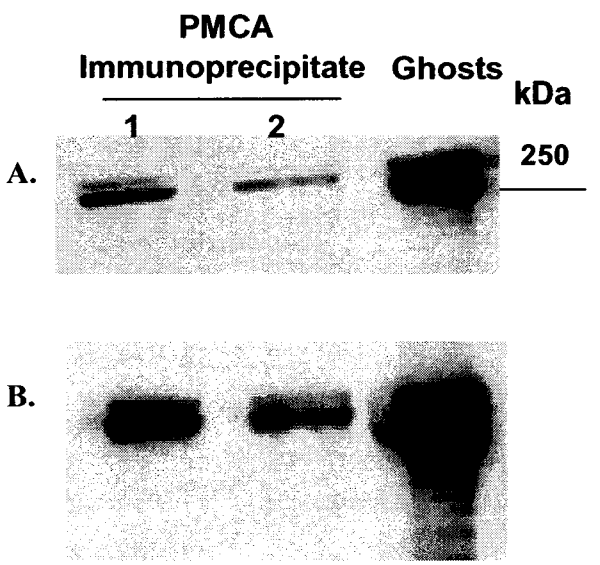


**Fig. 3.19. 3Bpa1c2-biotin selectively photolabels PMCA in erythrocyte ghosts.**

Ghosts (25 μg/50 μl) were photolabeled with 100 μM 3Bpa1c2-biotin for 30 min. PMCA from the photolabeled ghosts was immunoprecipitated and eluted from Protein A agarose as two fractions: PMCA immunoprecipitate 1 and 2. Biotin was detected in Western blots. The same blot was exposed to X-ray film for 3 min (**A**) or 10 min (**B**). Apparent molecular weights of the protein are shown in kDa. The experiment was repeated 7 times with similar results.

## 3.3 Aim 3: Develop caloxins using exdom 1Y for screening Ph.D libraries

The exdom 1 of human PMCA4 consists of residues 116-147 (SLVLSFYRPAGEENELCGQVATTPEDENEAQA). As described in section *3.1.1.1*, the exdom 1 was divided into exdom 1X exdom 1Y around the cysteine. In this Aim, the exdom 1Y (CGQVATTPEDENEAQA) of PMCA4 was used as a target to obtain a caloxin. The rationale for using exdom 1Y as a target was: a) the sequences between PMCA isoforms 1-4 differ from each other more in the exdom 1Y than in the exdom 1X (Fig. 1.2), which could lead to obtaining a caloxin with higher PMCA4 isoform selectivity than caloxin 1c2, b) caloxin 1c2 and an exdom 1Y selective high affinity caloxin can be used to form a bidentate caloxin with extremely high affinity and PMCA4 isoform selectivity.

### 3.3.1 Two-step screening of Ph.D-12 library using exdom 1Y of PMCA4

The two-step screening procedure used for obtaining caloxin 1b1 in 3.1.1.1 was used to select a phage that recognizes the exdom 1Y. The mixture of the synthetic exdom 1Y peptide and its KHLH conjugate was used as a target, while exdom 1Y-ovalbumin conjugate was used for the elution of the phage bound specifically to the target in 3 rounds of screening. This was followed by 2 rounds of phage screening by affinity chromatography with PMCA protein purified from human erythrocyte ghosts as described for the exdom 1X. The input pfu for affinity chromatography was kept constant with $2x10^8$ pfu. After two rounds of affinity chromatography, the phage pool was subjected to screening with the synthetic exdom 1Y as a target with $10^{11}$ pfu. This was followed by a

final round of affinity chromatography with $2x10^8$ pfu and the phage from the final round was titered and a total of 48 phage clones were picked and amplified and the phage DNA was sequenced. The consensus 12-amino acid peptide sequence encoded by 7 out of a total of 48 clones was HGWINYQSLYAW. Three clones were without any peptide insert and the remaining clones were present with 1 or 2 copy number. The phage-encoded peptide that appeared with highest frequency was synthesized and termed caloxin 1b2 (HGWINYQSLYAWGGGSK-amide).

The effect of caloxin 1b2 on the $Ca^{2+}$-$Mg^{2+}$ATPase activity of PMCA in leaky human erythrocyte ghosts was determined in a coupled enzyme assay (Fig. 3.20). Caloxin 1b2 produced 50 % inhibition of PMCA activity at a concentration of 31 ± 2 μM. The effect of different concentrations of caloxin 1b2 was also tested on the $Ca^{2+}$-$Mg^{2+}$ATPase activity in the PM enriched fraction from rabbit duodenal mucosa, which expresses mainly PMCA1 isoform (Fig. 3.20). Caloxin 1b2 inhibited PMCA1 activity with a 3 fold lower affinity ($K_i$: 100 ± 8 μM) as compared to PMCA4 ($K_i$: 31 ± 2 μM). Thus, caloxin 1b2 showed a preference for PMCA4 over PMCA1 isoform. To further increase the affinity of caloxin 1b2, a Ph.D caloxin 1b2-like peptide library was constructed as described for the library of caloxin 1b1-like peptides in section 3.1.2. Another student in the lab will screen the Ph.D caloxin 1b2-like peptide library.

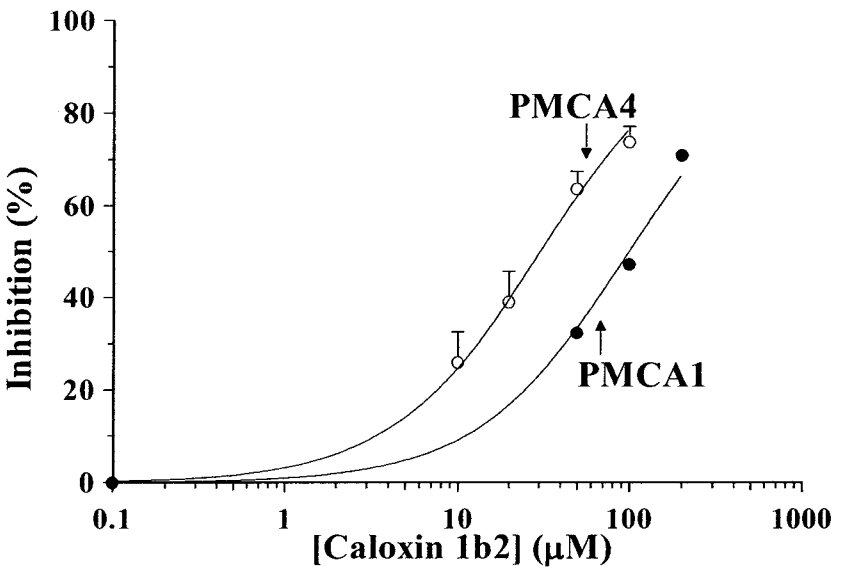


**Fig. 3.20. Caloxin 1b2 inhibition of $Ca^{2+}$-$Mg^{2+}$ATPase activity of PMCA isoforms 1 and 4 measured in a coupled enzyme assay.**

Sources of the two PMCA isoforms are: PMCA1 (PM fraction of rabbit duodenal mucosa) and PMCA4 (leaky human erythrocyte ghosts). Each value is the mean of 3-4 experiments done on 2-4 different days. For each day, the data were normalized, with the mean value of the activity in the absence of caloxin 1b2 taken as 100 %. The data fit best with the $K_i$ values of 100 ± 8 μM (PMCA1) and 31 ± 2 μM (PMCA4).

### 3.3.2 Screening a cysteine bridge constrained Ph.D-C7C library

The Ph.D-12 library screened for obtaining caloxins 1b1 and 1b2 expressed linear 12-amino acid random peptides. Libraries encoding cyclical peptides are also commercially available. One such library is the Ph.D-C7C that contains phage encoding random heptapeptides flanked by a pair of cysteine residues, which form an internal disulfide bridge during the phage assembly. This conformational strain in the peptides in the Ph.D-C7C library can lead to the selection of ligands with higher affinity[177]. The Ph.D-C7C library contains $3.7x10^9$ independent clones and thus is sufficiently complex to contain $1.28x10^9$ possible 7-amino acid peptide sequences. Therefore, the potential of the Ph.D-C7C library to obtain caloxins with higher affinity than caloxins 2a1 and 3a1 was tested by screening using only the synthetic exdom 1Y target. The screening with $10^{11}$ pfu of the Ph.D-C7C library was carried out for 6 rounds as described in the Experimental Methods. The phage eluted after each round was amplified to keep the input pfu ($10^{11}$ pfu) constant for the next round. The titer of the eluted phage increased with each round and became constant in rounds 5 and 6 of screening. The phage pool from the $6^{th}$ round was tested for its selectivity for binding to the synthetic exdom 1Y. The titer of the eluted phage was highest when the binding was carried out with the phage from the $6^{th}$ round of screening using the selective target (Fig. 3.21). Thus, as expected the phage enriched by screening bound selectively to the exdom 1Y target and the binding was much higher than for the random library. From this phage pool, 24 plaques were picked and amplified, and

the phage DNA sequenced. Two phage-encoded peptides (ACPIWQPHYCGGG) and (ACPWWSPHACGGG) appeared with higher frequency than the others and were synthesized.

Caloxin 1a1 (ACPWWSPHACGGG) was tested further due to the lower yields of the second peptide during its synthesis. The effect of caloxin 1a1 on the $Ca^{2+}$-$Mg^{2+}$ATPase activity of PMCA in leaky human erythrocyte ghosts was determined by monitoring the hydrolysis of [$\gamma$-$^{33}$P]-ATP (Fig. 3.22). Caloxin 1a1 inhibited PMCA activity with a $K_i$ value of 86 ± 12 μM. A similar $K_i$ value was obtained by testing the effect of caloxin 1a1 on PMCA $Ca^{2+}$-$Mg^{2+}$ATPase activity in leaky human erythrocyte ghosts using the coupled enzyme assay (Fig. 3.23).

The importance of the internal disulfide bridge in caloxin 1a1 sequence was tested using the reducing agent DTT. Inhibition with caloxin 1a1 was examined using a coupled enzyme assay. DTT increased the $K_i$ value from 86 ± 12 μM to 1939 ± 246 μM (Fig. 3.23). Thus the presence of the internal disulfide bridge is important for the inhibitory potential of caloxin 1a1. Further, it was tested whether the disulfide bridge alone was the mechanism of inhibition of PMCA $Ca^{2+}$-$Mg^{2+}$ATPase by caloxin 1a1. Addition of glutathione dimer at a concentration of 1 mM (= 10x $K_i$ of caloxin 1a1) to the assay solution did not inhibit PMCA activity (Fig. 3.24). Therefore, the inhibitory effect of caloxin 1a1 is specific to its disulfide constrained peptide sequence.

Caloxin 1a1 at a concentration of 200 μM inhibited the $Ca^{2+}$-$Mg^{2+}$ATPase activity of SERCA by 74 ± 2 %. Thus, caloxin 1a1 differs from other caloxins in

this respect. To test whether the disulfide bridge in caloxin 1a1 is enough to cause the non-specific inhibition of SERCA, the effect of glutathione dimer was tested (Fig. 3.24).

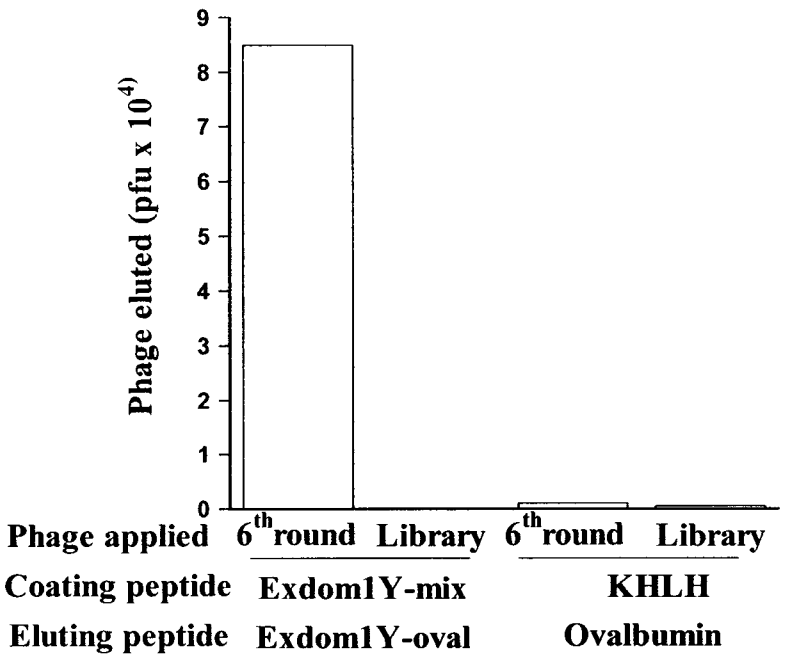


**Fig. 3.21. Selectivity of the phage pool from the 6th round of screening.**

The protocol was similar to that described in Fig. 3.1 except that the exdom 1Y peptide and its conjugates were used as target and for elution. $10^{10}$ pfu of the phage pool enriched after 6 rounds of screening was used for the test.

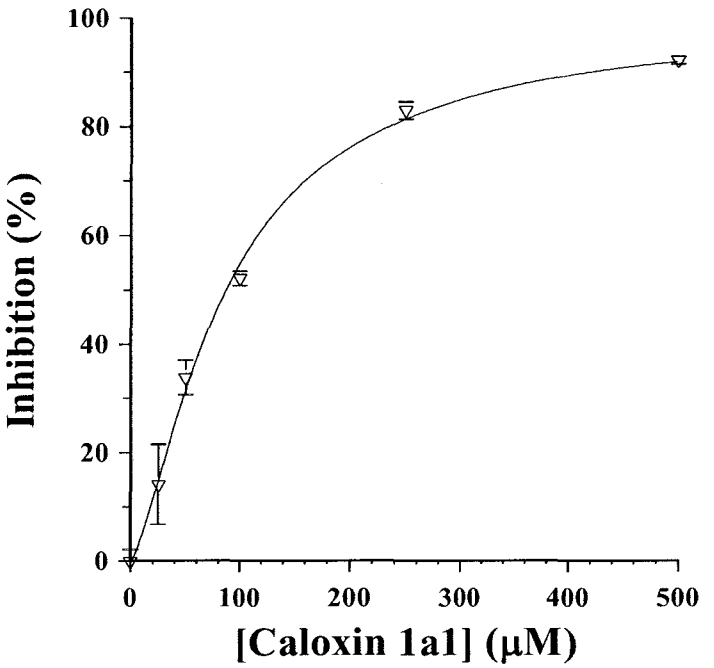


**Fig. 3.22. Caloxin 1a1 inhibition of PMCA activity in leaky human erythrocyte ghosts measured by monitoring the hydrolysis of [γ-$^{33}$P]-ATP.**

The difference in the ATPase activity before and after the addition of $Ca^{2+}$ is the $Ca^{2+}$-$Mg^{2+}$ATPase activity of PMCA. The activity in the absence of caloxin 1a1 was taken as 100 % and the decrease in the activity in its presence was used to compute the % inhibition. Each value is mean ± SE from 3-4 experiments. The data fit best with the $K_i$ value of 86 ± 12 μM. Modified from reference 173.

The glutathione dimer strongly inhibited SERCA activity. Thus, the presence of the disulfide bridge in caloxin 1a1 and glutathione dimer is enough to inhibit SERCA activity. However, caloxin 1a1 is unlikely to enter cells and be accessible to SERCA. Therefore, it is anticipated that in intact cells, caloxin 1a1 would inhibit only PMCA, but in cell preparations it would inhibit both PMCA and SERCA (App.1).

The effect of caloxin 1a1 was tested on the acylphosphate formation from [$\gamma$-$^{33}$P]-ATP in the reaction cycle of PMCA (Fig. 3.25). Preincubation of the erythrocyte ghosts with 1 mM caloxin 1a1 before the phosphorylation reaction increased the intensity of the band at 140 kDa by 150 $\pm$ 5 % ($P < 0.05$) as measured in 5 gels (lane 3). This increase is similar to that observed with caloxin 1b1 which was selected by using the exdom 1X as a target. Thus, both caloxins 1a1 and 1b1, which have their binding domains on the exdom 1 of PMCA, increased the steady state level of PMCA acylphosphate intermediate.

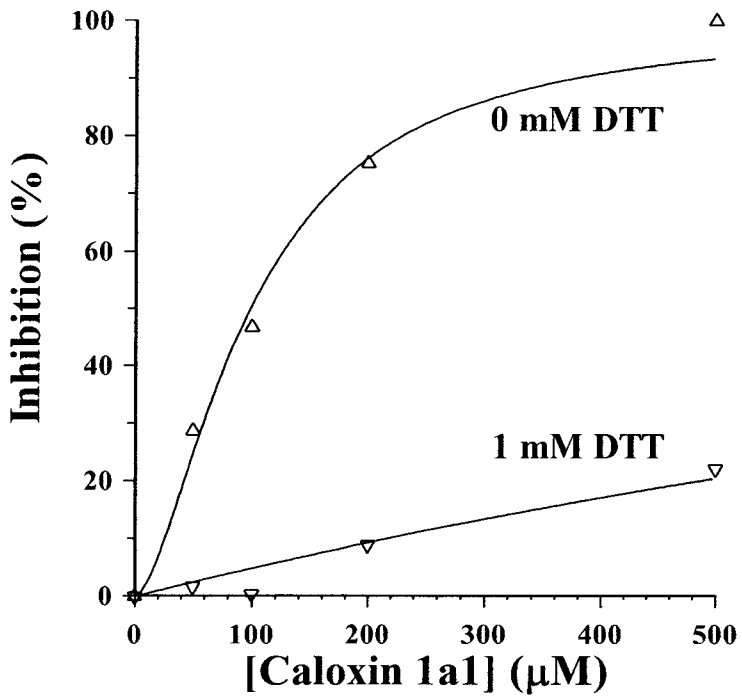


**Fig. 3.23. Effect of DTT on caloxin 1a1 inhibition of PMCA activity in leaky human erythrocyte ghosts.**

The difference in the ATPase activity before and after the addition of $Ca^{2+}$ is the $Ca^{2+}$-$Mg^{2+}$ATPase activity of PMCA. The activity in the absence of caloxin 1a1 was taken as 100 % and the decrease in the activity in its presence was used to compute the % inhibition. Each value is the mean from 3-4 experiments. The data fit best with the $K_i$ value of 86 ± 12 μM in the absence of DTT and 1939 ± 246 μM in the presence of DTT. Modified from reference 173.

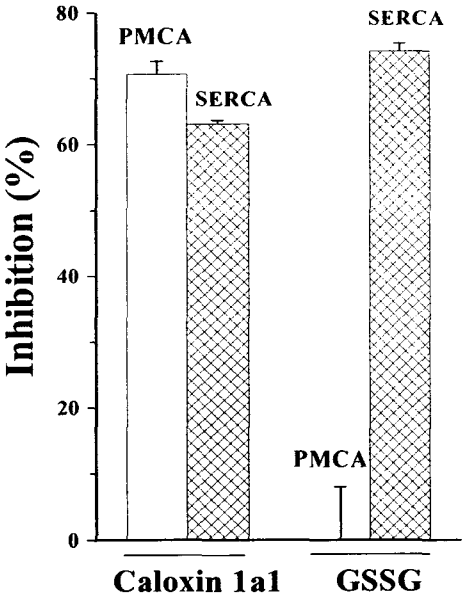


**Fig. 3.24. Effect of caloxin 1a1 (200 μM) and glutathione dimer GSSG (1 mM) on the $Ca^{2+}$-$Mg^{2+}$ATPase activity of SERCA and PMCA.**

The difference in the ATPase activity before and after the addition of $Ca^{2+}$ is the $Ca^{2+}$-$Mg^{2+}$ATPase activity measured in the coupled enzyme assay. The activity in the absence of caloxin 1a1 was taken as 100 % and the decrease in the activity in their presence was used to compute the % inhibition. Each value is mean ± SE from 3-4 experiments. Modified from reference 173.

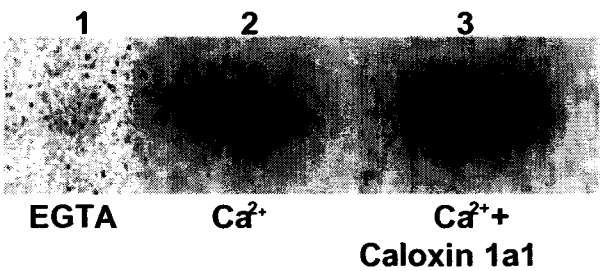


**Fig. 3.25. Effect of caloxin 1a1 on the 140-kDa acylphosphate intermediate of PMCA.**

The erythrocyte ghosts were preincubated with 1 mM caloxin 1a1. The acylphosphate formation was carried out with [$\gamma$-$^{33}$P]-ATP and the samples analyzed by acid gel electrophoresis. Lane 1 contained 1 mM EGTA, the $Ca^{2+}$ chelator. Modified from reference 173.

# 4.0 DISCUSSION

The Ph.D random peptide libraries were screened to obtain caloxins that bind to the exdom 1 that forms the extracellular loop connecting the TM helices 1 and 2 of PMCA. The N-terminal half of the exdom 1 (exdom 1X) of PMCA4 was used as a target in an improved two-step screening of the linear Ph.D-12 library to obtain caloxin 1b1. Caloxin 1b1 inhibited the $Ca^{2+}$-$Mg^{2+}$ATPase activity of PMCA with a 10 fold higher affinity as compared to the prototype caloxin 2a1 and showed slight preference for PMCA4 isoform over PMCA1. The Ph.D caloxin 1b1-like peptide library was designed by limited mutagenesis of caloxin 1b1 sequence and was screened to select caloxin 1c2. Caloxin 1c2 had 20 fold higher affinity and greater PMCA4 isoform selectivity than the parent caloxin 1b1. The exdom 1X of PMCA was experimentally verified as the binding site of caloxin 1c2. Caloxin 1c2 produced physiological effects by altering $[Ca^{2+}]_i$ when added to the medium containing tissues. The discussion focuses on the methods used to improve the affinity of caloxins, selectivity and mechanism of action of caloxins and their potential in understanding the role of PMCA in the cellular environment.

## 4.1 Two-step screening and mutagenesis to improve affinity of caloxins

The Ph.D libraries expressing linear random peptides have been successfully screened to obtain binding sequences using targets that have natural ligands[162]. For instance, the molecular chaperone protein BiP, found in the SER lumen binds the newly synthesized proteins as they are translocated across the

SER membrane. Screening two different Ph.D libraries expressing random octapeptides and dodecapeptides using BiP as a target identified ligands with a consensus motif[178]. Similarly, a hexapeptide selected from a Ph.D random peptide library bound to the S protein of the RNAse with an affinity, which is only 50 fold lower than that of its natural ligand[179]. However, screening the combinatorial linear peptide libraries to obtain peptide mimics of non-peptide ligands or peptides that bind to targets with no known ligands is difficult and may lead to selection of low affinity sequences[162,180]. The low affinity of the linear peptides may result due to the large unfavorable entropy change resulting from the loss of flexibility of the linear structure that offsets the favorable enthalpy change resulting from the binding of the peptide to the target[162,181]. For example, the peptide mimics of biotin obtained by screening the combinatorial linear peptide libraries for binding to streptavidin contained the consensus motif HPQ, with little amino acid conservation on either side of this motif. The peptides bound streptavidin with low affinity ($K_d$: 0.1-1 mM) as compared to streptavidin-biotin complex ($K_d$: $\sim 10^{-11}$ mM). The crystal structure of the peptide-streptavidin complex confirmed the interaction of the motif HPQ at the same site as biotin, however the peptide used only a subset of possible interaction sites of the binding pocket leading to its lower affinity[181]. The Ph.D peptide library may also be used for identifying antigenic epitopes of an antibody and to identify antibodies for the antigens[180]. The Ph.D antibody library has been used to overcome the innate tolerance of the immune system to certain post-translational modifications that

have no known natural ligands due to their non-immunogenic and ubiquitous nature[182]. The screening of the Ph.D antibody library usually results in the selection of antibodies that have low affinity for the antigen ($K_d$: ~0.1 mM). The affinity of the selected antibody can be increased further by mutagenesis to the level observed *in vivo*[163]. Therefore, screening of the Ph.D libraries followed by affinity maturation of the obtained peptides by mutagenesis can be used to obtain high affinity ligands for a target.

The conformation of the target used for screening the libraries is also an important determinant in obtaining high affinity ligands. The antibody directed against the nicotinic acetylcholine receptor shows a conformation dependent binding to its epitope. The antibody does not bind to the denatured receptor or the synthetic peptides derived from the receptor sequence, underlining the importance of the spatial conformation of the epitope[183]. The Ph.D libraries have been successfully screened to obtain high affinity ligands for the target receptors overexpressed in cells, thereby maintaining their structural complexity in the natural environment[184,185]. A recent alternative approach is biochromatography, in which the TM proteins can be incorporated into a phospholipid monolayer of an immobilized artificial membrane stationary phase that mimics their cellular environment. The membrane proteins like nicotinic acetylcholine receptors and the G-protein coupled receptors have been immobilized on the artificial membrane stationary phase while retaining their ligand binding specificity. Since such immobilized stationary phases are stable, they can be used in high

throughput screening with the Ph.D libraries to identify novel ligands that can bind the protein in its native conformation[186,187].

Caloxins 2a1 and 3a1 were obtained by screening the Ph.D-12 library for binding to the synthetic peptides based on the sequence of the exdoms of PMCA. The synthetic exdoms can differ in their conformation from the native exdoms in the membrane protein and therefore, the phage binding tightly to the synthetic exdom may not bind to PMCA protein with similar affinity. PMCA is a low abundant protein and is also difficult to overexpress to high levels[67]. Furthermore, the exdoms form only a small part of PMCA protein and hence using purified PMCA as a target for screening can lead to selection of non-exdom targeted peptides. Therefore, a two-step screening procedure was developed. In the first step, the Ph.D-12 library was first screened to bind to the synthetic exdom 1 of PMCA4 to enrich the phage pool in sequences with some bias towards the exdom. In the second step, the enriched phage pool was screened by affinity chromatography to select phage clones that bind to the exdom as part of PMCA protein immobilized on the calmodulin column. PMCA4 is the major isoform expressed in human erythrocyte ghosts[47]. Under the experimental conditions used, PMCA protein solubilized from human erythrocyte ghosts is the only major protein captured on the calmodulin column[99]. PMCA bound to calmodulin in the presence of $Ca^{2+}$ and the PMCA-phage complex was eluted in solution containing the $Ca^{2+}$ chelator[169]. The two-step screening of the Ph.D-12 library led to selection of phage clones with consensus sequences for caloxin 1b1 and 1b2. Caloxin 1b1

and 1b2 inhibited the $Ca^{2+}$-$Mg^{2+}$ ATPase activity of PMCA in erythrocyte ghosts with 10-15 fold higher affinity as compared to the prototype caloxin 2a1, and showed preference for PMCA4 isoform[169]. To further improve the affinity and PMCA4 isoform selectivity, a Ph.D caloxin 1b1-like peptide library was constructed and screened by affinity chromatography to select for caloxins with greater inhibitory potential. Designing phage libraries displaying mutants of low affinity ligands have been successfully screened to obtain high affinity inhibitors of growth hormone and type 1-interleukin receptors[188,189]. A phage clone selected from caloxin 1b1-like library encoded for caloxin 1c2. Caloxin 1c2 inhibited PMCA activity in human erythrocyte ghosts with a 20-fold higher affinity as compared to the parent caloxin 1b1 and 200-fold higher affinity as compared to caloxin 2a1 (Fig. 4.1). Caloxin 1c2 also had a ten-fold or higher selectivity for PMCA4 as compared to other PMCA isoforms.

## 4.2 Screening the Ph.D-C7C library

The Ph.D libraries displaying peptides constrained by a disulfide bridge are advantageous in selection of high affinity ligands. For instance, screening a disulfide constrained peptide library using streptavidin as a target resulted in selection of clones with conserved HPQ motif similar to those obtained from the Ph.D linear peptide library. However, the disulfide constrained peptides with HPQ motif bound streptavidin with a higher affinity than the linear peptides[177]. Similarly, a high affinity ligand for platelet integrin was obtained from disulfide constrained library but not from an equivalent linear peptide library[165]. Caloxin

1a1, which was obtained by screening the Ph.D-C7C library, has five-fold higher affinity as compared to caloxin 2a1. However, as in thiol dimer, the presence of disulfide bridge in caloxin 1a1 led to inhibition of SERCA activity. Studies have shown that SERCA is highly susceptible to the loss of activity due to oxidation of its sulfhydryl groups[128]. The high sensitivity of SERCA towards oxidants is used in its reversible S-glutathiolation during nitric oxide induced muscle relaxation under physiological conditions while leading to irreversible thiol oxidation under pathological conditions[190]. Therefore, the use of caloxins based on the disulfide-constrained peptides is limited to studying the role of PMCA only in intact cells and tissues[173].

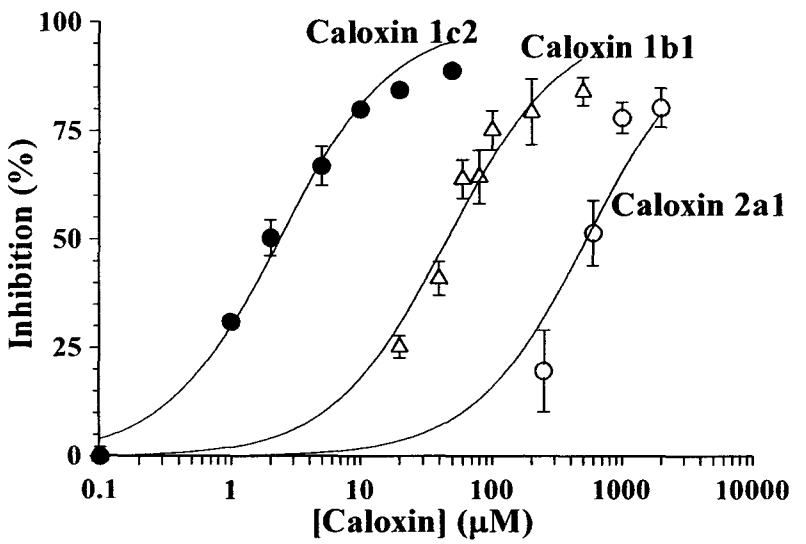


**Fig. 4.1. Comparison of affinities of caloxins.**

Caloxin 1c2 ($K_i$: 2.3 μM) inhibited the $Ca^{2+}$-$Mg^{2+}$ATPase activity of PMCA in human erythrocyte ghosts with 20-fold higher affinity as compared to caloxin 1b1 ($K_i$: 46 μM) and 200-fold higher affinity as compared to caloxin 2a1 ($K_i$: 529 μM). Modified from reference 74.

## 4.3 Selectivity of caloxins

Other than caloxins, there are no known extracellularly acting specific inhibitors of PMCA. PMCA shares sequence similarities, and the key features of ATP hydrolysis and the central core of the TM helices with other members of P-type ATPases that include SERCA and the $Na^+$-$K^+$ ATPase[53]. The alignment of the homologous regions of various P-type ATPases with SERCA sequence and their mapping onto SERCA structure has revealed extensive similarity in the cytosolic domains of SERCA, PMCA and $Na^+$-$K^+$ ATPase[54]. There are conserved amino acid residues in the TM domains of P-type ATPases that are proposed to mediate ion translocation. PMCA lacks two of these conserved residues in the TM domains 5 and 8. The recombinant PMCA with mutation of a single amino acid residue in the TM domain 5 to the conserved residue found in other P-type ATPases acquired properties of SERCA[191]. These studies show the extent of similarity between the members of P-type ATPases and the difficulty in obtaining PMCA specific inhibitors.

Caloxins are selected by screening the combinatorial peptide libraries displayed on phage particles for binding to the exdoms of PMCA that connect the TM domains on the extracellular side of the PM. A BLAST search of protein sequences in the SWISS-PORT Expert Protein Analysis System showed that the exdoms of PMCA do not share any significant homology with other P type ATPases and the sequence is unique to PMCA. Thus as expected, caloxins specifically inhibited the $Ca^{2+}$-$Mg^{2+}$ ATPase activity of PMCA without any effect

on other ATPases tested[3,166,167,169,173]. Randomization of the sequences of caloxins did not produce any inhibition of the $Ca^{2+}$-$Mg^{2+}$ ATPase activity of PMCA. Furthermore, a BLAST search showed that caloxin sequences are unique without any similarity to a naturally occurring protein. Thapsigargin, which is a specific and potent inhibitor of SERCA pump, has its binding site in the luminal loops between TM3/TM4 and TM7/TM8[192]. The luminal loops of SERCA correspond to the exdoms of PMCA. Ouabain inhibits the $Na^+$-$K^+$-ATPase by binding to its extracellular TM1/TM2 loop[193]. The specific reversible inhibitor of the gastric $H^+$-$K^+$-ATPase SCH28080, binds to the cavity surrounded by the TM 1,4,5,6,8 and the extracellular loops TM5/TM6, TM7/TM8 and TM9/TM10[194]. Omeprazole inhibits the gastric $H^+$-$K^+$-ATPase irreversibly by covalently modifying the cysteine in the TM5/TM6 extracellular loop[195]. Therefore, the unique sequences of the short extracytoplasmic loops of P-type ATPases are the binding sites of their known specific inhibitors.

### 4.4 Mechanism of inhibition by caloxins

The cysteine residue in the middle of the exdom 1 of PMCA4 was used to divide the exdom to synthesize two peptides corresponding to the sequence of exdom 1X and 1Y. The exdom 1X was used as a target to obtain caloxin 1b1, while the exdom 1Y was used to obtain caloxins 1b2 and 1a1. Caloxins inhibited PMCA activity in human erythrocyte ghosts and affected the steady state level of the acylphosphate intermediate formed during the reaction cycle of PMCA. Caloxins are expected to produce their modulatory effect on PMCA activity by

binding to their target exdom in PMCA. The photoactivable derivative of caloxin 1c2, a high affinity mutant of caloxin 1b1, photolabeled PMCA protein in the erythrocyte ghosts and the photolabeling was inhibited in the presence of excess synthetic exdom 1X as discussed in section 4.5. Therefore, caloxins may modulate PMCA activity by binding to their target exdom in the pump. A number of crystal structures of SERCA representing well-defined states of its reaction cycle have shown conformational changes occurring as a result of the concerted movements of the TM helices[56-61]. The luminal loops connecting the TM helices of SERCA also undergo changes in its functional cycle. Binding of thapsigargin to the luminal loops prevents the movements of the TM domains of SERCA leading to its inhibition. The luminal loops of SERCA correspond to the exdoms of PMCA. Therefore, the exdoms may also undergo conformational changes during the reaction cycle of PMCA and caloxins may inhibit those movements.

The exdom 1 of PMCA connects the TM domains 1 and 2. The TM domain 1 undergoes movements, which are important in relation to the cation translocation steps in both SERCA and the $Na^+$-$K^+$ ATPase. A contact point is formed between glycine and a bulky residue in the TM domains 1 and 3 to allow bending of the TM domain 1 that leads to the opening of the extracytoplasmic access pathway for the ions in both SERCA and the $Na^+$ pump. A conserved hydrophobic residue in the middle of the TM domain 1 facilitates the interaction and occlusion of $Ca^{2+}$and $K^+$ ions in SERCA and the $Na^+$ pump, respectively[196]. The TM domain 2 on the cytosolic side is connected to the actuator domain in

PMCA and other P-type ATPases. The sequence of the actuator domain is conserved and therefore it can be assumed that it has a similar 3-dimensional structure in all P-type ATPases. Studies on SERCA have shown that the coupling of phosphorylation that occurs at the cytosolic side, to the cation binding that occurs at the TM sites, is transmitted through the movement of the actuator domain. The large-scale movement of the actuator domain exerts a powerful drag on the TM1/2 and TM3/4, forcing them and their connecting luminal loops to separate from the rest of the TM domains of SERCA to form an open luminal pathway for the ion[57]. The actuator domain contains a conserved 'TGES' sequence that plays an important role in the dephosphorylation of the E2P conformation in the reaction cycle of both SERCA and the $Na^+$ pump. The movement of the actuator domain brings the 'TGES' sequence into close contact with the phosphorylated aspartate residue in the catalytic site to promote dephosphorylation of the pumps[197,198]. Thus, the TM domains 1 and 2 are involved in the long-range interactions essential for coupling the energy of ATP hydrolysis to the transport of ions in P-type ATPases. Further support for the importance of TM domains 1 and 2 in the P-type ATPases comes from the inhibition of the $Na^+$ pump activity upon binding of ouabain to the extracellular loop connecting the TM 1/2[193].

Caloxins obtained for binding to the different exdoms of PMCA have different effect on the steady state level of acylphosphate intermediate formed during its reaction cycle. Caloxins 1b1 and 1a1, obtained using the exdom 1 as a

target, caused an increase in the amount of acylphosphate formed during the reaction cycle of PMCA[169,173]. This is in contrast to the decrease in the acylphosphate formation by caloxin 2a1, which was obtained using the exdom 2 as a target[166]. Caloxin 3a1, obtained using the exdom 3 as a target, did not affect the level of acylphosphate intermediate[167]. Thus, caloxins binding to the different exdoms of PMCA may be inhibiting its activity by affecting different conformational states of the pump. Thapsigargin and ouabain inhibit the steady state amount of acylphosphate intermediate in the reaction cycle of SERCA and the $Na^+$ pump, respectively[175,199]. Lanthanum, which inhibits the ATPase activity of both PMCA and SERCA, causes an increase in the steady state level of acylphosphate in PMCA while decreasing its level in SERCA[1].

### 4.5 PMCA-binding domain of caloxin 1c2

Caloxin 1c2 (TAWSEVLDLLRR) showed higher affinity and PMCA4 isoform selectivity as compared to the parent caloxin 1b1 (TAWSEVLHLLSR). Two photoactivable derivatives of caloxin 1c2 with a C-terminal biotin tag were used to identify the binding site of caloxin 1c2. Of the two derivatives, 3Bpa1c2-biotin inhibited PMCA activity in the erythrocyte ghosts with a much lower affinity ($K_i$: 50 μM) than 16Bpa1c2-biotin ($K_i$: 5.1 μM). The affinity of 16Bpa1c2-biotin was comparable to that of caloxin 1c2 ($K_i$: 2.3 μM). However, at 50 or 100 μM, more intense photolabeling of the erythrocyte ghosts was observed with 3Bpa1c2-biotin than with 16Bpa1c2-biotin, even though the latter inhibited PMCA activity in ghosts with a much higher affinity. A likely

explanation is that W at position 3 in caloxin 1c2 sequence is crucial for binding. A comparison of the sequences selected after first screening of the Ph.D caloxin-1b1 like peptide library and those selected after competition show that the sequence (WSEVL) at position 3-7 is important for binding to PMCA. The residues (WSEVL) at position 3-7 in caloxin 1b1 appeared with their conservative substitutions (WS(E/D)V(L/V) in 88 % of the clones sequenced after first screening (Table. 3.3) and in 96 % of the clones selected after competition (Table. 3.4). The residue 'W' at position 3 appeared in 95 % of the clones selected after the first screening (Table. 3.3) and in 100 % of the clones selected after competition (Table. 3.4). Therefore, W at position 3 is part of the moiety (WS(E/D)V(L/V) that appears to be important for binding to PMCA protein and is also essential for the inhibitory potential of caloxin as seen with an increase in $K_i$ following its substitution by Bpa in 3Bpa1c2-biotin. Thus W at position 3 may form a crucial contact point for caloxin 1c2 binding to PMCA. The intense UV-crosslinking observed with 3Bap1c2-biotin is also consistent with this assertion. The residues lying outside the selective 12-mer domain unique to caloxin 1c2 and separated from it by glycines, do not appear to play a role in binding and inhibiting PMCA activity as observed with substitution of S at position 16 and the addition of a C-terminal biotin tag in 16Bpa1c2-biotin that had minimal effect on its inhibitory potential.

The photoactivable derivatives 3Bpa1c2-biotin and 16Bpa1c2-biotin formed a photoadduct, which appeared as a high molecular weight doublet at 250-

270 kDa detected both with streptavidin and the PMCA specific antibodies. However, Western blots using the PMCA specific antibodies, JA9 (anti-PMCA4) and 5F10 (anti-PMCA) showed most of PMCA protein at 130-140 kDa, suggesting that only a small fraction of PMCA protein was present as a high molecular weight photoadduct. Furthermore, the 250-270 kDa photoadduct was confirmed to be PMCA by its immunoprecipitation using the PMCA specific antibody. PMCA is a single chain integral membrane protein with approximate $M_r$ of ~138 kDa on the SDS-PAGE. However, PMCA protein purified from the erythrocyte membranes by calmodulin affinity chromatography yields a protein band with a molecular weight in excess of 200 kDa in addition to the major band at 138 kDa[40]. This high molecular weight band that forms an acylphosphate intermediate is thought to be a dimer of PMCA. A similar high molecular weight band was also observed with PMCA protein crosslinked to $^{125}$I-azido modified calmodulin under non-denaturing PAGE[200]. The radiation inactivation experiments on the erythrocyte membranes have estimated the size of PMCA to be ~251 kDa, which is close to twice that of the monomer, suggesting that it exists as a dimer in the native erythrocyte membranes[200,201]. However, the size obtained with radiation inactivation may also include the lipid annulus around PMCA protein. The reversible concentration dependent oligomerization of purified PMCA has been demonstrated by measurements of fluorescence resonance energy transfer between the labeled PMCA molecules[202-204]. The extent of oligomerization of purified PMCA and mass of the active dimer was

determined by equilibrium ultracentrifugation to be ~260 kDa[205]. Studies with purified PMCA have shown that the calmodulin-binding domain and a second region that may be related to the intracellular sites, which bind the autoinhibitory C-terminal domain of the pump are involved in promoting its oligomerization[203,204]. PMCA dimerization leads to calmodulin independent stimulation of the ATPase activity, although the dimer retains the ability to bind to calmodulin[202,204]. A study on the oligomerization of PMCA in phospholipid/detergent micelles suggests that PMCA dimerization may constitute a mechanism of self-protection against denaturation[206]. Radiation inactivation has determined that the αβ subunit complex of the $Na^+$ pump also exists as a dimer in the native membranes[200,207]. Studies co expressing different isoforms of the α subunit of the $Na^+$ pump have suggested a role for this subunit in the formation of specific and stable oligomers[208]. Therefore, there is evidence that P type ATPases exist as functional oligomers in the PM.

### 4.6 Studies using caloxins

Caloxins have been used to study the role of PMCA in cell physiology. In a study to determine the role of PM $Ca^{2+}$ efflux transporters in the generation of agonist independent $[Ca^{2+}]_i$ oscillations, both carboxyeosin and caloxin were used to inhibit PMCA in human mesenchymal stem cells. Caloxin 2a1 transiently elevated $[Ca^{2+}]_i$ that returned to basal levels with complete blocking of the $[Ca^{2+}]_i$ oscillations. Carboxyeosin, on the other hand, caused a sustained elevation of the basal $[Ca^{2+}]_i$ before blocking the $[Ca^{2+}]_i$ oscillations. An effect similar to that of

carboxyeosin was also observed by the inhibition of NCX by removal of extracellular $Na^+$ that elevated the basal $[Ca^{2+}]_i$ before blocking the $[Ca^{2+}]_i$ oscillations[209]. In another study, a similar transient increase in $[Ca^{2+}]_i$ was observed by PMCA inhibition by caloxin 2a1, while carboxyeosin caused a monotonic increase in $[Ca^{2+}]_i$ in mouse embryonic stem cells[210]. The effect of caloxin 2a1 can result by specific inhibition of the $Ca^{2+}$ extrusion by PMCA, while the elevation of the basal $[Ca^{2+}]_i$ by carboxyeosin can be explained by the inhibition of both PMCA and the $Na^+$ pump. Inhibition of the $Na^+$ pump by carboxyeosin can lead to $Ca^{2+}$ entry by NCX. Caloxin 2a1 has been used to study the role of $Ca^{2+}$ extruded by PMCA in stimulating the extracellular $Ca^{2+}$ sensing receptor expressed in HEK-293 cells. The study reported the novel autocrine and paracrine mechanism for the stimulation of the receptor by PMCA mediated increase in extracellular $Ca^{2+}$, which leads to generation of $Ca^{2+}$ spikes independent of the gap junction mediated cell-cell communication of $Ca^{2+}$ [211]. Caloxin 2a1 has also been used to study the mechanism of domoate-induced cytosolic acidification in the cerebellar granule cells and the effect of PMCA inhibition in the lens cell cultures[212,213].

The isoform selective caloxins will help to understand the role of PMCA isoforms 1-4 in cell physiology. Caloxin 1b1 selected using the exdom 1X of PMCA4 as a target showed slight preference for PMCA4 isoform. The endothelial cells from the pig coronary artery express mainly PMCA1 isoform, while the smooth muscle cells express both PMCA 1 and 4 isoforms. Caloxin 1b1 when

added extracellularly caused an increase in $[Ca^{2+}]_i$ in both the cell types. However, the increase in $[Ca^{2+}]_i$ was much greater in the smooth muscle cells than in the endothelial cells. Similarly, caloxin 1b1 increased the force of contraction in the smooth muscle in de-endothelialized rat aorta without potentiating the endothelium-induced relaxation. Caloxin 1c2 that inhibits PMCA4 isoform with higher affinity as compared to other PMCA isoforms caused an increase in the basal tone of the de-endothelialized pig coronary artery rings. This effect was similar at caloxin 1c2 concentrations of 10 and 50 μM. Since lower concentrations of caloxin 1c2 will primarily inhibit PMCA4 isoform, it suggests a primary role of this isoform in maintaining the basal tone. There are numerous examples where the different PMCA isoforms may be present in different cell types in the same tissue (e.g. brain, pancreas) or even in different microdomains of the PM, like caveolae or lipid rafts in the same cell. The isoform selective caloxins will help to delineate the role of various PMCA isoforms in their cellular environment.

### 4.7 Conclusions and Future experiments

This study filled a major gap in PMCA biology by the introduction of PMCA4 isoform selective inhibitor caloxin 1c2. In doing so, it established the role of exdoms in PMCA reaction cycle. In the process of inventing caloxin 1c2 and its predecessors, this study introduced novel methods. Finally, it also leads to encouraging future possibilities in the field of PMCA biology.

Exdoms in PMCA1-4 differ in their sequences and this difference was exploited to obtain caloxin 1b1 and then the PMCA4 selective high affinity caloxin 1c2. To the best of our knowledge, there are no known isoform specific inhibitors of any other P-type ATPases. Thus the invention of caloxin 1c2 is a major advance. It's implications become apparent when considering the differences in PMCA isoform expression between tissues such as coronary artery smooth muscle and endothelium.

The experimental evidence that caloxin 1c2 binds to the exdom 1X of PMCA protein is important in establishing that caloxins mediate their inhibitory effects by binding specifically to their target exdoms in PMCA. Previously, the exdoms of PMCA were not considered to play any role in PMCA function. This study has shown that caloxins that bind the exdoms can inhibit PMCA activity, indicating that the exdoms are involved in the reaction cycle of PMCA.

Phage display has been normally screened with varied success in different studies or phage display has been usually screened with varied success in different studies. This study advanced this technology as follows. Since the synthetic exdom peptides may differ in conformation from their native counterparts, the concept of two-step screening was introduced. The phage libraries may be biased due to differences in the frequencies and amplification efficiencies of individual phage clones. Therefore, the concept of competition between equal copy number of each of the phage particles was introduced. The selectivity and affinity of peptides can often be enhanced by limited mutagenesis. However, systematic

mutagenesis is labor intensive and costly. Therefore, the concept of creating caloxin 1b1-like libraries was brought in to obtain the mutant caloxin 1c2. All these methods can be used not only to obtain better caloxins, but to also enhance the field of phage display.

Whereas this study is a major advancement, it also opens new avenues. For instance, the exact binding site of caloxin 1c2 can be determined by proteomics. The affinities of biotinylated caloxins can be determined by methods such as surface plasmon resonance to understand the role of exdom 1X in the PMCA reaction cycle. Methods of displacement of the biotinylated caloxins may be used in throughput screening to develop non-peptide inhibitors.

Caloxins have been used to inhibit PMCA activity in physiological studies in our labs and by others. Future studies with PMCA4 specific caloxins can be used to: a) study the effect of co-localization of PMCA4 with other signaling molecules like nNOS in caveolae; b) understand the mechanism of the antinecrotic role of PMCA4 inhibition in certain cell types; c) study the importance of PMCA4 in sperm motility; and d) understand the role of PMCA4 in hypertension. Thus, it is anticipated that PMCA isoform specific caloxins will advance the field of PMCA physiology and pathophysiology.

## 5.0 REFERENCES


1. Carafoli,E. Calcium pump of the plasma membrane. *Physiol Rev.* **71**, 129-153 (1991).
2. Carafoli,E. The Ca2+ pump of the plasma membrane. *J. Biol. Chem.* **267**, 2115-2118 (1992).
3. Pande,J. & Grover,A.K. Plasma membrane calcium pumps in smooth muscle: from fictional molecules to novel inhibitors. *Can. J. Physiol Pharmacol.* **83**, 743-754 (2005).
4. Szewczyk,M.M. *et al.* Ca2+-pumps and Na2+-Ca2+-exchangers in coronary artery endothelium versus smooth muscle. *J. Cell Mol. Med.* **11**, 129-138 (2007).
5. Carafoli,E. Calcium-mediated cellular signals: a story of failures. *Trends Biochem. Sci.* **29**, 371-379 (2004).
6. Heyliger,C.E., Prakash,A. & McNeill,J.H. Alterations in cardiac sarcolemmal Ca2+ pump activity during diabetes mellitus. *Am. J. Physiol* **252**, H540-H544 (1987).
7. Kozel,P.J. *et al.* Balance and hearing deficits in mice with a null mutation in the gene encoding plasma membrane Ca2+-ATPase isoform 2. *J. Biol. Chem.* **273**, 18693-18696 (1998).
8. Kwan,C.Y., Belbeck,L. & Daniel,E.E. Abnormal biochemistry of vascular smooth muscle plasma membrane as an important factor in the initiation and maintenance of hypertension in rats. *Blood Vessels* **16**, 259-268 (1979).
9. Lehotsky,J., Kaplan,P., Murin,R. & Raeymaekers,L. The role of plasma membrane Ca2+ pumps (PMCAs) in pathologies of mammalian cells. *Front Biosci.* **7**, d53-d84 (2002).
10. Missiaen,L. *et al.* Abnormal intracellular ca(2+)homeostasis and disease. *Cell Calcium* **28**, 1-21 (2000).
11. Monteith,G.R., McAndrew,D., Faddy,H.M. & Roberts-Thomson,S.J. Calcium and cancer: targeting Ca2+ transport. *Nat. Rev. Cancer* **7**, 519-530 (2007).
12. Oceandy,D., Buch,M.H., Cartwright,E.J. & Neyses,L. The emergence of plasma membrane calcium pump as a novel therapeutic target for heart disease. *Mini. Rev. Med. Chem.* **6**, 583-588 (2006).
13. Schuh,K. *et al.* Plasma membrane Ca2+ ATPase 4 is required for sperm motility and male fertility. *J. Biol. Chem.* **279**, 28220-28226 (2004).
14. Tappia,P.S. *et al.* Role of oxidative stress in catecholamine-induced changes in cardiac sarcolemmal Ca2+ transport. *Arch. Biochem. Biophys.* **387**, 85-92 (2001).
15. Berridge,M.J., Bootman,M.D. & Roderick,H.L. Calcium signalling: dynamics, homeostasis and remodelling. *Nat. Rev. Mol. Cell Biol.* **4**, 517-529 (2003).

16. Carafoli,E., Santella,L., Branca,D. & Brini,M. Generation, control, and processing of cellular calcium signals. *Crit Rev. Biochem. Mol. Biol.* **36**, 107-260 (2001).
17. Clapham,D.E. Calcium signaling. *Cell* **131**, 1047-1058 (2007).
18. Bootman,M.D. *et al.* Calcium signalling--an overview. *Semin. Cell Dev. Biol.* **12**, 3-10 (2001).
19. Carafoli,E. The signaling function of calcium and its regulation. *J. Hypertens. Suppl* **12**, S47-S56 (1994).
20. Carafoli,E. Calcium signaling: a tale for all seasons. *Proc. Natl. Acad. Sci. U. S. A* **99**, 1115-1122 (2002).
21. Carafoli,E. Intracellular calcium homeostasis. *Annu. Rev. Biochem.* **56**, 395-433 (1987).
22. Marin,J., Encabo,A., Briones,A., Garcia-Cohen,E.C. & Alonso,M.J. Mechanisms involved in the cellular calcium homeostasis in vascular smooth muscle: calcium pumps. *Life Sci.* **64**, 279-303 (1999).
23. Berridge,M.J., Lipp,P. & Bootman,M.D. The versatility and universality of calcium signalling. *Nat. Rev. Mol. Cell Biol.* **1**, 11-21 (2000).
24. Thomas,A.P., Bird,G.S., Hajnoczky,G., Robb-Gaspers,L.D. & Putney,J.W., Jr. Spatial and temporal aspects of cellular calcium signaling. *FASEB J.* **10**, 1505-1517 (1996).
25. Penniston,J.T. & Enyedi,A. Modulation of the plasma membrane Ca2+ pump. *J. Membr. Biol.* **165**, 101-109 (1998).
26. Meldolesi,J. & Pozzan,T. The endoplasmic reticulum Ca2+ store: a view from the lumen. *Trends Biochem. Sci.* **23**, 10-14 (1998).
27. Brini,M. & Carafoli,E. Calcium signalling: a historical account, recent developments and future perspectives. *Cell Mol. Life Sci.* **57**, 354-370 (2000).
28. Missiaen,L. *et al.* Ca2+ extrusion across plasma membrane and Ca2+ uptake by intracellular stores. *Pharmacol. Ther.* **50**, 191-232 (1991).
29. Missiaen,L., De Smedt,H., Droogmans,G., Himpens,B. & Casteels,R. Calcium ion homeostasis in smooth muscle. *Pharmacol. Ther.* **56**, 191-231 (1992).
30. Missiaen,L., Dode,L., Vanoevelen,J., Raeymaekers,L. & Wuytack,F. Calcium in the Golgi apparatus. *Cell Calcium* **41**, 405-416 (2007).
31. Wuytack,F. & Raeymaekers,L. The Ca(2+)-transport ATPases from the plasma membrane. *J. Bioenerg. Biomembr.* **24**, 285-300 (1992).
32. Wuytack,F., Raeymaekers,L. & Missiaen,L. Molecular physiology of the SERCA and SPCA pumps. *Cell Calcium* **32**, 279-305 (2002).
33. Wuytack,F., Raeymaekers,L. & Missiaen,L. PMR1/SPCA Ca2+ pumps and the role of the Golgi apparatus as a Ca2+ store. *Pflugers Arch.* **446**, 148-153 (2003).
34. Guerini,D., Coletto,L. & Carafoli,E. Exporting calcium from cells. *Cell Calcium* **38**, 281-289 (2005).

35. Philipson,K.D. *et al.* The Na+/Ca2+ exchange molecule: an overview. *Ann. N. Y. Acad. Sci.* **976**, 1-10 (2002).
36. Schnetkamp,P.P. The SLC24 Na+/Ca2+-K+ exchanger family: vision and beyond. *Pflugers Arch.* **447**, 683-688 (2004).
37. Carafoli,E. Historical review: mitochondria and calcium: ups and downs of an unusual relationship. *Trends Biochem. Sci.* **28**, 175-181 (2003).
38. Kirichok,Y., Krapivinsky,G. & Clapham,D.E. The mitochondrial calcium uniporter is a highly selective ion channel. *Nature* **427**, 360-364 (2004).
39. Penniston,J.T., Enyedi,A., Verma,A.K., Adamo,H.P. & Filoteo,A.G. Plasma membrane Ca2+ pumps. *Ann. N. Y. Acad. Sci.* **834**, 56-64 (1997).
40. Carafoli,E. & Zurini,M. The Ca2+-pumping ATPase of plasma membranes. Purification, reconstitution and properties. *Biochim. Biophys. Acta* **683**, 279-301 (1982).
41. Carafoli,E. Biogenesis: plasma membrane calcium ATPase: 15 years of work on the purified enzyme. *FASEB J.* **8**, 993-1002 (1994).
42. Carafoli,E. Plasma membrane calcium pump: structure, function and relationships. *Basic Res. Cardiol.* **92 Suppl 1**, 59-61 (1997).
43. DUNHAM,E.T. & GLYNN,I.M. Adenosinetriphosphatase activity and the active movements of alkali metal ions. *J. Physiol* **156**, 274-293 (1961).
44. Schatzmann,H.J. ATP-dependent Ca++-extrusion from human red cells. *Experientia* **22**, 364-365 (1966).
45. Carafoli,E., Garcia-Martin,E. & Guerini,D. The plasma membrane calcium pump: recent developments and future perspectives. *Experientia* **52**, 1091-1100 (1996).
46. Grover,A.K. & Khan,I. Calcium pump isoforms: diversity, selectivity and plasticity. Review article. *Cell Calcium* **13**, 9-17 (1992).
47. Stauffer,T.P., Guerini,D. & Carafoli,E. Tissue distribution of the four gene products of the plasma membrane Ca2+ pump. A study using specific antibodies. *J. Biol. Chem.* **270**, 12184-12190 (1995).
48. Strehler,E.E. & Zacharias,D.A. Role of alternative splicing in generating isoform diversity among plasma membrane calcium pumps. *Physiol Rev.* **81**, 21-50 (2001).
49. Monteith,G.R. & Roufogalis,B.D. The plasma membrane calcium pump--a physiological perspective on its regulation. *Cell Calcium* **18**, 459-470 (1995).
50. Monteith,G.R., Wanigasekara,Y. & Roufogalis,B.D. The plasma membrane calcium pump, its role and regulation: new complexities and possibilities. *J. Pharmacol. Toxicol. Methods* **40**, 183-190 (1998).
51. Wang,K.K., Villalobo,A. & Roufogalis,B.D. The plasma membrane calcium pump: a multiregulated transporter. *Trends Cell Biol.* **2**, 46-52 (1992).
52. Apell,H.J. How do P-type ATPases transport ions? *Bioelectrochemistry.* **63**, 149-156 (2004).

53. Moller,J.V., Juul,B. & le Maire,M. Structural organization, ion transport, and energy transduction of P-type ATPases. *Biochim. Biophys. Acta* **1286**, 1-51 (1996).
54. Sweadner,K.J. & Donnet,C. Structural similarities of Na,K-ATPase and SERCA, the Ca(2+)-ATPase of the sarcoplasmic reticulum. *Biochem. J.* **356**, 685-704 (2001).
55. Carafoli,E. & Brini,M. Calcium pumps: structural basis for and mechanism of calcium transmembrane transport. *Curr. Opin. Chem. Biol.* **4**, 152-161 (2000).
56. Olesen,C., Sorensen,T.L., Nielsen,R.C., Moller,J.V. & Nissen,P. Dephosphorylation of the calcium pump coupled to counterion occlusion. *Science* **306**, 2251-2255 (2004).
57. Olesen,C. *et al.* The structural basis of calcium transport by the calcium pump. *Nature* **450**, 1036-1042 (2007).
58. Toyoshima,C., Nakasako,M., Nomura,H. & Ogawa,H. Crystal structure of the calcium pump of sarcoplasmic reticulum at 2.6 A resolution. *Nature* **405**, 647-655 (2000).
59. Toyoshima,C. & Nomura,H. Structural changes in the calcium pump accompanying the dissociation of calcium. *Nature* **418**, 605-611 (2002).
60. Toyoshima,C. & Mizutani,T. Crystal structure of the calcium pump with a bound ATP analogue. *Nature* **430**, 529-535 (2004).
61. Toyoshima,C., Nomura,H. & Tsuda,T. Lumenal gating mechanism revealed in calcium pump crystal structures with phosphate analogues. *Nature* **432**, 361-368 (2004).
62. Gadsby,D.C. Structural biology: ion pumps made crystal clear. *Nature* **450**, 957-959 (2007).
63. Kosk-Kosicka,D., Scaillet,S. & Inesi,G. The partial reactions in the catalytic cycle of the calcium-dependent adenosine triphosphatase purified from erythrocyte membranes. *J. Biol. Chem.* **261**, 3333-3338 (1986).
64. Rega,A.F. & Garrahan,P.J. Calcium ion-dependent phosphorylation of human erythrocyte membranes. *J. Membr. Biol.* **22**, 313-327 (1975).
65. Chiesi,M., Zurini,M. & Carafoli,E. ATP synthesis catalyzed by the purified erythrocyte Ca-ATPase in the absence of calcium gradients. *Biochemistry* **23**, 2595-2600 (1984).
66. Adamo,H.P., Rega,A.F. & Garrahan,P.J. The E2 in equilibrium E1 transition of the Ca2(+)-ATPase from plasma membranes studied by phosphorylation. *J. Biol. Chem.* **265**, 3789-3792 (1990).
67. Adamo,H.P., Rega,A.F. & Garrahan,P.J. Pre-steady-state phosphorylation of the human red cell Ca2+-ATPase. *J. Biol. Chem.* **263**, 17548-17554 (1988).
68. Filomatori,C.V. & Rega,A.F. On the mechanism of activation of the plasma membrane Ca2+-ATPase by ATP and acidic phospholipids. *J. Biol. Chem.* **278**, 22265-22271 (2003).

69. Garrahan,P.J. & Rega,A.F. Activation of partial reactions of the Ca2+-ATPase from human red cells by Mg2+ and ATP. *Biochim. Biophys. Acta* **513**, 59-65 (1978).
70. Grover,A.K. & Samson,S.E. Pig coronary artery smooth muscle: substrate and pH dependence of the two calcium pumps. *Am. J. Physiol* **251**, C529-C534 (1986).
71. Salvador,J.M., Inesi,G., Rigaud,J.L. & Mata,A.M. Ca2+ transport by reconstituted synaptosomal ATPase is associated with H+ countertransport and net charge displacement. *J. Biol. Chem.* **273**, 18230-18234 (1998).
72. Niggli,V., Sigel,E. & Carafoli,E. The purified Ca2+ pump of human erythrocyte membranes catalyzes an electroneutral Ca2+-H+ exchange in reconstituted liposomal systems. *J. Biol. Chem.* **257**, 2350-2356 (1982).
73. Carafoli,E. & Stauffer,T. The plasma membrane calcium pump: functional domains, regulation of the activity, and tissue specificity of isoform expression. *J. Neurobiol.* **25**, 312-324 (1994).
74. Szewczyk,M.M., Pande,J. & Grover,A.K. Caloxins: a novel class of selective plasma membrane Ca(2+) pump inhibitors obtained using biotechnology. *Pflugers Arch.* **456**, 255-266 (2008).
75. James,P. *et al.* Identification and primary structure of a calmodulin binding domain of the Ca2+ pump of human erythrocytes. *J. Biol. Chem.* **263**, 2905-2910 (1988).
76. Hofmann,F., James,P., Vorherr,T. & Carafoli,E. The C-terminal domain of the plasma membrane Ca2+ pump contains three high affinity Ca2+ binding sites. *J. Biol. Chem.* **268**, 10252-10259 (1993).
77. Paszty,K. *et al.* Asp1080 upstream of the calmodulin-binding domain is critical for autoinhibition of hPMCA4b. *J. Biol. Chem.* **277**, 36146-36151 (2002).
78. Falchetto,R., Vorherr,T., Brunner,J. & Carafoli,E. The plasma membrane Ca2+ pump contains a site that interacts with its calmodulin-binding domain. *J. Biol. Chem.* **266**, 2930-2936 (1991).
79. Falchetto,R., Vorherr,T. & Carafoli,E. The calmodulin-binding site of the plasma membrane Ca2+ pump interacts with the transduction domain of the enzyme. *Protein Sci.* **1**, 1613-1621 (1992).
80. Hilfiker,H., Guerini,D. & Carafoli,E. Cloning and expression of isoform 2 of the human plasma membrane Ca2+ ATPase. Functional properties of the enzyme and its splicing products. *J. Biol. Chem.* **269**, 26178-26183 (1994).
81. Chicka,M.C. & Strehler,E.E. Alternative splicing of the first intracellular loop of plasma membrane Ca2+-ATPase isoform 2 alters its membrane targeting. *J. Biol. Chem.* **278**, 18464-18470 (2003).
82. Hill,J.K. *et al.* Splice-site A choice targets plasma-membrane Ca2+-ATPase isoform 2 to hair bundles. *J. Neurosci.* **26**, 6172-6180 (2006).

83. Reinhardt,T.A., Lippolis,J.D., Shull,G.E. & Horst,R.L. Null mutation in the gene encoding plasma membrane Ca2+-ATPase isoform 2 impairs calcium transport into milk. *J. Biol. Chem.* **279**, 42369-42373 (2004).
84. Strehler,E.E. *et al.* Plasma membrane Ca2+ ATPases as dynamic regulators of cellular calcium handling. *Ann. N. Y. Acad. Sci.* **1099**, 226-236 (2007).
85. Fanning,A.S. & Anderson,J.M. PDZ domains: fundamental building blocks in the organization of protein complexes at the plasma membrane. *J. Clin. Invest* **103**, 767-772 (1999).
86. Schuh,K., Uldrijan,S., Gambaryan,S., Roethlein,N. & Neyses,L. Interaction of the plasma membrane Ca2+ pump 4b/CI with the Ca2+/calmodulin-dependent membrane-associated kinase CASK. *J. Biol. Chem.* **278**, 9778-9783 (2003).
87. DeMarco,S.J., Chicka,M.C. & Strehler,E.E. Plasma membrane Ca2+ ATPase isoform 2b interacts preferentially with Na+/H+ exchanger regulatory factor 2 in apical plasma membranes. *J. Biol. Chem.* **277**, 10506-10511 (2002).
88. Brandt,P., Neve,R.L., Kammesheidt,A., Rhoads,R.E. & Vanaman,T.C. Analysis of the tissue-specific distribution of mRNAs encoding the plasma membrane calcium-pumping ATPases and characterization of an alternately spliced form of PMCA4 at the cDNA and genomic levels. *J. Biol. Chem.* **267**, 4376-4385 (1992).
89. Zacharias,D.A. & Kappen,C. Developmental expression of the four plasma membrane calcium ATPase (Pmca) genes in the mouse. *Biochim. Biophys. Acta* **1428**, 397-405 (1999).
90. Filoteo,A.G. *et al.* Plasma membrane Ca2+ pump in rat brain. Patterns of alternative splices seen by isoform-specific antibodies. *J. Biol. Chem.* **272**, 23741-23747 (1997).
91. Guerini,D. The significance of the isoforms of plasma membrane calcium ATPase. *Cell Tissue Res.* **292**, 191-197 (1998).
92. Varadi,A., Molnar,E. & Ashcroft,S.J. A unique combination of plasma membrane Ca2+-ATPase isoforms is expressed in islets of Langerhans and pancreatic beta-cell lines. *Biochem. J.* **314 ( Pt 2)**, 663-669 (1996).
93. Kuo,T.H. *et al.* Co-ordinated regulation of the plasma membrane calcium pump and the sarco(endo)plasmic reticular calcium pump gene expression by Ca2+. *Cell Calcium* **21**, 399-408 (1997).
94. Guerini,D. *et al.* The expression of plasma membrane Ca2+ pump isoforms in cerebellar granule neurons is modulated by Ca2+. *J. Biol. Chem.* **274**, 1667-1676 (1999).
95. Guerini,D., Wang,X., Li,L., Genazzani,A. & Carafoli,E. Calcineurin controls the expression of isoform 4CII of the plasma membrane Ca(2+) pump in neurons. *J. Biol. Chem.* **275**, 3706-3712 (2000).

96. Hammes,A. *et al.* Differentiation-specific isoform mRNA expression of the calmodulin-dependent plasma membrane Ca(2+)-ATPase. *FASEB J.* **8**, 428-435 (1994).
97. Keller,D. & Grover,A.K. Nerve growth factor treatment alters Ca2+ pump levels in PC12 cells. *Neuroreport* **11**, 65-68 (2000).
98. Niggli,V., Ronner,P., Carafoli,E. & Penniston,J.T. Effects of calmodulin on the (Ca2+ + Mg2+)ATPase partially purified from erythrocyte membranes. *Arch. Biochem. Biophys.* **198**, 124-130 (1979).
99. Niggli,V., Adunyah,E.S., Penniston,J.T. & Carafoli,E. Purified (Ca2+-Mg2+)-ATPase of the erythrocyte membrane. Reconstitution and effect of calmodulin and phospholipids. *J. Biol. Chem.* **256**, 395-401 (1981).
100. Downes,P. & Michell,R.H. Human erythrocyte membranes exhibit a cooperative calmodulin-dependent Ca2+-ATPase of high calcium sensitivity. *Nature* **290**, 270-271 (1981).
101. Osborn,K.D., Zaidi,A., Mandal,A., Urbauer,R.J. & Johnson,C.K. Single-molecule dynamics of the calcium-dependent activation of plasma-membrane Ca2+-ATPase by calmodulin. *Biophys. J.* **87**, 1892-1899 (2004).
102. Caride,A.J. *et al.* The plasma membrane calcium pump displays memory of past calcium spikes. Differences between isoforms 2b and 4b. *J. Biol. Chem.* **276**, 39797-39804 (2001).
103. Enyedi,A. *et al.* The Ca2+ affinity of the plasma membrane Ca2+ pump is controlled by alternative splicing. *J. Biol. Chem.* **269**, 41-43 (1994).
104. Verma,A.K., Enyedi,A., Filoteo,A.G., Strehler,E.E. & Penniston,J.T. Plasma membrane calcium pump isoform 4a has a longer calmodulin-binding domain than 4b. *J. Biol. Chem.* **271**, 3714-3718 (1996).
105. Caride,A.J. *et al.* The rate of activation by calmodulin of isoform 4 of the plasma membrane Ca(2+) pump is slow and is changed by alternative splicing. *J. Biol. Chem.* **274**, 35227-35232 (1999).
106. Caride,A.J. *et al.* Delayed activation of the plasma membrane calcium pump by a sudden increase in Ca2+: fast pumps reside in fast cells. *Cell Calcium* **30**, 49-57 (2001).
107. Elwess,N.L., Filoteo,A.G., Enyedi,A. & Penniston,J.T. Plasma membrane Ca2+ pump isoforms 2a and 2b are unusually responsive to calmodulin and Ca2+. *J. Biol. Chem.* **272**, 17981-17986 (1997).
108. Caride,A.J., Filoteo,A.G., Penniston,J.T. & Strehler,E.E. The plasma membrane Ca2+ pump isoform 4a differs from isoform 4b in the mechanism of calmodulin binding and activation kinetics: implications for Ca2+ signaling. *J. Biol. Chem.* **282**, 25640-25648 (2007).
109. Penheiter,A.R. *et al.* A model for the activation of plasma membrane calcium pump isoform 4b by calmodulin. *Biochemistry* **42**, 12115-12124 (2003).

110. Guerini,D., Pan,B. & Carafoli,E. Expression, purification, and characterization of isoform 1 of the plasma membrane Ca2+ pump: focus on calpain sensitivity. *J. Biol. Chem.* **278**, 38141-38148 (2003).
111. Filoteo,A.G., Enyedi,A., Verma,A.K., Elwess,N.L. & Penniston,J.T. Plasma membrane Ca(2+) pump isoform 3f is weakly stimulated by calmodulin. *J. Biol. Chem.* **275**, 4323-4328 (2000).
112. Gromadzinska,E., Lachowicz,L., Walkowiak,B. & Zylinska,L. Calmodulin effect on purified rat cortical plasma membrane Ca(2+)-ATPase in different phosphorylation states. *Biochim. Biophys. Acta* **1549**, 19-31 (2001).
113. Bruce,J.I., Yule,D.I. & Shuttleworth,T.J. Ca2+-dependent protein kinase--a modulation of the plasma membrane Ca2+-ATPase in parotid acinar cells. *J. Biol. Chem.* **277**, 48172-48181 (2002).
114. Baggaley,E., McLarnon,S., Demeter,I., Varga,G. & Bruce,J.I. Differential regulation of the apical plasma membrane Ca(2+) -ATPase by protein kinase A in parotid acinar cells. *J. Biol. Chem.* **282**, 37678-37693 (2007).
115. Furukawa,K., Tawada,Y. & Shigekawa,M. Regulation of the plasma membrane Ca2+ pump by cyclic nucleotides in cultured vascular smooth muscle cells. *J. Biol. Chem.* **263**, 8058-8065 (1988).
116. Vrolix,M., Raeymaekers,L., Wuytack,F., Hofmann,F. & Casteels,R. Cyclic GMP-dependent protein kinase stimulates the plasmalemmal Ca2+ pump of smooth muscle via phosphorylation of phosphatidylinositol. *Biochem. J.* **255**, 855-863 (1988).
117. Enyedi,A., Verma,A.K., Filoteo,A.G. & Penniston,J.T. Protein kinase C activates the plasma membrane Ca2+ pump isoform 4b by phosphorylation of an inhibitory region downstream of the calmodulin-binding domain. *J. Biol. Chem.* **271**, 32461-32467 (1996).
118. Kuo,T.H., Wang,K.K., Carlock,L., Diglio,C. & Tsang,W. Phorbol ester induces both gene expression and phosphorylation of the plasma membrane Ca2+ pump. *J. Biol. Chem.* **266**, 2520-2525 (1991).
119. Enyedi,A. *et al.* Protein kinase C phosphorylates the "a" forms of plasma membrane Ca2+ pump isoforms 2 and 3 and prevents binding of calmodulin. *J. Biol. Chem.* **272**, 27525-27528 (1997).
120. Verma,A.K., Paszty,K., Filoteo,A.G., Penniston,J.T. & Enyedi,A. Protein kinase C phosphorylates plasma membrane Ca2+ pump isoform 4a at its calmodulin binding domain. *J. Biol. Chem.* **274**, 527-531 (1999).
121. Roelofsen,B. & Schatzmann,H.J. The lipid requirement of the (Ca2+ + Mg2+)-ATPase in the human erythrocyte membrane, as studied by various highly purified phospholipases. *Biochim. Biophys. Acta* **464**, 17-36 (1977).
122. Enyedi,A., Flura,M., Sarkadi,B., Gardos,G. & Carafoli,E. The maximal velocity and the calcium affinity of the red cell calcium pump may be regulated independently. *J. Biol. Chem.* **262**, 6425-6430 (1987).
123. Niggli,V., Adunyah,E.S. & Carafoli,E. Acidic phospholipids, unsaturated fatty acids, and limited proteolysis mimic the effect of calmodulin on the

purified erythrocyte Ca2+ - ATPase. *J. Biol. Chem.* **256**, 8588-8592 (1981).
124. Choquette,D. *et al.* Regulation of plasma membrane Ca2+ ATPases by lipids of the phosphatidylinositol cycle. *Biochem. Biophys. Res. Commun.* **125**, 908-915 (1984).
125. Brodin,P., Falchetto,R., Vorherr,T. & Carafoli,E. Identification of two domains which mediate the binding of activating phospholipids to the plasma-membrane Ca2+ pump. *Eur. J. Biochem.* **204**, 939-946 (1992).
126. Pinto,F.T. & Adamo,H.P. Deletions in the acidic lipid-binding region of the plasma membrane Ca2+ pump. A mutant with high affinity for Ca2+ resembling the acidic lipid-activated enzyme. *J. Biol. Chem.* **277**, 12784-12789 (2002).
127. Wanaverbecq,N., Marsh,S.J., Al Qatari,M. & Brown,D.A. The plasma membrane calcium-ATPase as a major mechanism for intracellular calcium regulation in neurones from the rat superior cervical ganglion. *J. Physiol* **550**, 83-101 (2003).
128. Grover,A.K. & Samson,S.E. Effect of superoxide radical on Ca2+ pumps of coronary artery. *Am. J. Physiol* **255**, C297-C303 (1988).
129. Zylinska,L. & Soszynski,M. Plasma membrane Ca2+-ATPase in excitable and nonexcitable cells. *Acta Biochim. Pol.* **47**, 529-539 (2000).
130. Bautista,D.M., Hoth,M. & Lewis,R.S. Enhancement of calcium signalling dynamics and stability by delayed modulation of the plasma-membrane calcium-ATPase in human T cells. *J. Physiol* **541**, 877-894 (2002).
131. Foder,B. & Scharff,O. Solitary calcium spike dependent on calmodulin and plasma membrane Ca2+ pump. *Cell Calcium* **13**, 581-591 (1992).
132. Klishin,A., Sedova,M. & Blatter,L.A. Time-dependent modulation of capacitative Ca2+ entry signals by plasma membrane Ca2+ pump in endothelium. *Am. J. Physiol* **274**, C1117-C1128 (1998).
133. Usachev,Y.M., DeMarco,S.J., Campbell,C., Strehler,E.E. & Thayer,S.A. Bradykinin and ATP accelerate Ca(2+) efflux from rat sensory neurons via protein kinase C and the plasma membrane Ca(2+) pump isoform 4. *Neuron* **33**, 113-122 (2002).
134. Blaustein,M.P., Juhaszova,M., Golovina,V.A., Church,P.J. & Stanley,E.F. Na/Ca exchanger and PMCA localization in neurons and astrocytes: functional implications. *Ann. N. Y. Acad. Sci.* **976**, 356-366 (2002).
135. Brandt,P.C. & Vanaman,T.C. The plasma membrane calcium pump: not just another pretty ion translocase. *Glycobiology* **6**, 665-668 (1996).
136. DeMarco,S.J. & Strehler,E.E. Plasma membrane Ca2+-atpase isoforms 2b and 4b interact promiscuously and selectively with members of the membrane-associated guanylate kinase family of PDZ (PSD95/Dlg/ZO-1) domain-containing proteins. *J. Biol. Chem.* **276**, 21594-21600 (2001).
137. Daniel,E.E., Jury,J. & Wang,Y.F. nNOS in canine lower esophageal sphincter: colocalized with Cav-1 and Ca2+-handling proteins? *Am. J. Physiol Gastrointest. Liver Physiol* **281**, G1101-G1114 (2001).

138. Schuh,K., Uldrijan,S., Telkamp,M., Rothlein,N. & Neyses,L. The plasmamembrane calmodulin-dependent calcium pump: a major regulator of nitric oxide synthase I. *J. Cell Biol.* **155**, 201-205 (2001).
139. Bredt,D.S. Nitric oxide signaling specificity--the heart of the problem. *J. Cell Sci.* **116**, 9-15 (2003).
140. Periasamy,M. & Kalyanasundaram,A. SERCA pump isoforms: their role in calcium transport and disease. *Muscle Nerve* **35**, 430-442 (2007).
141. Rossi,A.E. & Dirksen,R.T. Sarcoplasmic reticulum: the dynamic calcium governor of muscle. *Muscle Nerve* **33**, 715-731 (2006).
142. Dolphin,A.C. A short history of voltage-gated calcium channels. *Br. J. Pharmacol.* **147 Suppl 1**, S56-S62 (2006).
143. Villereal,M.L. Mechanism and functional significance of TRPC channel multimerization. *Semin. Cell Dev. Biol.* **17**, 618-629 (2006).
144. Rose,A.M. & Valdes,R., Jr. Understanding the sodium pump and its relevance to disease. *Clin. Chem.* **40**, 1674-1685 (1994).
145. Brini,M. *et al.* A comparative functional analysis of plasma membrane Ca2+ pump isoforms in intact cells. *J. Biol. Chem.* **278**, 24500-24508 (2003).
146. Graf,E. *et al.* Molecular properties of calcium-pumping ATPase from human erythrocytes. *Biochemistry* **21**, 4511-4516 (1982).
147. Aiton,J.F. & Cramb,G. The effects of vanadate on rabbit ventricular muscle adenylate cyclase and sodium pump activities. *Biochem. Pharmacol.* **34**, 1543-1548 (1985).
148. Tiffert,T. & Lew,V.L. Kinetics of inhibition of the plasma membrane calcium pump by vanadate in intact human red cells. *Cell Calcium* **30**, 337-342 (2001).
149. Skou,J.C. & Esmann,M. Eosin, a fluorescent probe of ATP binding to the (Na+ + K+)-ATPase. *Biochim. Biophys. Acta* **647**, 232-240 (1981).
150. Adamo,H.P. *et al.* Overexpression of the erythrocyte plasma membrane Ca2+ pump in COS-1 cells. *Biochem. J.* **285 ( Pt 3)**, 791-797 (1992).
151. Brini,M., Bano,D., Manni,S., Rizzuto,R. & Carafoli,E. Effects of PMCA and SERCA pump overexpression on the kinetics of cell Ca(2+) signalling. *EMBO J.* **19**, 4926-4935 (2000).
152. Enyedi,A., Verma,A.K., Filoteo,A.G. & Penniston,J.T. A highly active 120-kDa truncated mutant of the plasma membrane Ca2+ pump. *J. Biol. Chem.* **268**, 10621-10626 (1993).
153. Guerini,D., Schroder,S., Foletti,D. & Carafoli,E. Isolation and characterization of a stable Chinese hamster ovary cell line overexpressing the plasma membrane Ca(2+)-ATPase. *J. Biol. Chem.* **270**, 14643-14650 (1995).
154. Tribe,R.M., Moriarty,P. & Poston,L. Calcium homeostatic pathways change with gestation in human myometrium. *Biol. Reprod.* **63**, 748-755 (2000).

155. Hammes,A. *et al.* Expression of the plasma membrane Ca2+-ATPase in myogenic cells. *J. Biol. Chem.* **271**, 30816-30822 (1996).
156. Liu,B.F., Xu,X., Fridman,R., Muallem,S. & Kuo,T.H. Consequences of functional expression of the plasma membrane Ca2+ pump isoform 1a. *J. Biol. Chem.* **271**, 5536-5544 (1996).
157. Okunade,G.W. *et al.* Targeted ablation of plasma membrane Ca2+-ATPase (PMCA) 1 and 4 indicates a major housekeeping function for PMCA1 and a critical role in hyperactivated sperm motility and male fertility for PMCA4. *J. Biol. Chem.* **279**, 33742-33750 (2004).
158. Gros,R. *et al.* Plasma membrane calcium ATPase overexpression in arterial smooth muscle increases vasomotor responsiveness and blood pressure. *Circ. Res.* **93**, 614-621 (2003).
159. Schuh,K. *et al.* Regulation of vascular tone in animals overexpressing the sarcolemmal calcium pump. *J. Biol. Chem.* **278**, 41246-41252 (2003).
160. Hammes,A. *et al.* Overexpression of the sarcolemmal calcium pump in the myocardium of transgenic rats. *Circ. Res.* **83**, 877-888 (1998).
161. Williams,J.C. *et al.* The Sarcolemmal Calcium Pump, {alpha}-1 Syntrophin, and Neuronal Nitric-oxide Synthase Are Parts of a Macromolecular Protein Complex. *J. Biol. Chem.* **281**, 23341-23348 (2006).
162. Clackson,T. & Wells,J.A. In vitro selection from protein and peptide libraries. *Trends Biotechnol.* **12**, 173-184 (1994).
163. Gram,H. *et al.* In vitro selection and affinity maturation of antibodies from a naive combinatorial immunoglobulin library. *Proc. Natl. Acad. Sci. U. S. A* **89**, 3576-3580 (1992).
164. Lowman,H.B. Bacteriophage display and discovery of peptide leads for drug development. *Annu. Rev. Biophys. Biomol. Struct.* **26**, 401-424 (1997).
165. O'Neil,K.T. *et al.* Identification of novel peptide antagonists for GPIIb/IIIa from a conformationally constrained phage peptide library. *Proteins* **14**, 509-515 (1992).
166. Chaudhary,J., Walia,M., Matharu,J., Escher,E. & Grover,A.K. Caloxin: a novel plasma membrane Ca2+ pump inhibitor. *Am. J. Physiol Cell Physiol* **280**, C1027-C1030 (2001).

166a. Holmes,M.E., Chaudhary,J. & Grover,A.K. Mechanism of action of the novel plasma membrane Ca2+pump inhibitor caloxin. *Cell Calcium* **33**, 241-245 (2003).
167. Pande,J., Mallhi,K.K. & Grover,A.K. Role of third extracellular domain of plasma membrane Ca2+-Mg2+-ATPase based on the novel inhibitor caloxin 3A1. *Cell Calcium* **37**, 245-250 (2005).
168. Hajduk,P.J., Meadows,R.P. & Fesik,S.W. Discovering high-affinity ligands for proteins. *Science* **278**, 497,499 (1997).

169. Pande,J. *et al.* Aortic smooth muscle and endothelial plasma membrane Ca2+ pump isoforms are inhibited differently by the extracellular inhibitor caloxin 1b1. *Am. J. Physiol Cell Physiol* **290**, C1341-C1349 (2006).

169a. Pande,J. Szewczyk,M.M., Kuszczak,I., Grover,S., Escher,E. & Grover,A.K. Functional effects of caloxin 1c2, a novel engineered selective inhibitor of plasma membrane Ca(2+) pump isoform 4, on coronary artery. J. Cell. Mol. Med. 2008; 12(3):1049-60.

170. Laemmli,U.K. Cleavage of structural proteins during the assembly of the head of bacteriophage T4. *Nature* **227**, 680-685 (1970).

171. Jarrett,H.W. & Penniston,J.T. Purification of the Ca2+-stimulated ATPase activator from human erythrocytes. Its membership in the class of Ca2+-binding modulator proteins. *J. Biol. Chem.* **253**, 4676-4682 (1978).

172. Narayanan,N., Newland,M. & Neudorf,D. Inhibition of sarcoplasmic reticulum calcium pump by cytosolic protein(s) endogenous to heart and slow skeletal muscle but not fast skeletal muscle. *Biochim. Biophys. Acta* **735**, 53-66 (1983).

173. Pande,J., Mallhi,K.K. & Grover,A.K. A novel plasma membrane Ca(2+)-pump inhibitor: caloxin 1A1. *Eur. J. Pharmacol.* **508**, 1-6 (2005).

174. Seto-Young,D., Na,S., Monk,B.C., Haber,J.E. & Perlin,D.S. Mutational analysis of the first extracellular loop region of the H(+)-ATPase from Saccharomyces cerevisiae. *J. Biol. Chem.* **269**, 23988-23995 (1994).

175. Papp,B. *et al.* Demonstration of two forms of calcium pumps by thapsigargin inhibition and radioimmunoblotting in platelet membrane vesicles. *J. Biol. Chem.* **266**, 14593-14596 (1991).

176. Dorman,G. & Prestwich,G.D. Benzophenone photophores in biochemistry. *Biochemistry* **33**, 5661-5673 (1994).

177. McLafferty,M.A., Kent,R.B., Ladner,R.C. & Markland,W. M13 bacteriophage displaying disulfide-constrained microproteins. *Gene* **128**, 29-36 (1993).

178. Blond-Elguindi,S. *et al.* Affinity panning of a library of peptides displayed on bacteriophages reveals the binding specificity of BiP. *Cell* **75**, 717-728 (1993).

179. Smith,G.P., Schultz,D.A. & Ladbury,J.E. A ribonuclease S-peptide antagonist discovered with a bacteriophage display library. *Gene* **128**, 37-42 (1993).

180. Winter,G., Griffiths,A.D., Hawkins,R.E. & Hoogenboom,H.R. Making antibodies by phage display technology. *Annu. Rev. Immunol.* **12**, 433-455 (1994).

181. Weber,P.C., Pantoliano,M.W. & Thompson,L.D. Crystal structure and ligand-binding studies of a screened peptide complexed with streptavidin. *Biochemistry* **31**, 9350-9354 (1992).

182. Kehoe,J.W. *et al.* Using phage display to select antibodies recognizing post-translational modifications independently of sequence context. *Mol. Cell Proteomics.* **5**, 2350-2363 (2006).

183. Balass,M. *et al.* Identification of a hexapeptide that mimics a conformation-dependent binding site of acetylcholine receptor by use of a phage-epitope library. *Proc. Natl. Acad. Sci. U. S. A* **90**, 10638-10642 (1993).
184. Goodson,R.J., Doyle,M.V., Kaufman,S.E. & Rosenberg,S. High-affinity urokinase receptor antagonists identified with bacteriophage peptide display. *Proc. Natl. Acad. Sci. U. S. A* **91**, 7129-7133 (1994).
185. Szardenings,M. *et al.* Phage display selection on whole cells yields a peptide specific for melanocortin receptor 1. *J. Biol. Chem.* **272**, 27943-27948 (1997).
186. Beigi,F. & Wainer,I.W. Syntheses of immobilized G protein-coupled receptor chromatographic stationary phases: characterization of immobilized mu and kappa opioid receptors. *Anal. Chem.* **75**, 4480-4485 (2003).
187. Zhang,Y., Xiao,Y., Kellar,K.J. & Wainer,I.W. Immobilized nicotinic receptor stationary phase for on-line liquid chromatographic determination of drug-receptor affinities. *Anal. Biochem.* **264**, 22-25 (1998).
188. Lowman,H.B. & Wells,J.A. Affinity maturation of human growth hormone by monovalent phage display. *J. Mol. Biol.* **234**, 564-578 (1993).
189. Yanofsky,S.D. *et al.* High affinity type I interleukin 1 receptor antagonists discovered by screening recombinant peptide libraries. *Proc. Natl. Acad. Sci. U. S. A* **93**, 7381-7386 (1996).
190. Adachi,T. *et al.* S-Glutathiolation by peroxynitrite activates SERCA during arterial relaxation by nitric oxide. *Nat. Med.* **10**, 1200-1207 (2004).
191. Guerini,D., Zecca-Mazza,A. & Carafoli,E. Single amino acid mutations in transmembrane domain 5 confer to the plasma membrane Ca2+ pump properties typical of the Ca2+ pump of endo(sarco)plasmic reticulum. *J. Biol. Chem.* **275**, 31361-31368 (2000).
192. Young,H.S., Xu,C., Zhang,P. & Stokes,D.L. Locating the thapsigargin-binding site on Ca(2+)-ATPase by cryoelectron microscopy. *J. Mol. Biol.* **308**, 231-240 (2001).
193. De Fusco,M. *et al.* Haploinsufficiency of ATP1A2 encoding the Na+/K+ pump alpha2 subunit associated with familial hemiplegic migraine type 2. *Nat. Genet.* **33**, 192-196 (2003).
194. Asano,S. *et al.* The cavity structure for docking the K(+)-competitive inhibitors in the gastric proton pump. *J. Biol. Chem.* **279**, 13968-13975 (2004).
195. Lambrecht,N., Corbett,Z., Bayle,D., Karlish,S.J. & Sachs,G. Identification of the site of inhibition by omeprazole of a alpha-beta fusion protein of the H,K-ATPase using site-directed mutagenesis. *J. Biol. Chem.* **273**, 13719-13728 (1998).
196. Einholm,A.P., Andersen,J.P. & Vilsen,B. Roles of transmembrane segment M1 of Na+,K+-ATPase and Ca2-ATPase, the gatekeeper and the pivot. *J. Bioenerg. Biomembr.* **39**, 357-366 (2007).

197. Clausen,J.D., Vilsen,B., McIntosh,D.B., Einholm,A.P. & Andersen,J.P. Glutamate-183 in the conserved TGES motif of domain A of sarcoplasmic reticulum Ca2+-ATPase assists in catalysis of E2/E2P partial reactions. *Proc. Natl. Acad. Sci. U. S. A* **101**, 2776-2781 (2004).
198. Toustrup-Jensen,M. & Vilsen,B. Importance of conserved Thr214 in domain A of the Na+,K+ -ATPase for stabilization of the phosphoryl transition state complex in E2P dephosphorylation. *J. Biol. Chem.* **278**, 11402-11410 (2003).
199. Ng,Y.C. & Akera,T. Two classes of ouabain binding sites in ferret heart and two forms of Na+-K+-ATPase. *Am. J. Physiol* **252**, H1016-H1022 (1987).
200. Minocherhomjee,A.M., Beauregard,G., Potier,M. & Roufogalis,B.D. The molecular weight of the calcium-transport-ATPase of the human red blood cell determined by radiation inactivation. *Biochem. Biophys. Res. Commun.* **116**, 895-900 (1983).
201. Cavieres,J.D. Calmodulin and the target size of the (Ca2+ + Mg2+)-ATPase of human red-cell ghosts. *Biochim. Biophys. Acta* **771**, 241-244 (1984).
202. Kosk-Kosicka,D. & Bzdega,T. Activation of the erythrocyte Ca2+-ATPase by either self-association or interaction with calmodulin. *J. Biol. Chem.* **263**, 18184-18189 (1988).
203. Levi,V., Rossi,J.P., Castello,P.R. & Gonzalez Flecha,F.L. Oligomerization of the plasma membrane calcium pump involves two regions with different thermal stability. *FEBS Lett.* **483**, 99-103 (2000).
204. Vorherr,T., Kessler,T., Hofmann,F. & Carafoli,E. The calmodulin-binding domain mediates the self-association of the plasma membrane Ca2+ pump. *J. Biol. Chem.* **266**, 22-27 (1991).
205. Sackett,D.L. & Kosk-Kosicka,D. The active species of plasma membrane Ca2+-ATPase are a dimer and a monomer-calmodulin complex. *J. Biol. Chem.* **271**, 9987-9991 (1996).
206. Levi,V., Rossi,J.P., Castello,P.R. & Gonzalez Flecha,F.L. Structural significance of the plasma membrane calcium pump oligomerization. *Biophys. J.* **82**, 437-446 (2002).
207. Schrijen,J.J., Groningen-Luyben,W.A., Nauta,H., De Pont,J.J. & Bonting,S.L. Studies on (K+ + H+)-ATPase. VI. Determination on the molecular size by radiation inactivation analysis. *Biochim. Biophys. Acta* **731**, 329-337 (1983).
208. Blanco,G., Koster,J.C. & Mercer,R.W. The alpha subunit of the Na,K-ATPase specifically and stably associates into oligomers. *Proc. Natl. Acad. Sci. U. S. A* **91**, 8542-8546 (1994).
209. Kawano,S., Otsu,K., Shoji,S., Yamagata,K. & Hiraoka,M. Ca(2+) oscillations regulated by Na(+)-Ca(2+) exchanger and plasma membrane Ca(2+) pump induce fluctuations of membrane currents and potentials in human mesenchymal stem cells. *Cell Calcium* **34**, 145-156 (2003).

210. Yanagida,E. *et al.* Functional expression of Ca2+ signaling pathways in mouse embryonic stem cells. *Cell Calcium* **36**, 135-146 (2004).
211. De Luisi,A. & Hofer,A.M. Evidence that Ca(2+) cycling by the plasma membrane Ca(2+)-ATPase increases the 'excitability' of the extracellular Ca(2+)-sensing receptor. *J. Cell Sci.* **116**, 1527-1538 (2003).
212. Vale-Gonzalez,C., Alfonso,A., Sunol,C., Vieytes,M.R. & Botana,L.M. Role of the plasma membrane calcium adenosine triphosphatase on domoate-induced intracellular acidification in primary cultures of cerebelar granule cells. *J. Neurosci. Res.* **84**, 326-337 (2006).
213. Vale-Gonzalez,C., Gomez-Limia,B., Vieytes,M.R. & Botana,L.M. Effects of the marine phycotoxin palytoxin on neuronal pH in primary cultures of cerebellar granule cells. *J. Neurosci. Res.* **85**, 90-98 (2007).

## 6.0 Appendix 1: Physiological studies using caloxins

Since caloxins are obtained by screening the Ph.D peptide library for binding to the exdoms of PMCA, they are expected to inhibit PMCA activity by binding to the extracellular surface of the cells. Different individuals in the lab carried out experiments to examine the physiological effects of adding caloxins extracellularly. This included the effects on $[Ca^{2+}]_i$ in the cells cultured from the pig coronary artery smooth muscle (SMC) or endothelium (EC) whose isolation and phenotypic characterization has been described previously and effects on the contractility of the rat aorta and the pig coronary artery[169,173]. Together these studies show that PMCA inhibition by caloxins affects $[Ca^{2+}]_i$ levels and thereby influencing arterial function.

### A1.1 Effects of caloxin 1b1 on [Ca2+]i and the arterial contractility

The effect of caloxin 1b1 on $[Ca^{2+}]_i$ levels was studied using the cultured SMC and the EC. The SMC express PMCA isoforms 1 and 4, while the EC express mainly PMCA1[4]. Caloxin 1b1 (50 or 200 μM) was added to the medium containing the SMC and the EC. Caloxin 1b1 caused an increase in $[Ca^{2+}]_i$ in both the cell types (Fig. A1.1). However, the increase was more pronounced in the SMC than the EC. The RP1b1 (200 μM) or ethanol at the same final concentration as in the caloxin 1b1 treated cells had no effect on $[Ca^{2+}]_i$ in either cell type.

The effect of caloxin 1b1 was also tested on the cultured SMC and the EC stimulated with a low concentration of the non-fluorescent $Ca^{2+}$ ionophore, 4-

bromo-A23187. The ionophore caused a rapid but transient increase in $[Ca^{2+}]_i$ in both the cell types (Fig. A1.2). Caloxin 1b1 or RP1b1 at a concentration of 200 μM was added to the cells after the $[Ca^{2+}]_i$ decreased to a steady level. Caloxin 1b1 caused an increase in $[Ca^{2+}]_i$ in both the cell types, however, the increase in $[Ca^{2+}]_i$ was greater in the SMC than in the EC (Fig. A1.2). RP1b1 or ethanol at the same final concentration as in caloxin 1b1 treated cells had no effect on $[Ca^{2+}]_i$ dynamics in both the cell types. Thus, caloxin 1b1 caused an increase in the $[Ca^{2+}]_i$ when added to the medium containing cells stimulated with the calcium ionophore.

The effect of caloxin 1b1 on the arterial contractility was tested using the rat aorta. Increasing $[Ca^{2+}]_i$ in the smooth muscle and the endothelium has opposite effects on the arterial contractility. Elevated $[Ca^{2+}]_i$ in the endothelium causes relaxation while increase in $[Ca^{2+}]_i$ in the smooth muscle causes contraction. Here, caloxin 1b1 was used to study the effects of PMCA inhibition in these two tissues in the rat aorta.

The effect of caloxin 1b1 was tested on the contractility of the de-endothelialized rat aortic rings that were partially precontracted with submaximum concentration (0.1 μM) of phenylephrine. Caloxin 1b1 (200 μM) increased the contractile force in the partially precontracted rat aortic rings (Fig. A1.3). The addition of RP1b1 or ethanol to the precontracted aortic rings at the same final concentration as in caloxin 1b1 treated rings had no effect on their contractile state.

The rat aorta produces an endothelium dependent relaxation in response to carbachol and this relaxation is blocked by the inhibition of the nitric oxide synthase. The rat aortic rings with intact endothelium were fully contracted with 1 μM phenylephrine and then partially relaxed with submaximum concentration (0.3 μM) of carbachol. Addition of 200 μM caloxin 1b1 to the partially relaxed rat aortic rings did not increase the relaxation; instead it contracted the aortic rings (Fig. A1.4.). Greater inhibition of PMCA in smooth muscle by caloxin 1b1 may have led to a contractile response without potentiating the endothelium dependent relaxation.

Caloxin 1b1 exhibited a slight preference for PMCA4 isoform. It was also more effective in increasing $[Ca^{2+}]_i$ in the SMC than in the EC. It increased smooth muscle dependent contraction in the rat aorta but did not potentiate the endothelium dependent relaxation. These results are consistent with the observation that caloxin 1b1 has higher affinity for PMCA4 ($K_i$: 46 ± 5 μM) expressed only in the smooth muscle than PMCA1 isoform ($K_i$: 105 ± 11 μM) expressed in both the endothelium and the smooth muscle. These results can also be obtained due to the differences in the abundance of PMCA between the smooth muscle and the endothelium and hence the different roles of this transporter in the two tissues.

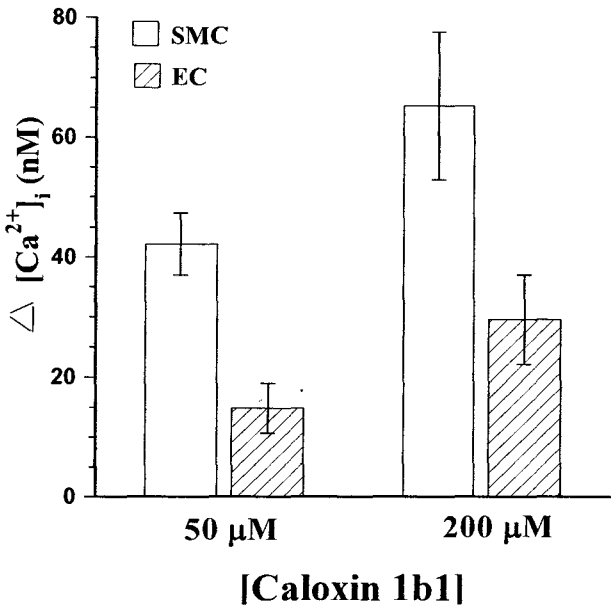


**Fig. A1.1. Effect of caloxin 1b1 on $[Ca^{2+}]_i$ in cultured SMC and the EC.**

Caloxin 1b1 (50 or 200 μM) was added to the medium containing cells. Caloxin 1b1 caused a greater increase in $[Ca^{2+}]_i$ in the SMC (PMCA1 and 4) than in the EC (PMCA1). The data are mean ± SE of 4 replicates. This experiment was carried out in our lab by Sue E. Samson. Modified from reference 169.

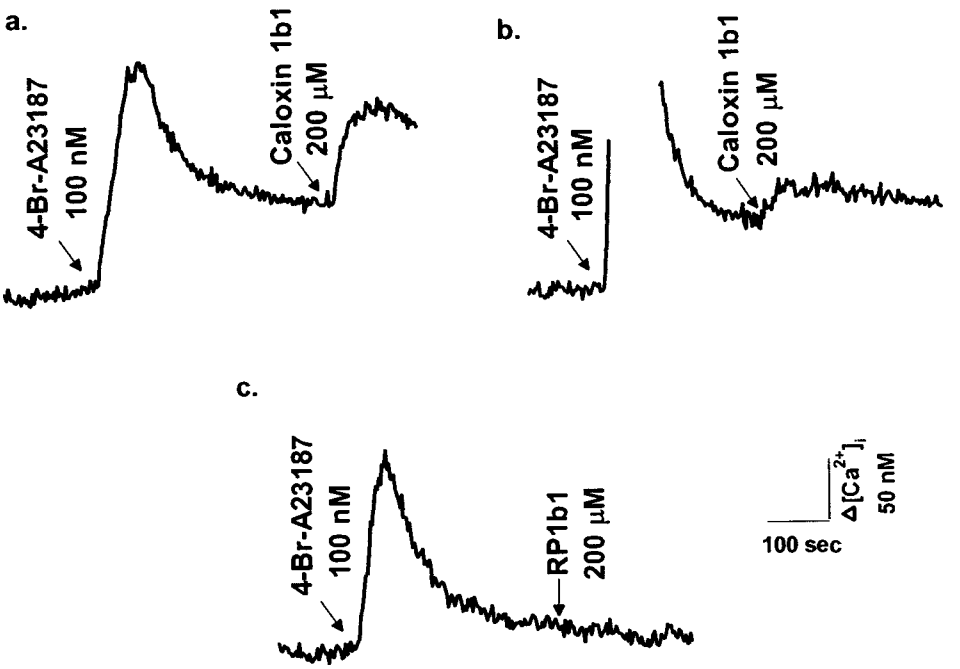


**Fig. A1.2. Effect of caloxin 1b1 on $[Ca^{2+}]_i$ dynamics.**

The SMC (a, c) and the EC (b) were stimulated with $Ca^{2+}$ ionophore, 4-Br-A23187, which caused a transient increase in $[Ca^{2+}]_i$. Addition of 200 µM caloxin 1b1 caused a greater increase in $[Ca^{2+}]_i$ in the SMC (PMCA1 and 4) than in EC (PMCA1). RP1b1 had no effect on $[Ca^{2+}]_i$. The scale $\triangle[Ca^{2+}]_i$ indicates the change in the fluorescence of Fluo-3 corresponding to 50 nM $Ca^{2+}$. Each experiment was replicated on 3 different days. Sue E. Samson carried out this experiment in our lab. Modified from reference 169.

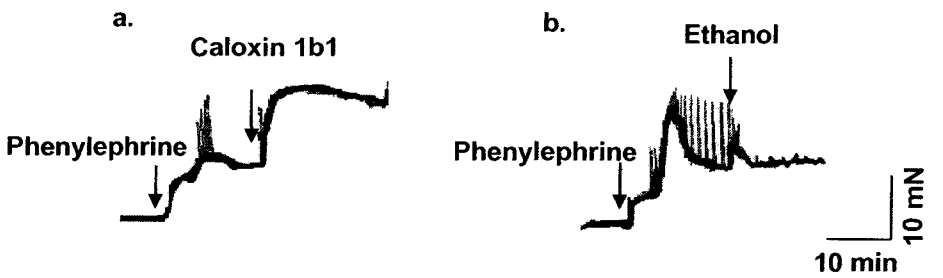


**Fig. A1.3. Effect of caloxin 1b1 on the de-endothelialized rat aortic rings.**

The rings were partially contracted with 0.1 μM phenylephrine, followed by the addition of 200 μM caloxin 1b1 (a) or ethanol (b) at the time points indicated by the arrows. The final concentration of ethanol in the control aortic rings was the same (0.1 %) as in the caloxin 1b1 treated aortic rings. Alex Kitson carried out this experiment in our lab. Modified from reference 169.

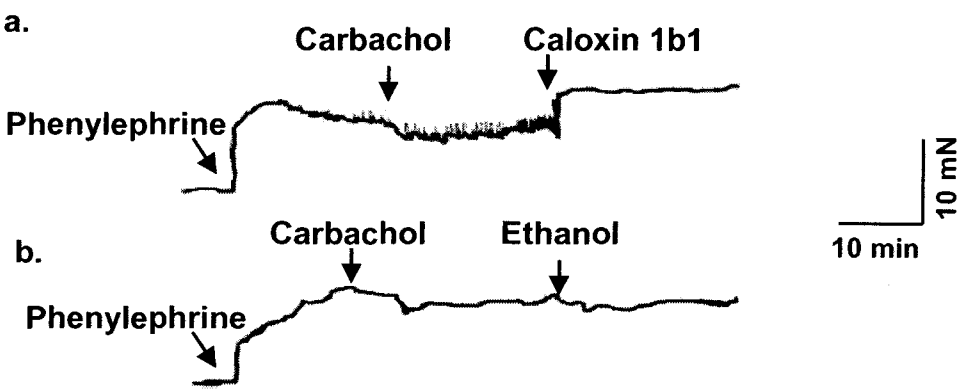


**Fig. A1.4. Effect of caloxin 1b1 on the endothelium dependent relaxation of the rat aortic rings.**

The rings fully contracted with 1 μM phenylephrine were partially relaxed by the addition of 0.3 μM carbachol at the time indicated by the arrow. This was followed by the addition of 200 μM caloxin 1b1 (a) or ethanol (b) at the time points indicated by the arrows. The final concentration of ethanol in the control aortic rings was the same (0.1 %) as in the caloxin 1b1 treated aortic rings. Alex Kitson carried out this experiment in our lab. Modified from reference 169.

## A1.2. Effect of caloxin 1c2 on the arterial contractility

The effect of 0, 10, 20 and 50 μM caloxin 1c2 was tested on the basal tone of the de-endothelialized pig coronary artery in the presence of L-NAME, the inhibitor of nitric oxide synthase. At all three concentrations of caloxin 1c2, there was an increase in the basal tone, which leveled off after 20 min at 2-3% of the maximum contraction obtained with 60 mM KCl (Fig. A1.5) A multiple comparison test with one-way ANOVA negated the hypothesis that the differences in the tone at 0, 10, 20 and 50 μM caloxin 1c2 were purely due to chance ($p= 0.0015$). In a Tukey-Kramer multiple comparison test, q values greater than 3.807 indicates that a group differs from another comparison group. In this test, there was a significant difference between the control tissues and those treated with 10 ($q = 4.085$, $p < 0.05$), 20 ($q = 5.235$, $p<0.05$) and 50 ($q = 4.156$, $p<0.05$) μM caloxin 1c2. There was no significant difference between tissues treated with 10 or 20 ($q = 1.435$, $p>0.05$), 10 or 50 ($q = 0.7679$, $p>0.05$) and 20 or 50 ($q = 0.5133$, $p>0.05$) μM caloxin 1c2.

The effect of caloxin 1c2 was also tested on the de-endothelialized coronary artery rings in which the forward mode of the NCX and the SERCA were inhibited. $Na^+$ loading the arteries by incubating them in the $K^+$ and $Ca^{2+}$ free Krebs' inhibited the forward mode of the NCX in which it extrudes $Ca^{2+}$ from the cell. The SERCA activity was inhibited by cyclopiazonic acid. With SERCA and NCX inhibited, PMCA was the only $Ca^{2+}$ extruding system operating under given conditions. The introduction of 0.05 mM $Ca^{2+}$ to the $Ca^{2+}$ free Krebs' containing

L-NAME caused arterial contraction. Caloxin 1c2 (20 μM) caused a significant increase in the force of contraction (p=0.019) as compared to the controls. Ethanol at the same final concentration as in the caloxin 1c2 treated rings had no effect. This increase in contractile force by caloxin 1c2 was observed only at low extracellular $Ca^{2+}$ concentration with no effect at 0.1 or 1.6 mM extracellular $Ca^{2+}$ concentrations (Fig. A1.6). Thus, caloxin 1c2 increased the $Ca^{2+}$ sensitivity of the tissue when other $[Ca^{2+}]_i$ lowering systems were inhibited without affecting the maximum contraction.

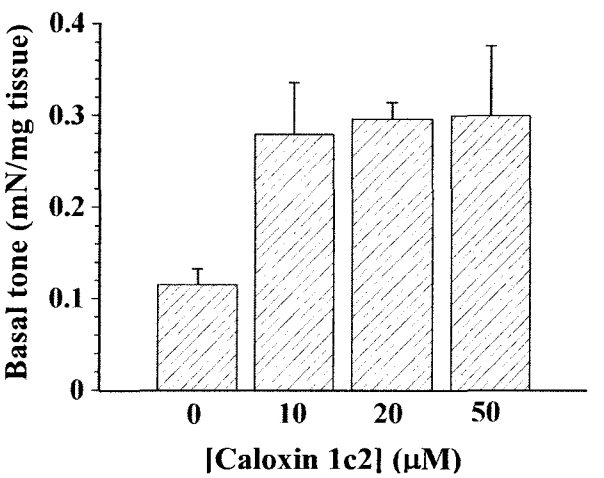


**Fig. A1.5. Effect of caloxin 1c2 on the basal tone of de-endothelialized pig coronary artery rings.**

The given concentrations of caloxin 1c2 were added to the de-endothelialized coronary artery rings in the presence of L-NAME. Ethanol was added to the control at the same final concentration as in the caloxin 1c2 treated coronary rings. An increase in the basal tone in 20 min after the addition of caloxin 1c2 was determined as mN/mg tissue weight. The values are mean ± SEM of 18, 12, 7 and 7 replicates for 0, 10, 20 and 50 μM caloxin 1c2, respectively. Iwona Kuszczak and Fareeha Qayyum carried out this experiment in our lab. Modified from reference 169a.

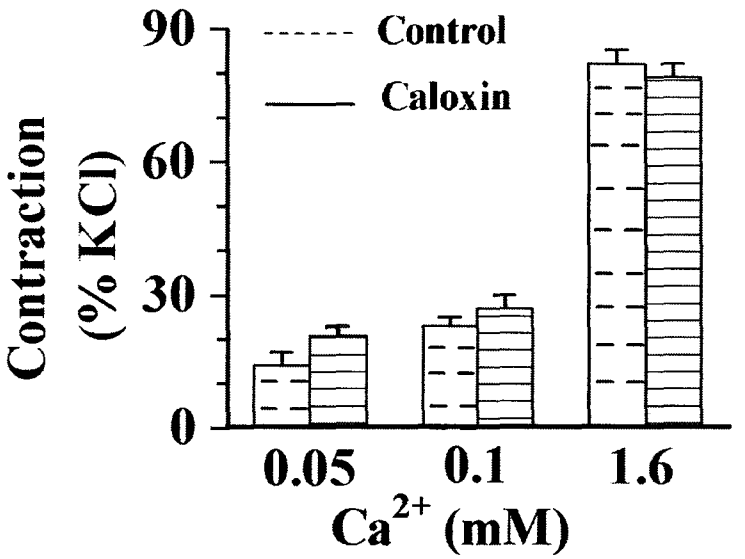


**Fig. A1.6. Effect of caloxin 1c2 on the contractility of de-endothelialized coronary artery rings.**

The SERCA and forward mode of the NCX were inhibited in the rings that were incubated in the $K^+$ and $Ca^{2+}$ free Krebs' containing L-NAME. Caloxin 1c2 at a concentration of 20 μM was added to the coronary artery rings. Ethanol at the same final concentration as in the caloxin 1c2 treated rings was added to the control tissues. Introduction of 0.05 mM, 0.1 mM and 1.6 mM $Ca^{2+}$ to the $Ca^{2+}$ free Krebs' caused arterial contraction. Caloxin 1c2 at 20 μM caused a significant increase in the force of contraction at only 0.05 mM $Ca^{2+}$ ($p=0.019$). Contraction of each artery is expressed as % of that obtained with 60 mM KCl. The values are mean ± SEM of 11 replicates. Iwona Kuszczak carried out this experiment in our lab. Modified from reference 169a.

### A1.3. Effect of caloxin 1a1 on cells stimulated with $Ca^{2+}$ ionophore

The effect of caloxin 1a1 on $[Ca^{2+}]_i$ was tested using intact cultured EC. The EC were stimulated with the $Ca^{2+}$ ionophore, 4-bromo-A23187 (100 nM), in the presence of 10 μM cyclopiazonic acid to inhibit the SERCA activity. Caloxin 1a1 was added to the cells after $[Ca^{2+}]_i$ had decreased to a steady level following the transient increase. Addition of caloxin 1a1 caused a further increase in $[Ca^{2+}]_i$ which is consistent with the decreased ability of the cells to extrude $Ca^{2+}$ following the inhibition of PMCA (Fig. A1.7).

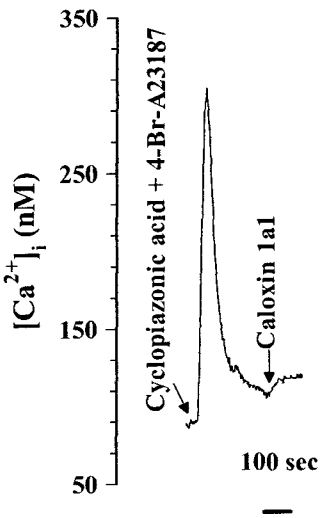


**Fig. A1.7. Effect of caloxin 1a1 on cell $[Ca^{2+}]_i$ dynamics.**

The EC stimulated with the $Ca^{2+}$ ionophore, 4-Br-A23187 in the presence of cyclopiazonic acid (SERCA inhibitor) caused a transient increase in $[Ca^{2+}]_i$. Addition of caloxin 1a1 (370 μM) at the time indicated by the arrow caused an increase in $[Ca^{2+}]_i$. Sue E. Samson carried out this experiment in our lab. Modified from reference 173.